องค์ประกอบทางเคมีและฤทธิ์ทางชีวภาพของเปลือกต้นสีเสียดน้ำ

นายก้องสินธุ์ เหลืองเรืองรอง

วิทยานิพนธ์นี้เป็นส่วนหนึ่งของการศึกษาตามหลักสูตรปริญญาเภสัชศาสตรมหาบัณฑิต
สาขาวิชาเภสัชเวท ภาควิชาเภสัชเวทและเภสัชพฤกษศาสตร์
คณะเภสัชศาสตร์ จุฬาลงกรณ์มหาวิทยาลัย
ปีการศึกษา 2556

CHEMICAL CONSTITUENTS AND BIOACTIVITIES OF *MALLOTUS PLICATUS* STEM BARK

Mr. Kongsin Luangruangrong

A Thesis Submitted in Partial Fulfillment of the Requirements
for the Degree of Master of Science in Pharmacy Program in Pharmacognosy
Department of Pharmacognosy and Pharmaceutical Botany
Faculty of Pharmaceutical Sciences
Chulalongkorn University
Academic Year 2013

Thesis Title	CHEMICAL CONSTITUENTS AND BIOACTIVITIES OF *MALLOTUS PLICATUS* STEM BARK
By	Mr. Kongsin Luangruangrong
Field of Study	Pharmacognosy
Thesis Advisor	Professor Kittisak Likhitwitayawuid, Ph.D.
Thesis Co-Advisor	Associate Professor Boonchoo Sritularak, Ph.D.

Accepted by the Faculty of Pharmaceutical Sciences, Chulalongkorn University in Partial Fulfillment of the Requirements for the Master's Degree

.....Dean of the Faculty of Pharmaceutical Sciences

(Assistant Professor Rungpetch Sakulbumrungsil, Ph.D.)

THESIS COMMITTEE

.....Chairman

(Associate Professor Surattana Amnuoypol, Ph.D.)

.....Thesis Advisor

(Professor Kittisak Likhitwitayawuid, Ph.D.)

.....Thesis Co-Advisor

(Associate Professor Boonchoo Sritularak, Ph.D.)

.....Examiner

(Associate Professor Vimolmas Lipipun, Ph.D.)

.....Examiner

(Associate Professor Suchada Sukrong, Ph.D.)

.....External Examiner

(Associate Professor Nijsiri Ruangrungsi, Ph.D.)

ก้องสินธุ์ เหลืองเรืองรอง : องค์ประกอบทางเคมีและฤทธิ์ทางชีวภาพของเปลือกต้นสีเสียดน้ำ. (CHEMICAL CONSTITUENTS AND BIOACTIVITIES OF *MALLOTUS PLICATUS* STEM BARK) อ.ที่ปรึกษาวิทยานิพนธ์หลัก: ศ. ภก. ดร. กิตติศักดิ์ ลิขิตวิทยาวุฒิ, อ.ที่ปรึกษาวิทยานิพนธ์ร่วม: รศ. ภก. ดร. บุญชู ศรีตุลารักษ์, 139 หน้า.

จากการคัดกรองพืชสมุนไพรที่มีฤทธิ์ต้านไวรัสเริม พบว่าสารสกัดหยาบเอทิลแอซิเตตและสารสกัดหยาบเมทานอลจากส่วนเปลือกต้นของสีเสียดน้ำมีฤทธิ์ดังกล่าว นำสารสกัดหยาบทั้งสองมาสกัดแยกสารบริสุทธิ์ด้วยวิธีการทางโครมาโทกราฟี สามารถแยกสารบริสุทธิ์ 9 ชนิด เมื่อนำมาศึกษาโครงสร้างสารด้วยวิธีทางสเปคโทรสโคปีได้แก่ UV, IR, MS และ NMR พบว่าเป็นสารใหม่ 2 ชนิดคือ bergenin-8-*O*-α-L-rhamnoside และ *seco*-bergenin-8-*O*-α-L-rhamnoside ส่วนสารอีก 7 ชนิดเป็นสารที่เคยมีรายงานมาแล้วได้แก่ aleuritolic acid 3-acetate, bergenin, daucosterol, protocatechuic acid, 11-*O*-acetylbergenin, scopoletin และ blumenol A เมื่อนำสารที่แยกได้มาทดสอบฤทธิ์ต้านไวรัสเริม พบว่าสาร *seco*-bergenin-8-*O*-α-L-rhamnoside และ protocatechuic acid มีฤทธิ์ต้านไวรัสเริมอย่างอ่อน ส่วนสารอื่นไม่มีฤทธิ์ นอกจากนี้ยังนำสารที่แยกได้บางสารไปทดสอบความเป็นพิษต่อเซลล์มะเร็ง KB และฤทธิ์ต้านอนุมูลอิสระ DPPH แต่พบว่าไม่มีสารชนิดใดมีฤทธิ์

ภาควิชา	เภสัชเวทและเภสัชพฤกษศาสตร์	ลายมือชื่อนิสิต .....
สาขาวิชา	เภสัชเวท	ลายมือชื่อ อ.ที่ปรึกษาวิทยานิพนธ์หลัก .....
ปีการศึกษา	2556	ลายมือชื่อ อ.ที่ปรึกษาวิทยานิพนธ์ร่วม .....

5476233233 : MAJOR PHARMACOGNOSY
KEYWORDS: MALLOTUS PLICATUS / CHEMICAL CONSTITUENTS / ANTI-HSV ACTIVITY

KONGSIN LUANGRUANGRONG: CHEMICAL CONSTITUENTS AND BIOACTIVITIES OF *MALLOTUS PLICATUS* STEM BARK. ADVISOR: PROF. KITTISAK LIKHITWITAYAWUID, Ph.D., CO-ADVISOR: ASSOC. PROF. BOONCHOO SRITULARAK, Ph.D., 139 pp.

During the course of our screening of medicinal plants for anti-Herpes simplex virus (HSV) activity, an ethyl acetate extract and a methanol extract prepared from the stem bark of *Mallotus plicatus* (Müll.Arg.) Airy Shaw showed significant anti-HSV potential. A chemical investigation was then conducted using several chromatographic techniques. This led to the isolation of nine compounds. The structure determinations of the isolated compounds were carried out using a combination of spectroscopic techniques (UV, IR, MS and NMR). Two of the isolates were structurally characterized as new compounds and named bergenin-8-*O*-α-L-rhamnoside and *seco*-bergenin-8-*O*-α-L-rhamnoside. The other seven compounds were identified as bergenin, daucosterol, protocatechuic acid, 11-*O*-acetylbergenin, scopoletin and blumenol A. The results from the anti-HSV activity assay showed that bergenin-8-*O*-α-L-rhamnoside and protocatechuic acid were weakly active against HSV. Some of the isolated compounds were also evaluated for cytotoxicity against KB cells and scavenging activity against DPPH free radicals, but none of them showed the activities.

Department:	Pharmacognosy and Pharmaceutical Botany	Student's Signature .....
		Advisor's Signature .....
Field of Study:	Pharmacognosy	Co-Advisor's Signature .....
Academic Year:	2013	

ACKNOWLEDGEMENTS

The author would like to thank his thesis advisor, Professor Dr. Kittisak Likhitwitayawuid of the Department of Pharmacognosy and Pharmaceutical Botany, Faculty of Pharmaceutical Sciences, Chulalongkorn University, for his useful advice, kindness, patience and constant encouragement throughout this research project.

The author would like to extend his gratitude to his co-advisor, Associate Professor Dr. Boonchoo Sritularak of the Department of Pharmacognosy and Pharmaceutical Botany, Faculty of Pharmaceutical Sciences, Chulalongkorn University, for his patience, useful guidance and kindness.

The author is very much obliged to the thesis committee for their useful, critical and constructive suggestions for this thesis.

The author is grateful to the Graduate School of Chulalongkorn University for granting partial financial support for this research project.

The author would like to thank Associate Professor Dr. Vimolmas Lipipun of the Department of Biochemistry and Microbiology, Faculty of Pharmaceutical Sciences, Chulalongkorn University, for her assistance in the in vitro anti-herpetic activity assay.

The author's gratitude is extended to the staff members and other graduate students of the Department of Pharmacognosy and Pharmaceutical Botany, Faculty of Pharmaceutical Sciences, Chulalongkorn University, for their assistance, useful advice and friendship throughout the period of his study.

Finally, the author would like to express his gratitude to his family for their understanding, love and encouragement.

CONTENTS

Page

Page

Page

Page

LIST OF TABLES

TABLE Page

LIST OF FIGURES

FIGURE Page

FIGURE Page

FIGURE Page

FIGURE Page

FIGURE Page

LIST OF SCHEMES

LIST OF ABBREVIATIONS

$[\alpha]^{20}_{D}$	=	Specific rotation at Sodium D line (589 nm)
Ac	=	Acetyl group
amu	=	Atomic mass unit
acetone-d_6	=	Deuterated acetone
α	=	Alpha
β	=	Beta
br	=	Broad (for NMR spectra)
br m	=	Broad multiplet (for NMR spectra)
br s	=	Broad singlet (for NMR spectra)
br t	=	Broad triplet (for NMR spectra)
Bu-i	=	Isobutyl group
BuOH	=	Butanol
c	=	Concentration
°C	=	Degree Celcius
calcd.	=	Calulate
CC	=	Column chromatography
CC_{50}	=	50% Cytotoxicity concentration
CD	=	Circular dichroism
$CDCl_3$	=	Deuterated chloroform
CD_3OD	=	Deuterated methanol
CH_2Cl_2	=	Dichloromethane
$CHCl_3$	=	Chloroform
cm	=	Centimeter
cm^{-1}	=	Reciprocal centimeter (unit of wave number)
^{13}C-NMR	=	Carbon-13 Nuclear Magnetic Resonance
DEPT	=	Distortionless Enhancement by Polarization Transfer

2D-NMR	=	Two Dimentional Nuclear Magnetic Resonance
d	=	Doublet (for NMR spectra)
dd	=	Doublet of doublets (for NMR spectra)
DMSO	=	Dimethyl sulfoxide
DMSO-d_6	=	Deuterated dimethyl sulfoxide
DPPH	=	2,2-diphenyl-1-picrylhydrazyl
δ	=	Chemical shift
ε	=	Molar absorptivity
ESI-MS	=	Electrospray ionization mass spectrometry
Et	=	Ethyl group
EtOAc	=	Ethyl acetate
EtOH	=	Ethanol
F_{254}	=	Fluorescence at 254 nm
FBS	=	Fetal bovine serum
FT	=	Fourier Transform
g	=	Gram
G	=	Gypsum
Glc	=	Glucose
hr	=	Hour
^{1}H-NMR	=	Proton Nuclear Magnetic Resonance
^{1}H-^{1}H COSY	=	Homonuclear (Proton-Proton) Correlation Spectroscopy
HMBC	=	^{1}H-detected Heteronuclear Multiple Bond Correlation
HR	=	High resolution
HSQC	=	Heteronuclear Single Quantum Coherence
HSV	=	Herpes simplex virus
Hz	=	Hertz
IR	=	Infrared spectrum
IC_{50}	=	50% Inhibitory concentration

J	=	Coupling constant
KBr	=	Potassium bromide
kg	=	Kilogram
L	=	Litre
λ_{max}	=	Wavelength at maximal absorption
µg	=	Microgram
µg/mL	=	Microgram per millilitre
µL	=	Microlitre
µM	=	Micromolar
$[M]^+$	=	Molecular ion
$[M+H]^+$	=	Protonated molecular ion
$[M-H]^-$	=	Deprotonated molecular ion
$[M+Na]^+$	=	Sodium-adduct molecular ion
m	=	Multiplet (for NMR spectra)
Me	=	Methyl group
MEM	=	Minimum essential medium
MeOH	=	Methanol
mg	=	Milligram
MHz	=	MegaHertz
MIC	=	Minimum inhibitory concentration
min	=	Minute
mL	=	Militer
mm	=	Millimeter
mp	=	Melting point
MS	=	Mass spectrometry
MW	=	Molecular weight
m/z	=	Mass to charge ratio
N	=	Normality

ν_{max}	=	Wave number at maximal absorption
nm	=	Nanometre
NMR	=	Nuclear Magnetic Resonance
No.	=	Number
NOESY	=	Nuclear Overhauser Enhancement Spectroscopy
OD	=	Optical density
ODS	=	Octadecylsilane
Ph	=	Phenyl group
ppm	=	Part-per-million
Pr-i	=	Isopropyl group
rel int	=	Relative intensity
R_f	=	Retention factor
Rha	=	Rhamnose
RP	=	Reverse phase
s	=	Singlet (for NMR spectra)
t	=	Triplet (for NMR spectra)
td	=	Triplet of doublets (for NMR spectra)
TLC	=	Thin Layer Chromatography
UV	=	Ultraviolet
v	=	Volume
v/v	=	Volume per volume
VIS	=	Visible

CHAPTER I

INTRODUCTION

The genus *Mallotus* is a member of the family Euphorbiaceae of the order Malphighiales. Most plants in this genus are shrubs and trees (Department of National Park, 2007;Rivière et al., 2010). They are also dioecious. They have simple or stellate hairs and whitish to reddish glandular trichomes. Leaves are alternate or opposite with caduceus stipules. The shape of the leaf is symmetric blade with denticulate margin. The upper surface is full of extrafloral nectaries, and the lower surface has grandular scales and domatia in nerve axils. Inflorescences arise from the axil of the leaf and the terminal of the stick. They are single, unbranched and racemes. Each flower has 3-6 sepals. Petals and disc are absent. Staminate flowers are in groups per nodes. They have no sepals. Stamens are 15-250. Pistillate flowers are 1 or 2 per node. Sepals exist. Each flower has one ovary with 3 locules, one ovule per lucule. Fruits are capsules with spines. Seeds are usually naked or with arils, especially when young (The Forest Herbarium, Department of National Park, Wildlife and Plant Conservation, 2007). There are approximately 150 species in the genus *Mallotus*. Most members are distributed mainly in East and Southeast Asia. Only 2 species, *M. oppositifolius* and *M. subulatus*, are found in Africa, and one species namely *M. baillonianus* Müll.Arg. is found only in Madagascar (Bollendorff et al., 2000;Rivière et al., 2010).

In Thailand, about 40 species have been reported (Department of National Park, 2007). In addition, two species namely *M. actinoneurus* and *M. tokiae* have been recently recorded (Welzen, 2013). All of them are shrubs or trees as follows (Table 1).

Table 1 Scientific names and vernacular (Thai) names of the *Mallotus* plants found in Thailand

Scientific Name	Thai Name
Mallotus actinoneurus Airy Shaw	-
M. bartatus Müll.Arg	Khi thao, Po tao, Tao khon and Tong tao
M. brevipetiolatus Gage	Po hun kan san
M. calocarpus Airy Shaw	-
M. coudercii (Gagnep.) Airy Shaw	Ta khe khum wang (Phetchaburi) and Tao tua mia (Ratchaburi)
M. decipiens Müll.Arg.	-
M. dispar (Blume) Müll.Arg.	-
M. floribundus (Blume) Müll.Arg.	Lo, Pik and Prik (Nakhon Si thammarat and Prachuap khiri khan)
M. glabriusculus (Kurz) Pax & K.Hoffm.	Kok krasum
M. garrettii Airy Shaw	-
M. glomerulatus Welzen	Mak lium
M. hispidospinosus Welzen & Chayam.	-
M. hymenophyllus Airy Shaw	-
M. khasianus Hook.f.	Nhao nok, Ngao-pa, Sipo and Sipo yang (Northern)
M. kingii	-
M. kongkandae Welzen & Phattar.	-
M. lanceolatus (Gagnep.) Airy Shaw	Pho (Central)
M. leptostachynus Hook.f.	-
M. leucocalyx Müll.Arg.	-
M. leucodermis Hook.f.	Ka dong dong

Table 1 Scientific names and vernacular (Thai) names of the *Mallotus* plants found in Thailand. (continued)

Scientific Name	Thai Name
M. macrostachyus (Miq.) Müll.Arg.	Plao yai, Lua (Nakhon Si thammarat), Fami, Lo khon (Trang) and Lo (Narathiwat)
M. metcalfianus Croizat	Plaothong (Northeastern)
M. miquelianus (Scheff.) Boerl.	-
M. metcalfianus Croizat	Plaothong (Northeastern)
M. miquelianus (Scheff.) Boerl.	-
M. pallidus (Airy Shaw) Airy Shaw	Kra duk kai khao (Southwestern)
M. paniculatus (Lam.) Müll.Arg.	Sati ton, Salad pang, Soi dao (Chanthaburi and Trat), Lo khon and Saet (Penisular)
M. peltatus (Geiseler) Müll.Arg.	Salad (Chanthaburi) and Khi tao (Ranong)
M. penangensis	-
M. philippensis (Lam.) Müll.Arg.	Kai khat hin, Makai khat, Kham dang, Kham saet, Ma khai, Thongthuai and Saet (Central)
M. pierrei (Gagnep.) Airy Shaw	-
M. plicatus (Müll.Arg.) Airy Shaw	-
M. repandus (Willd.) Müll.Arg.	Makai khruea and Mapop khruea (Northern)
M. resinosus (Blanco) Merr.	-
M. stipularis	Nut (Ranong)
M. subcuneatus (Gage) Airy Shaw	-
M. subpeltatus	Raeo (Phuket), Cha ngo phi, Dan mi and Han ton (Nakhon Si thammarat)
M. thorelii Gagnep.	-
M. tiliifolius (Blume) Müll.Arg.	-
M. tokiae Welzen	-

Mallotus plicatus (Müll.Arg.) Airy Shaw has several symnonyms: *Coccoceras plicatum* Müll.Arg., *Croton anisopodum* Gagnep., *Croton castaniofolius* Wall., *Croton*

eirocarpoides Wall., *Hymenocardia plicata* Kurz, *Mallotus anisopodus* (Gagnep.) Airy Shaw, *Mallotus eriocarpoides* Wall. ex Müll. Arg. and *Mallotus. wallichianus* Müll.Arg. It is a shrub or tree. Its height is up to 15 m. It has simple and stellate hairs and orange-red small grandular scales everywhere. Leaves are opposite or alternate with triangular stipules, 0.7-0.9 by ca. 0.3 mm, and petioles, 1.2-4 cm long. The shape of the leaf is blade elliptic to obovate. Its length and width is 5.5-16 and 2.5-8.5 cm, respectively, and the length/width ratio is 1.7-2.8. The margin is crenate with glands in sinuses. Its base is slightly emarginate to obtuse. The apex is round to bluntly acuminate. Inflorescences stick together 1-3. Their position is axillary and terminal, covered with triangular bracts, 1.2-1.8 by 0.8-1.2 mm. Their staminate inflorescences length is up to 18 cm. Every inflorescence composes of 3-7 flowers. Its diameter is about 4 mm, and the pedicel is about 2.5 mm long. Each flower has 3 or 4 sepals. Its shape is ovate to elliptic, 2-3 by 1.4-2 mm, and the color is yellow to reddish-brown. Stamens are 20-25. Their filaments are about 0.5-1.5 mm long. Each anther is about 0.3-0.5 mm long. Each pistillate inflorescence is about 7-21 cm long. The pistillate flower diameter is about 3-4 mm, and pedicels are about 1-3 mm long. Each flower has 5-6 sepals, 2-2.5 by 0.3-1 mm. One ovary composes of 2-4 locules. Stigma is subsessile, 2-2.5 mm long. Fruit is indehiscent woody capsules with obpyramidal winged lobed shape. It is 2-2.5 mm in diameter with brown colors. Seeds are subglobose with shiny, dark brown. Its diameter is about 4-5 mm. *M. plicatus* distributes in evergreen forests, 150 m above sea level. It has been found in Burma, Cambodia, Laos and Vietnam. In Thailand, this plant has been identified in Maha Sarakham and Saraburi provinces (Bollendorff et al., 2000;Department of National Park, 2007).

The leaves and branches of *M. plicatus* have been previously chemically studied under the name *M. anisopodus* (Van Minh et al., 2009), but the plant has never been investigated for biological activity. In this study, we evaluated the EtOAc and MeOH extracts of *M. plicatus* stem bark, and found them to have significant anti-

herpes simplex virus activity (See the Experimental). This investigation was therefore initiated with the primary goal of finding the anti-herpetic principles of *M. plicatus* bark. In addition, because several reports have described the cytotoxicity (Kiem et al., 2005;Rivière et al., 2010) and free radical scavenging activity (Arfan et al., 2007;Rivière et al., 2009) of the chemical constituents of the plants in the genus *Mallotus*, this study would also aim to evaluate the cytotoxic and antiradical properties of the isolates from *M. plicatus* stem bark. It is hoped that the chemical and biological data to be obtained in this study would be beneficial for the future chemotaxonomic study of members in the genus *Mallotus*, as well as for the development of useful medicinal agents.

In this study, the following objectives were put forward:

1. Separation and isolation bioactive compounds from the stem bark of *M. plicatus*

2. Structure characterization of the isolated compounds

3. Examination of biological activities including anti-HSV activity, cytotoxicity against cancer cells and antiradical activity against DPPH of the isolated compounds

Figure 1 *Mallotus plicatus* (Müll.Arg.) Airy Shaw

(Photographed by Associate Professor Thatree Phadungcharoen)

CHAPTER II

HISTORICAL

1. Chemical constituents of *Mallotus* species

Up to the present, there have been several studies on the chemical constituents of several members of this genus. Some species of *Mallotus*, for example, *M. apelta*, *M metcalfianus*, *M. philippensis*, *M. paniculatus* and *M. repandus*, have been reported to produce structurally diversified classes of secondary metabolites. The chemical compounds reported from the genus *Mallotus* can be categorized into 9 groups as diterpenoids, cardenolides, triterpenoids, steroids, coumarins, flavonoids, phloroglucinol derivatives, tannins and gallic acid derivatives, and miscellaneous compounds (Tables 2-10 and Figures 2-10).

1.1 Diterpenoids

There are several types of diterpenoids that have been found in the genus *Mallotus*. Compounds **1**-**3**, which have been isolated from *M. apelta*, can be classified as cembrane-type diterpenoids, whereas the diterpenoids **4** and **5** from the same plant are of dolabradane-type. The other categories include casbane-type diterpenoids [**6**-**8**], which have a 5-membered lactone ring from *M. hookerianus*, and the norclerodane-type diterpenoids [**9**-**12**] from *M. repandus*, in which the methyl group at C-5 of the clerodane structure is missing (Table 2 and Figure 2).

Table 2 Distribution of diterpenoids in *Mallotus* species

Name	Plant	References
10-Hydroxycembrene-5-one [**1**]	*M. apelta*	(Cheng and Chen, 1999)
6-Hydroxycembrene-5,10-dione [**2**]		(Cheng and Chen, 1999)
6,10-Dihydroxycembrene-5-one (malloapeltene) [**3**]		(Cheng et al., 1999)
2***α***,4***β***,15,16-Tetrahydroxydolabradane [**4**]		(Cheng and Chen, 1999)
4***α***,15,16-Trihydroxydolabradane (malloapeltin) [**5**]		(Cheng et al., 1999)
Hookerianolide A [**6**], B [**7**] and C [**8**]	*M. hookerianus*	(Bai et al., 2006)
Mallotucin A [**9**], B [**10**], C [**11**] And D [**12**]	*M. repandus*	(Rivière et al., 2010)

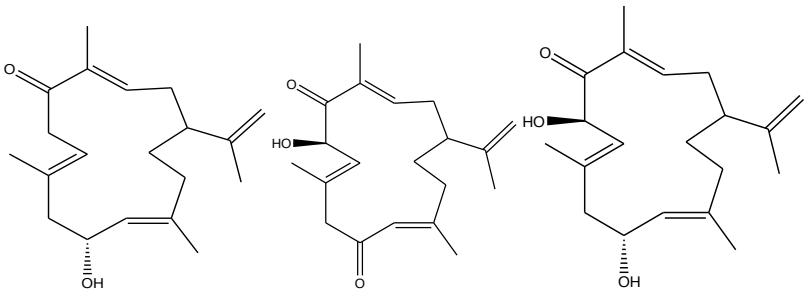

[1] [2] [3]

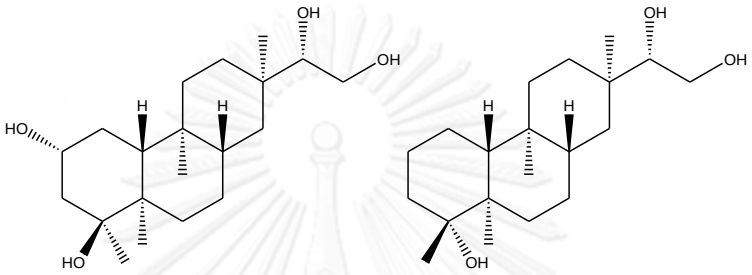

[4] [5]

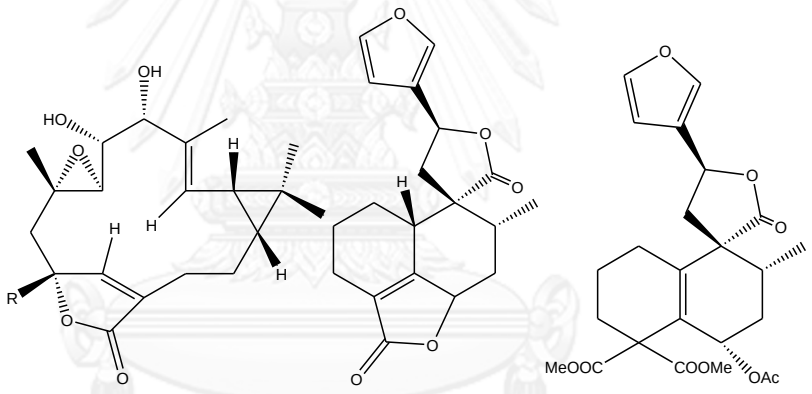

[6] R = OH

[7] R = H

[8] R = OEt

[9] [10]

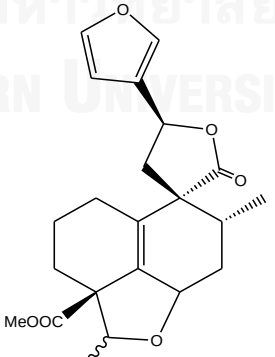

[11] R = *β*-OH

[12] R = *α*-OH

Figure 2 Diterpenoids from *Mallotus* species

1.2 Cardenolides

Cadenolides of the *Mallotus* can be classified into 2 groups: (1) the cardenolides with a sugar unit attached to C-3 [**15**-**17, 20 and 22**], which may be called cardiac glycosides, and (2) the cardenolides without a sugar part [**13, 14, 18**-**19 and 21**]. The sugar units have been found to be glucose or rhamnose (Table 3 and Figure 3).

Table 3 Distribution of cardenolides in *Mallotus* species

Name	Plant	References
5-Desarogenin [**13**] Mallogenin [**14**] Malloside [**15**] Panoside [**16**] Glucopanoside [**17**] Uzarigenin [**18**]	*M. paniculatus*	(Rivière et al., 2010)
Coroglaucigenin [**19**]	*M. paniculatus* *M. philippensis*	
Coroglaucigenin L-rhamnoside [**20**] Corotoxigenin [**21**] Corotoxigenin L-rhamnoside [**22**]	*M. philippensis*	

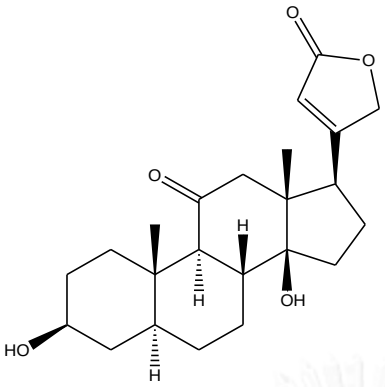

[**13**]

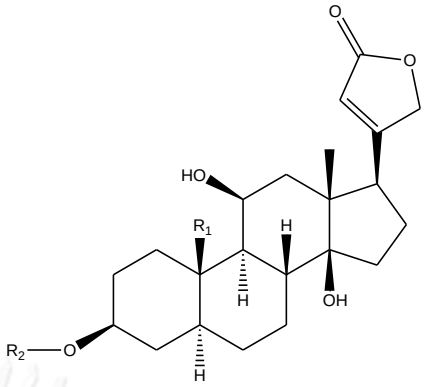

[**14**] R_1 = Me R_2 = H

[**15**] R_1 = Me R_2 = L-Rha

[**16**] R_1 = CH_2OH R_2 = L-Rha

[**17**] R_1 = CH_2OH R_2 = Glc

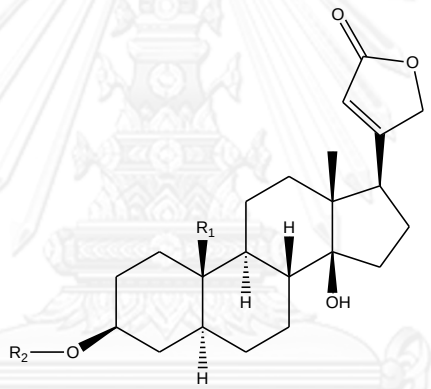

[**18**] R_1 = Me R_2 = H

[**19**] R_1 = CH_2OH R_2 = H

[**20**] R_1 = CH_2OH R_2 = L-Rha

[**21**] R_1 = CHO R_2 = H

[**22**] R_1 = CHO R_2 = L-Rha

Figure 3 Cardenolides from *Mallotus* species

1.3 Triterpenoids

Triterpenoids are chemical constituents widely found this genus. Several triterpenoids [**23**-**29**] are classified as lupane-type. Some of them are identified as friedelane [**30**-**35**], gennacrane [**36**-**38** and **40**], and oleanane [**39** and **41**] types. A large number of them [**42**-**54**] belong to the ursane-type (Table 4 and Figure 4).

Table 4 Distribution of triterpenoids in *Mallotus* species

Name	Plant	References
Hennadiol [**23**] 3***β***,29-Dihydroxylupane [**24**] 3***α***-Hydroxyhop-22(29)-ene or malloapelta A [**25**]	*M. apelta*	(Kiem et al., 2004) (Rivière et al., 2010)
29-Nor-21***α***H-hopan-3,22-dione [**26**]	*M. paniculatus*	(Wai-Haan and Man-Moon, 1976)
Betulin-3-acetate [**27**] Lupeol-3-acetate [**28**]	*M. philippensis*	(Bandopadhyay et al., 1972)
Lupeol [**29**]	*M. philippensis* *M. repandus*	(Bandopadhyay et al., 1972) (Wai-Haan and Man-Moon, 1976) (Wai-Haan and Man-Moon, 1977)
Friedelin [**30**]	*M. apelta* *M. hookerianus* *M. paniculatus* *M. philippensis* *M. repandus*	(Kiem et al., 2004) (Wai-Haan and Man-Moon, 1976) (Hui et al., 1969) (Nair and Madhusudana Rao, 1993) (Wai-Haan and Man-Moon, 1977)
Friedelinol or friedelin-3***α***-ol or friedelanol [**31**]	*M. apelta* *M. metcalfianus*	(Kiem et al., 2004) (Rivière et al., 2009)

Table 4 Distribution of triterpenoids in *Mallotus* species (continued)

Name	Plant	References
Epifriedelinol or friedelin-3***β***-ol or epifriedelanol [**32**]	*M. apelta* *M. hookerianus* *M. paniculatus*	(Kiem et al., 2004) (Wai-Haan and Man-Moon, 1976) (Hui et al., 1969)
3-Oxo-D:A-friedo-oleanan-27,16***α***-lactone [**33**] 3***α***-Benzoyloxy-D:A-friedo-oleanan-27,16***α***-lactone [**34**] 3***β***-Hydroxy-D:A-friedo-oleanan-27,16***α***-lactone [**35**]	*M. repandus*	(Sutthivaiyakit et al., 2001)
Taraxerone [**36**], Tarexerol [**37**], Epitaraxerol [**38**] and Erythrodiol-3-acetate [**39**]	*M. apelta*	(Kiem et al., 2004) (Rivière et al., 2010)
Acetylaleuritolic acid or aleuritolic acid acetate [**40**]	*M. apelta* *M. philippensis*	(Rivière et al., 2010) (Bandopadhyay et al., 1972)
3***β***-Acetoxy-22***β***-hydroxyolean-18-ene [**41**]	*M. philippensis*	(Nair and Madhusudana Rao, 1993)
α-Amyrin [**42**]	*M. philippensis* *M. repandus*	(Bandopadhyay et al., 1972) (Wai-Haan and Man-Moon, 1977)
Ursolic acid [**43**]	*M. apelta* *M. peltatus* *M. repandus*	(Rivière et al., 2010) (Chattopadhyay et al., 2002); (Chattopadhyay et al., 2003) (Wai-Haan and Man-Moon, 1977); (Huang et al., 1999)

Table 4 Distribution of triterpenoids in *Mallotus* species (continued)

Name	Plant	References
Ursolic acid acetate [**44**] 12-Ursen-3-one [**45**] 3-Hydroxy-12-ursen [**46**]	*M. apelta*	(Rivière et al., 2010)
3-Oxours-12-ene-27,28-dioic acid [**47**] 3*β*,28-Dihydroxyurs-12-en-27-oic acid [**48**]	*M. hookerianus*	(Wai-Haan and Man-Moon, 1976)
3*α*-Hydroxy-13*α*-ursan-28,12*β*-olide [**49**]	*M. repandus*	(Wai-Haan and Man-Moon, 1977)
3*α*-Hydroxy-13*α*-ursan-28,12*β*-olide 3-benzoate [**50**]		(Huang et al., 1999)
3*β*-Hydroxy-13*α*-ursan-28,12*β*-olide [**51**] 3*β*-Hydroxy-13α-ursan-28,12*β*-olide 3-benzoate [**52**]		(Wai-Haan and Man-Moon, 1977)
3α-Hydroxy-13*α*-ursan-28-oic acid [**53**] 3*β*-Hydroxy-28*β*-methoxy-13*α*-ursan-28,12*β*-epoxide 3-benzoate [**54**]		(Huang et al., 1999)

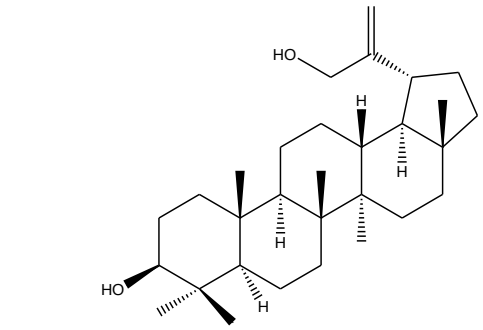

[23]

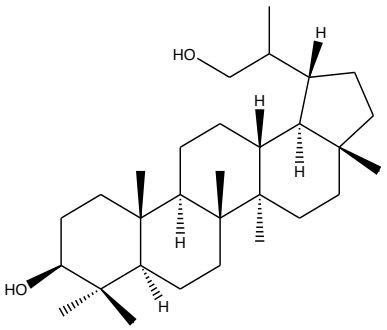

[24]

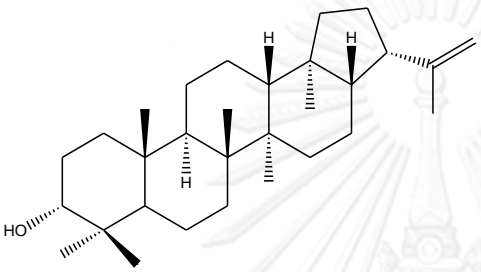

[25]

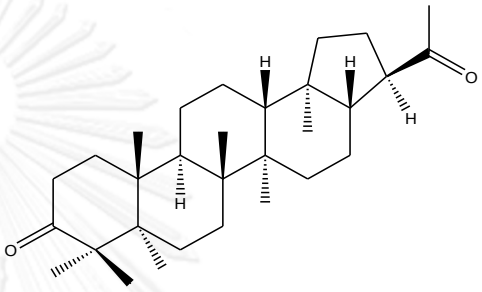

[26]

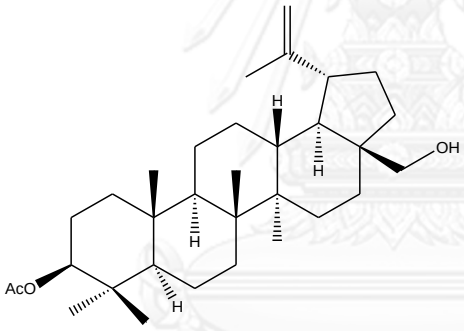

[27]

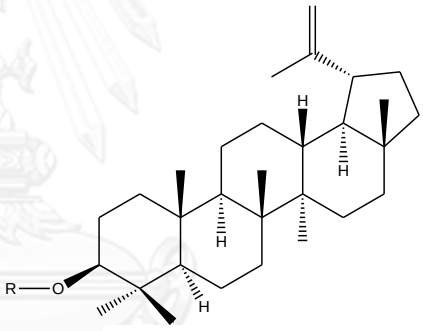

[28] R = Ac

[29] R = H

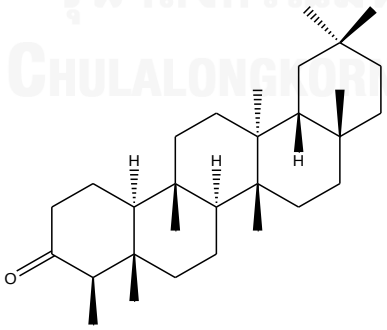

[30]

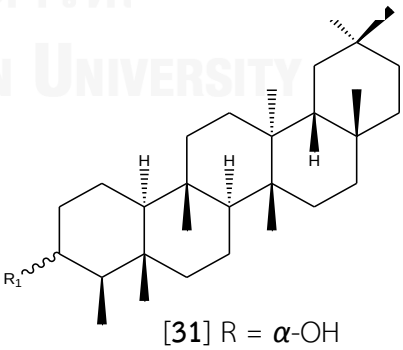

[31] R = α-OH

[32] R = β-OH

Figure 4 Triterpenoids from *Mallotus* species

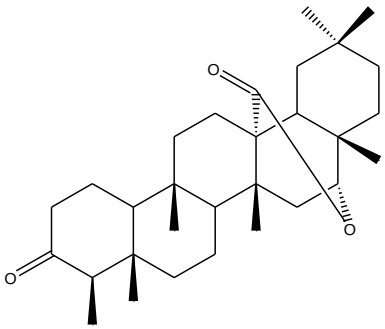

[33]

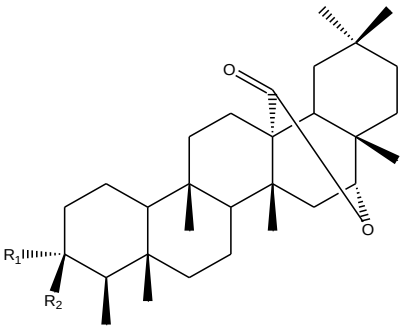

[34] R_1 = O-C(=O)Ph R_2 = H

[35] R_1 = H R_2 = OH

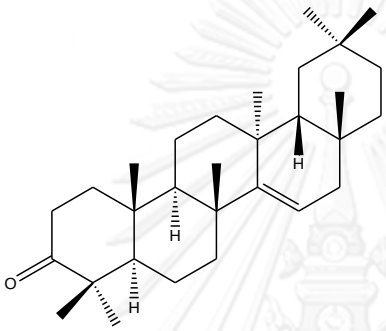

[36]

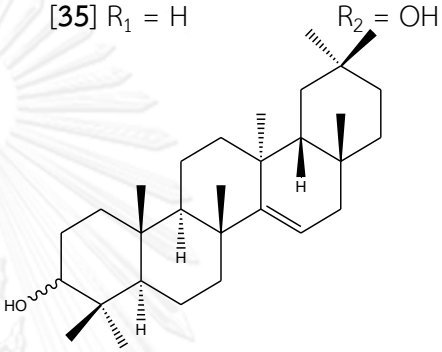

[37] R = *β*-OH

[38] R = *α*-OH

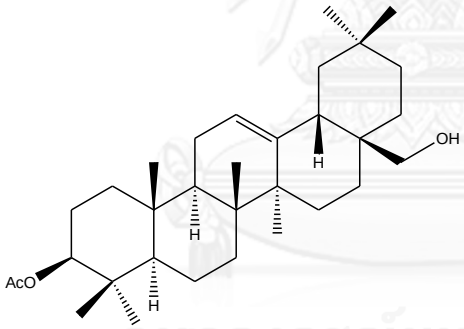

[39]

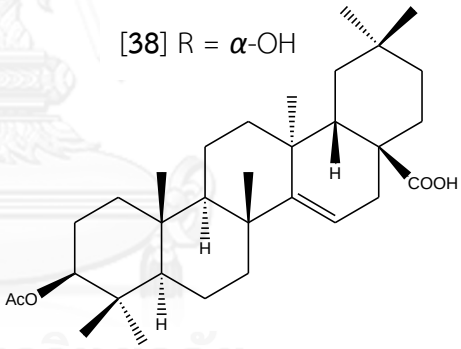

[40]

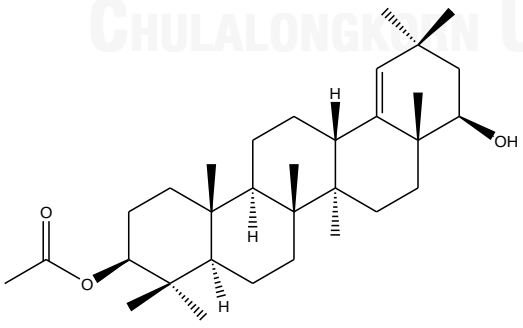

[41]

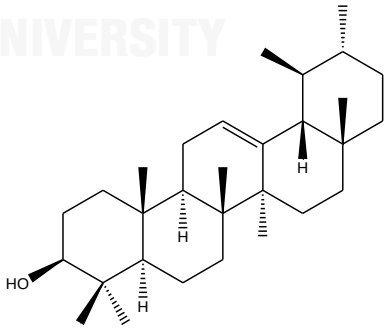

[42]

Figure 4 Triterpenoids from *Mallotus* species (continued)

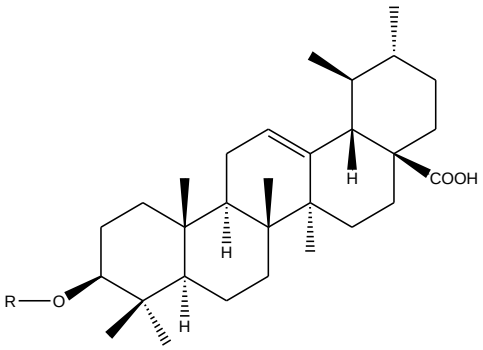

[**43**] R = H

[**44**] R = Ac

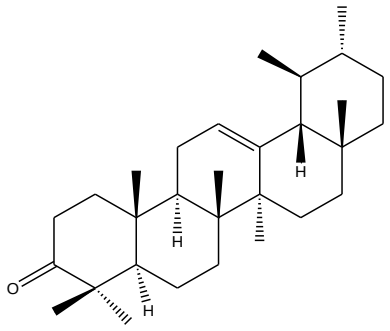

[**45**]

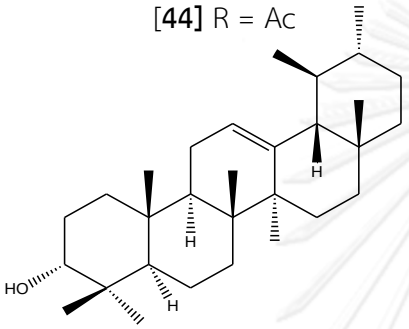

[**46**]

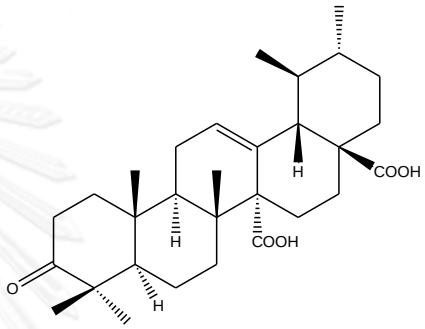

[**47**]

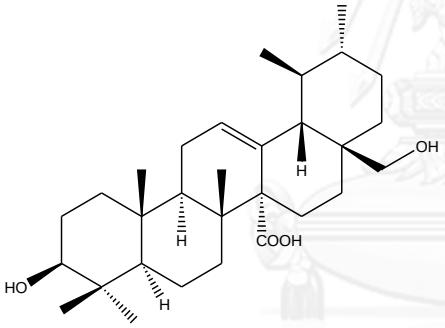

[**48**]

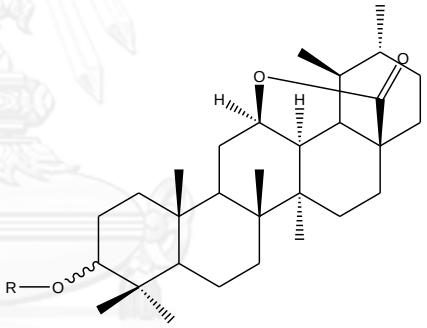

[**49**] R = *α*-H

[**50**] R = *α*-(C=O)Ph

[**51**] R = *β*-H

[**52**] R = *β*-(C=O)Ph

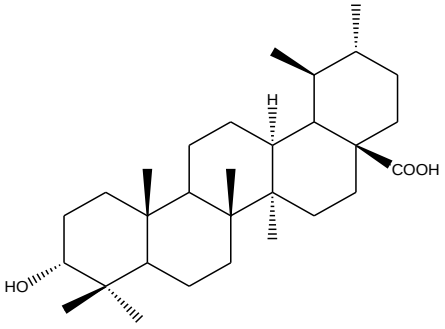

[**53**]

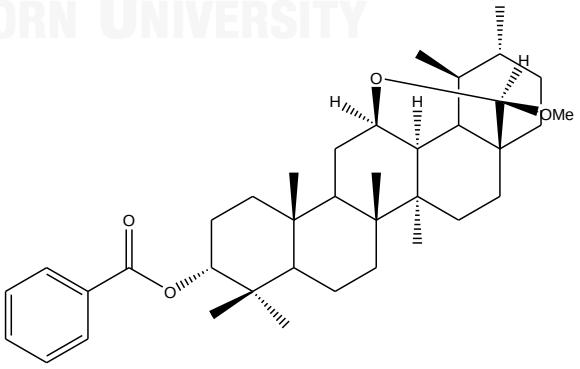

[**54**]

Figure 4 Triterpenoids from *Mallotus* species (continued)

1.4 Steroids

Only a few steroids have been reported from the genus *Mallotus*. *β*-sitosterol [**55**] can be found in several members of this genus (Table 5 and Figure 5).

Table 5 Distribution of steroids in *Mallotus* species

Name	Plant	References
β-sitosterol [**55**]	*M. apelta* *M. hookerianus* *M. paniculatus* *M. peltatus* *M. philippensis*	(Rivière et al., 2010) (Wai-Haan and Man-Moon, 1976) (Hui et al., 1969) (Chattopadhyay et al., 2002); (Chattopadhyay et al., 2003) (Bandopadhyay et al., 1972)
Daucosterol [**56**]	*M. apelta* *M. philippensis*	(Rivière et al., 2010) (Bandopadhyay et al., 1972)
Ergosterol [**57**]	*M. apelta*	(Rivière et al., 2010)
Stigmasterol [**58**]	*M. apelta* *M. paniculatus*	(Rivière et al., 2010) (Hui et al., 1969)

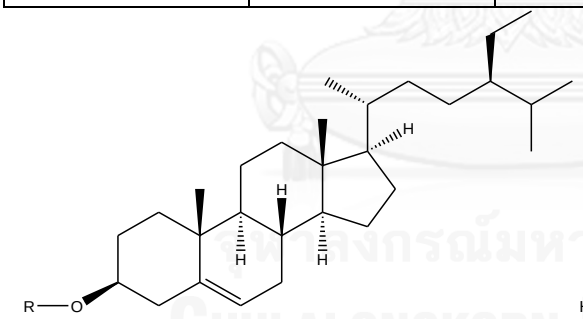

[**55**] R = H

[**56**] R = Glc

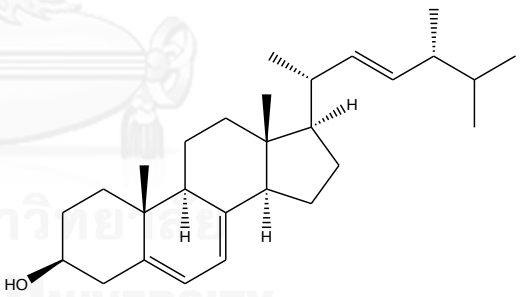

[**57**]

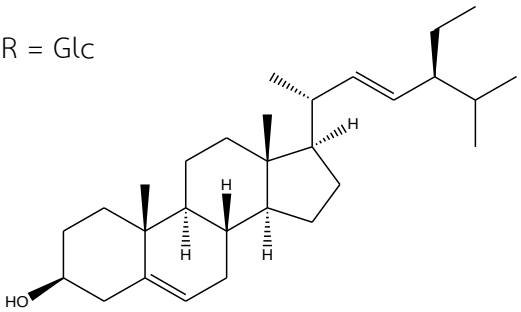

[**58**]

Figure 5 Steroids from *Mallotus* species

1.5 Coumarins

There are 2 types: coumarins [**59-61**] and coumarinolignoids [**62-68**] (Table 6 and Figure 6).

Table 6 Distribution of coumarins in *Mallotus* species

Name	Plant	References
Scopoletin [**59**]	*M. resinosus*	(Ma et al., 2004)
Isoscopoletin [**60**] and Isopimpinellin [**61**]	*M. apelta*	(Rivière et al., 2010)
Cleomiscosin A [**62**] and B [**63**] Malloapelin A [**64**], B [**65**] and C [**66**] 5′-Demethylaquillochin [**67**] Aquillochin [**68**]	*M. apelta*	(Cheng and Chen, 2000) (Xu et al., 2008)

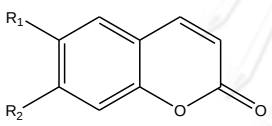

[**59**] R_1 = OMe R_2 = OH

[**60**] R_1 = OH R_2 = OMe

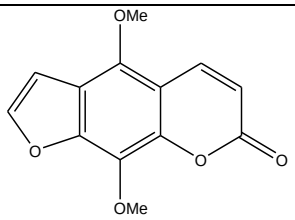

[**61**]

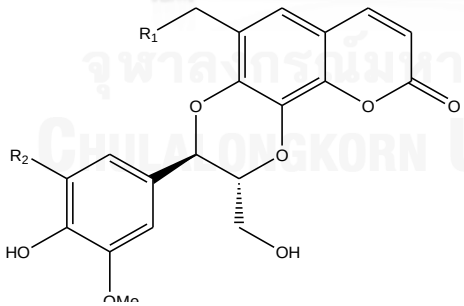

[**62**] R_1 = OMe R_2 = OH

[**63**] R_1 = OMe R_2 = H

[**64**] R_1 = OH R_2 = OH

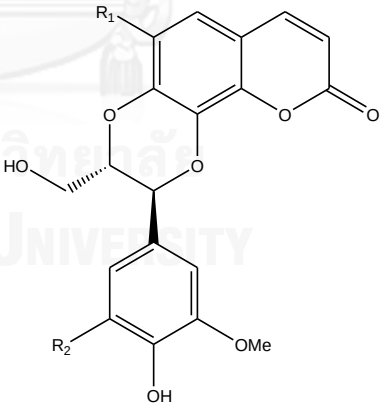

[**65**] R_1 = OH R_2 = OH

[**66**] R_1 = OMe R_2 = OH

[**67**] R_1 = OMe R_2 = H

[**68**] R_1 = OMe R_2 = OMe

Figure 6 Coumarins from *Mallotus* species

1.6 Flavonoids

Flavonoids can be classified into 5 subgroups: flavonol glycosides [**69**-**72**], a flavanonol glycoside [**73**], flavanones [**74 and 75**], flavones [**78 and 80**], flavone glycosides [**76, 77, 79** and **81**] and chalcones [**82**-**86**] (Table 7 and Figure 7).

Table 7 Distribution of favonoids in *Mallotus* species

Name	Plant	References
Quercitrin [**69**] and Astilbin [**75**]	*M. apelta* *M. metcalfianus*	(Rivière et al., 2010) (Rivière et al., 2009)
Kaempferol-3-*O*-***α***-L-rhamnose [**70**] Quercetin-3-*O*-***β***-neohesperoside [**71**] Kaempferol-3-*O*-***β***-neohesperoside [**72**]	*M. metcalfianus*	(Rivière et al., 2009)
Isoallorottlerin [**73**] Isorottlerin [**74**]	*M. philippensis*	(Lounasmaa et al., 1975) (Zaidi et al., 2009)
Luteolin-7-*O*-(4′-*O*-(E)-coumaroyl)-***β***-glucopyranoside [**76**] Chrysoeriol-7-*O*-(4′-*O*-(E)-coumaroyl)-***β***-glucopyranoside [**77**]	*M. metcalfianus*	(Rivière et al., 2009)
Apigenin [**78**] Apigenin-7-*O*-***β***-D-glucoside [**79**] Mallotusin [**80**] and Vicenin II [**81**]	*M. apelta*	(Rivière et al., 2010)
Kamalachalcone A [**82**] and B [**83**] Mallotophilippen C[**84**], D [**85**] and E [**86**]	*M. philippensis*	(Tanaka et al., 1998) (Daikonya et al., 2004)

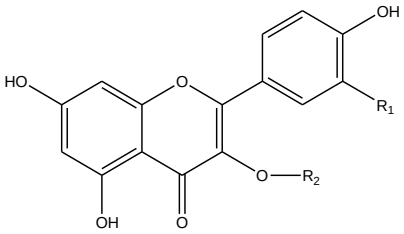

[**69**] R_1 = OH R_2 = Rha [**70**] R_1 = H R_2 = Rha

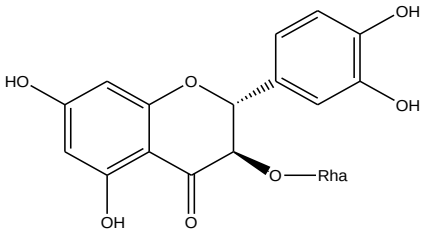

[**73**]

[**71**] R_1 = OH R_2 = Glc-Rha [**72**] R_1 = H R_2 = Glc-Rha

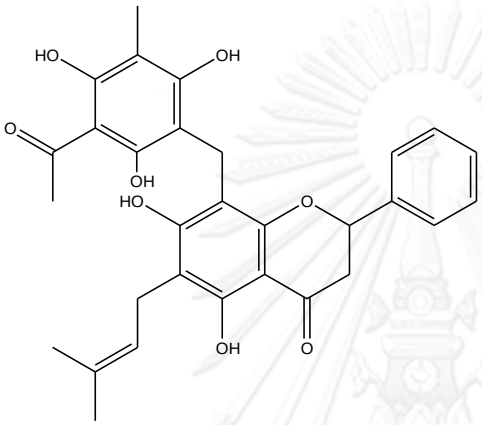

[**74**]

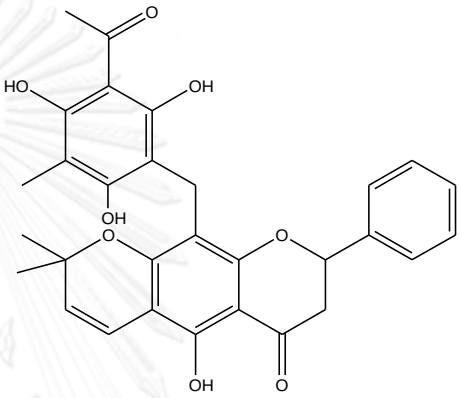

[**75**]

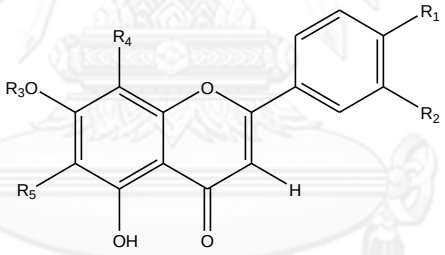

[**76**] R_1 = OH	R_2 = OH	R_3 = Glc-coumaroyl	R_4 = H	R_5 = H
[**77**] R_1 = OH	R_2 = OMe	R_3 = Glc-coumaroyl	R_4 = H	R_5 = H
[**78**] R_1 = OH	R_2 = H	R_3 = H	R_4 = H	R_5 = H
[**79**] R_1 = OH	R_2 = H	R_3 = Glc	R_4 = H	R_5 = H
[**80**] R_1 = H	R_2 = OMe	R_3 = H	R_4 = H	R_5 = CH_2-CH=C(Me)$_2$
[**81**] R_1 = OH	R_2 = H	R_3 = H	R_4 = Glc	R_5 = Glc

Figure 7 Flavonoids from *Mallotus* species

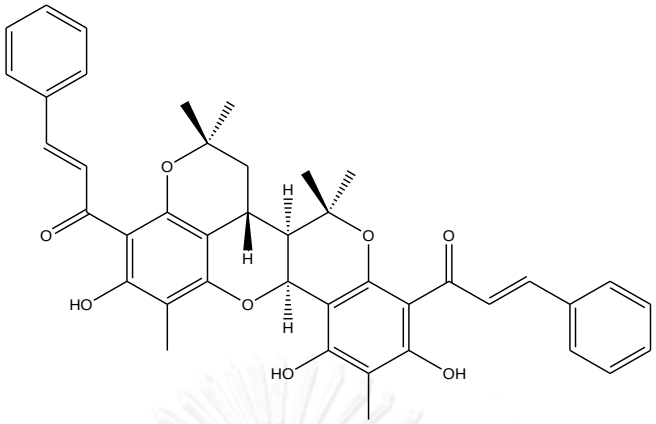

[**82**]

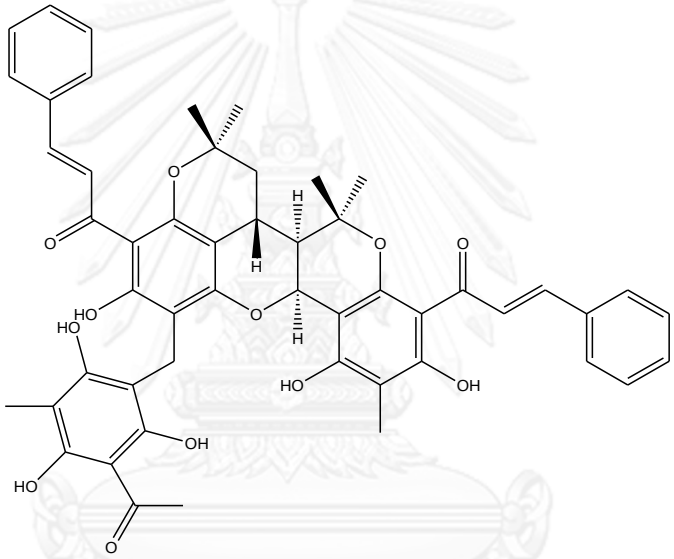

[**83**]

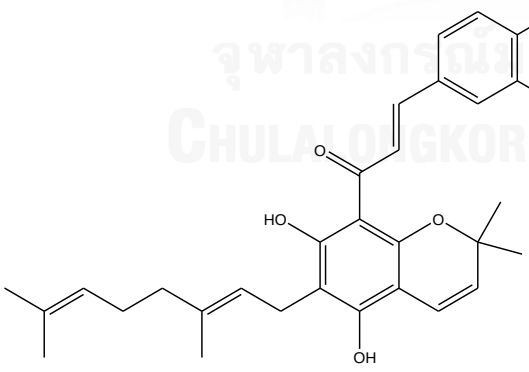

[**84**] R = H

[**85**] R = OH

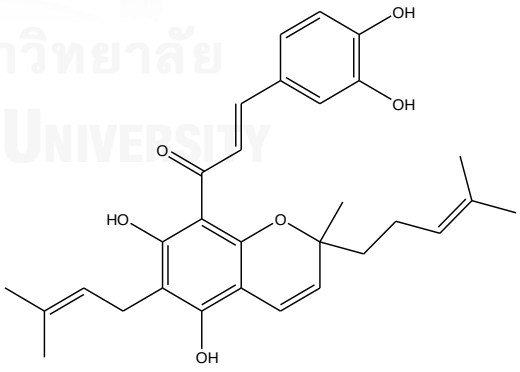

[**86**]

Figure 7 Flavonoids from *Mallotus* species (continued)

1.7 Phloroglucinol derivatives

Several phloroglucinol derivatives have been isolated from *Mallotus* species. Some contain an isoprenyl group [**87**-**88**], whereas the others are also conjugated with a benzopyrone ring [**89**-**92 and 98-100**]. One compound has a phenylpropanoid unit [**93**]. The others are the derivatives of chromones [**94-97** and **101-102**] (Table 8 and Figure 8).

Table 8 Distribution of phloroglucinol derivatives in *Mallotus* species

Name	Plant	References
Pallidusol [**87**], Dehydropallidusol [**88**], Pallidol [**89**], Mallopallidol [**90**] and Homomallopallidol [**91**]	*M. pallidus*	(Supudompol et al., 2004)
Mallopallidusol [**92**]		(Likhitwitayawuid et al., 2005)
Rottlerin [**93**]		(Lounasmaa et al., 1975)
4-Hydroxy-2,6-dimethyl-6-(3,7-dimethyl-2,6-octadienyl)-8-(3-methyl-2-butenyl)-2*H*-1-benzopyran-5,7(3*H*,6*H*)-dione [**94**]	*M. apelta*	(An et al., 2001)
4-Hydroxy-2,6,8-trimethyl-6-(3,7-dimethyl-2,6-octadienyl)-2*H*-1-benzopyran-5,7(3*H*,6*H*)-dione [**95**]		
5-Hydroxy-2,8-dimethyl-6-(3-methyl-2-butenyl)-8-(3,7-dimethyl-2,6-octadienyl)-2*H*-1-benzopyran-4,7(3*H*,8*H*)-dione [**96**]		
5-Hydroxy-2,6,8-trimethyl-8-(3,7-dimethyl-2,6-octadienyl)-2*H*-1-benzopyran-4,7(3*H*,8*H*)-dione [**97**]		
2,3-Dihydro-5,7-dihydroxy-2,6-dimethyl-8-(3-methyl-2-butenyl)-4*H*-1-benzopyran-4-one [**98**]		

Table 8 Distribution of phloroglucinol derivatives in *Mallotus* species (continued)

Name	Plant	References
2,3-Dihydro-5,7-dihydroxy-2,8-dimethyl-6-(3-methyl-2-butenyl)-4*H*-1-benzopyran-4-one [**99**]	*M. apelta*	(An et al., 2001)
2,3-Dihydro-5,7-dihydroxy-2,6,8-trimethyl-4*H*-1-benzopyran-4-one [**100**]		
6-Hydroxy-2,6,8-trimethyl-8-(3,7-dimethyl-2,6-octadienyl)-2*H*-1-benzopyran [**101**]		
6-Hydroxy-2,8-dimethyl-6-(3-methyl-2-butenyl)-8-(3,7-dimethyl-2,6-octadienyl)-2*H*-1-benzopyran-4,5,7(3*H*,6*H*,8*H*)-trione [**102**] 6-Hydroxy-2,8-dimethyl-6-(3-methyl-2-butenyl)-8-(3,7-dimethyl-2,6-octadienyl)-2*H*-1-benzopyran-4,5,7(3*H*,6*H*,8*H*)-trione or malloapelta B [**103**]		
8-(1′-Oxo-3′ (*R*)-hydroxy-butyl)-5,7-dimethoxy-2,2-dimethyl-2*H*-1-benzopyran [**104**]		(Rivière et al., 2010)
8-(Acetic acid 1′-oxo-3′ (*R*)-hydroxy-butyl ester)-5,7-dimethoxy-2,2-dimethyl-2*H*-1-benzopyran [**105**]		
6-(1′-Oxo-2′-en-butyl)-5,7-dimethoxy-2,2-dimethyl-2*H*-1-benzopyran [**106**]		
6-(1′-Oxo-3′ (*R*)-hydroxy-butyl)-5,7-dimethoxy-2,2-dimethyl-2*H*-1-benzopyran [**107**]		(Kiem et al., 2005)
6-(1′-Oxo-3′ (*R*)-methoxy-butyl)-5,7-dimethoxy-2,2-dimethyl-2*H*-1-benzopyran [**108**]		

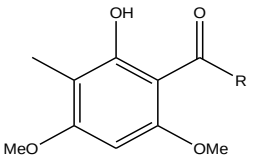

[**87**] R = Bu-i [**88**] R = CH=C(Me)$_2$

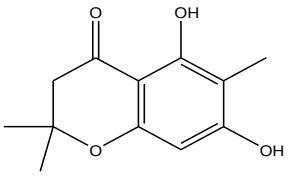

[**89**]

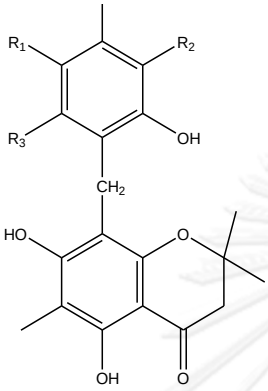

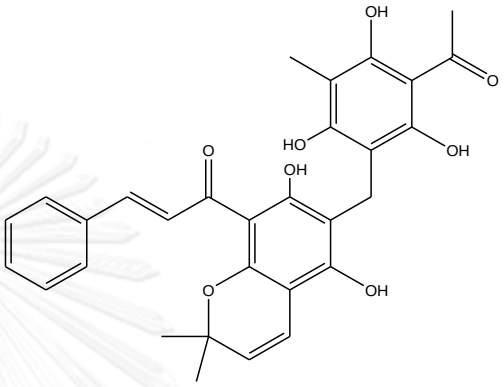

[**90**] R_1 = Me R_2 = C(=O)-Pr-i R_3 = OMe

[**91**] R_1 = Me R_2 = C(=O)-CH(Me)Et R_3 = OMe

[**92**] R_1 = C(=O)-Pr-i R_2 = Me R_3 = OH

[**93**]

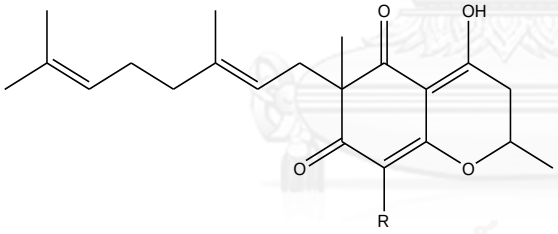

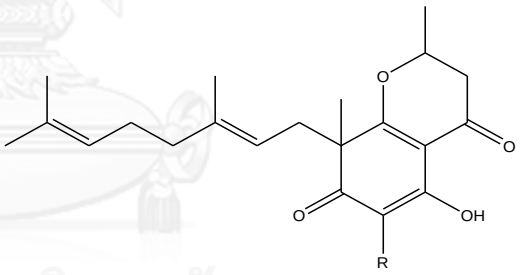

[**94**] R = CH_2-CH=C(Me)$_2$ [**96**] R = CH_2-CH=C(Me)$_2$

[**95**] R = Me [**97**] R = Me

Figure 8 Phloroglucinol derivatives from *Mallotus* species

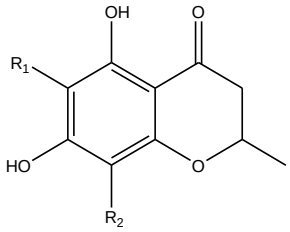

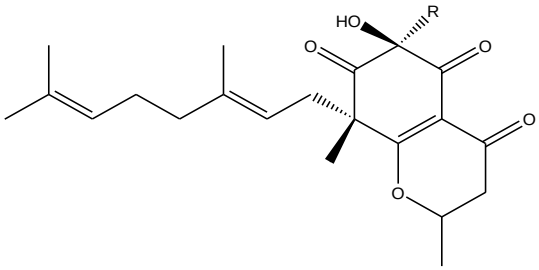

[**98**] R_1 = Me R_2 = CH_2-CH=C(Me)$_2$

[**99**] R_1 = CH_2-CH=C(Me)$_2$ R_2 = Me

[**100**] R_1 = Me R_2 = Me

[**101**] R = Me

[**102**] R = CH_2-CH=C(Me)$_2$

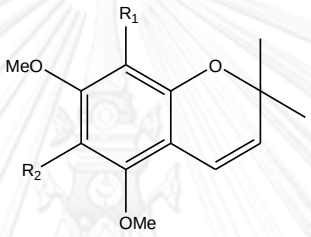

[**103**] R_1 = CO-CH=CH-CH_3 R_2 = H

[**104**] R_1 = CO-CH_2CH(CH_3)OH R_2 = H

[**105**] R_1 = CO-CH_2CH(CH_3)OAc R_2 = H

[**106**] R_1 = H R_2 = CO-CH=CH-CH_3

[**107**] R_1 = H R_2 = CO-CH_2CH(CH_3)OH

[**108**] R_1 = H R_2 = CO-CH_2CH(CH_3)OCH_3

Figure 8 Phloroglucinol derivatives from *Mallotus* species (continued)

1.8 Tannins and gallic acid derivatives

Tannins [**109, 110** and **112-120**] and gallic acid derivatives [**111, 121, 122** and **123**] are common chemical constituents of the genus *Mallotus*. So far, all of the tannins reported from *Mallotus* species are hydrolysable tannins because they contain glucose as the core structure connected with several units of gallic acid (Table 9 and Figure 9).

Table 9 Distribution of tannins and gallic acid derivatives in *Mallotus* species

Name	Plant	References
Corilagin [**109**] Mallotinic acid [**110**] Brevifolin carboxylic acid [**111**] Repandusinin [**112**] Repandusinic acid A [**113**] and B [**114**] Mallotinin [**115**] Punicafolin [**116**] Eugeniin [**117**] Furosin [**118**] Geraniin [**119**] Mallotusinic acid [**120**] Glucogallin [**121**]	*M. repandus*	(Saijo et al., 1989)
4,5,4′-Trimethyl-ellagic acid [**122**]	*M. apelta*	(Cheng et al., 1998)
Bergenin [**123**]	*M. philippensis* *M. repandus* *M. roxburghianus* *M. anisopodus*	(Bandopadhyay et al., 1972) (Huang et al., 1999) (Tomizawa et al., 1976) (Rana et al., 2005) (Van Minh et al., 2009)

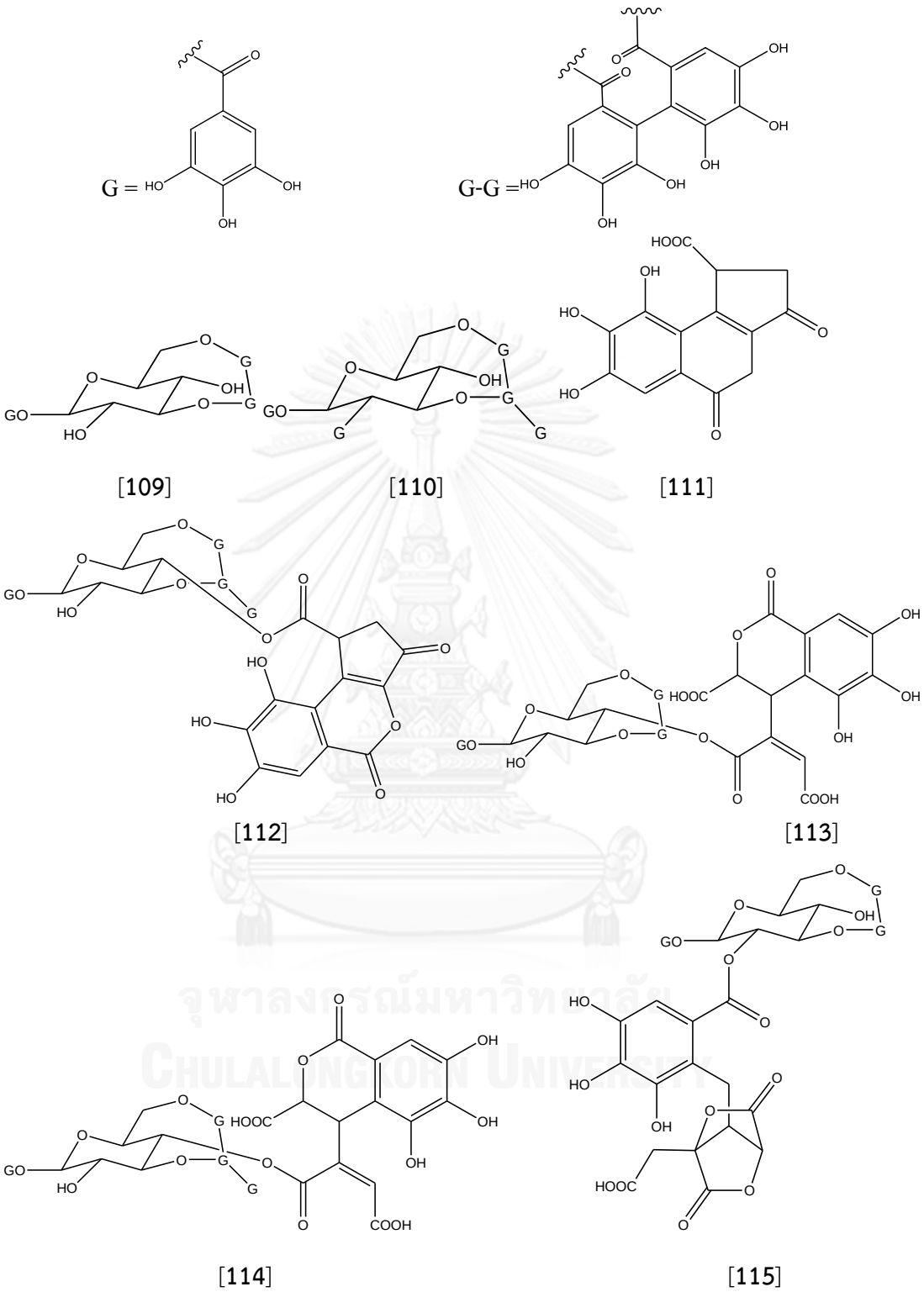

Figure 9 Tannins and gallic acid derivatives from *Mallotus* species

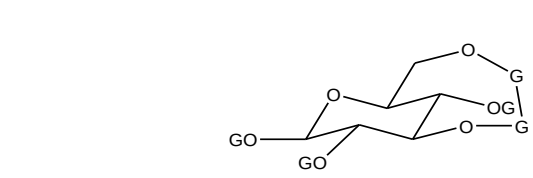

[116]

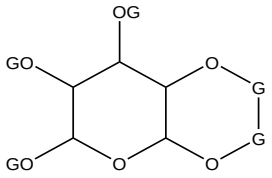

[117]

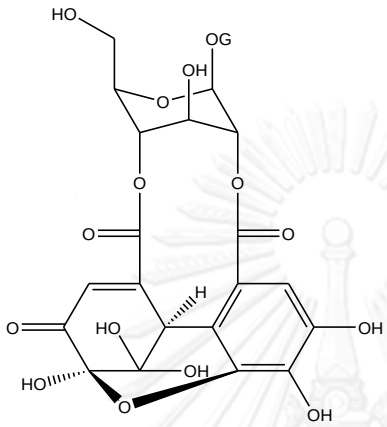

[118]

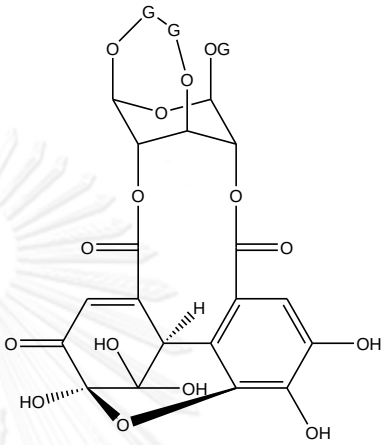

[119]

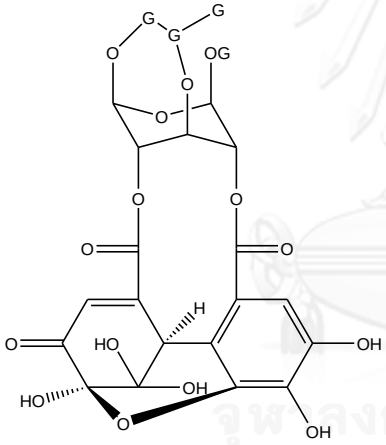

[120]

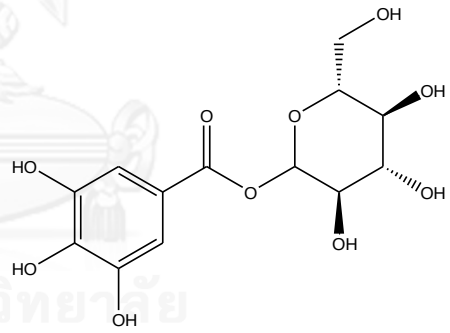

[121]

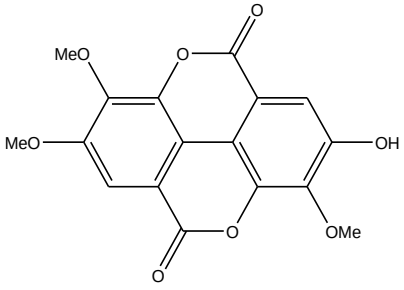

[122]

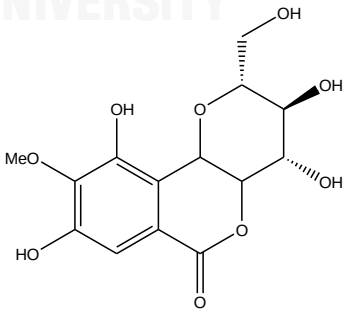

[123]

Figure 9 Tannins and gallic acid derivatives from *Mallotus* species (continued)

1.10 Miscellaneous compounds

Other secondary metabolites have been repoted, for example, a chromone [**124**], a phenylpropranoid [**125**], an anthraquinone [**126**], an iridoid [**127**], tocopherol [**128**], megasigmane glucoside [**129**], a long chain alcohol [**130**], benzoic acid glucosides [**131** and **138**], an amide [**132**], pyridine derivatives [**133** and **134**], a cyano-**γ**-pyridone [**135**], megastigmane sulphonoglucosides [**136** and **137**] (Table 10 and Figure 10).

Table 10 Distribution of miscellaneous compounds in *Mallotus* species

Name	Plant	References
6-Methoxy-benzopyran-4-one [**124**]	*M. apelta*	(Rivière et al., 2010)
Ferulic acid [**125**]	*M. metcalfianus*	(Rivière et al., 2009)
Chrysophanol [**126**]	*M. apelta*	(Rivière et al., 2010)
Mussaenoide [**127**]		
α-Tocopherol [**128**]	*M. apelta* *M. anisopodus*	(Rivière et al., 2010) (Van Minh et al., 2009)
Blumenol-*C*-glucoside [**129**] Methyl-2-*O*-**β**-D-glucopyranosylbenzoate [**130**]	*M. metcalfianus*	(Rivière et al., 2009)
Trans-2-carboxy-4-hydroxytetrahydrofuran-N,N-dimethylamide [**131**]	*M. cuneatus*	(Rivière et al., 2010)
n-Hexacosanol [**132**]	*M. metcalfianus*	(Rivière et al., 2009)
Nicotinic acid [**133**] and 4-Methoxy-3-cyano-pyridine 1-oxide (malloapeltine) [**134**]	*M. apelta*	(Rivière et al., 2010) (Cheng et al., 1998)
Mallorepine [**135**]	*M. repandus*	(Hikino et al., 1978)
Anisoposide A [**136**] and B [**137**] Junipetrioloside A [**138**]	*M. anisopodus*	(Van Minh et al., 2009)

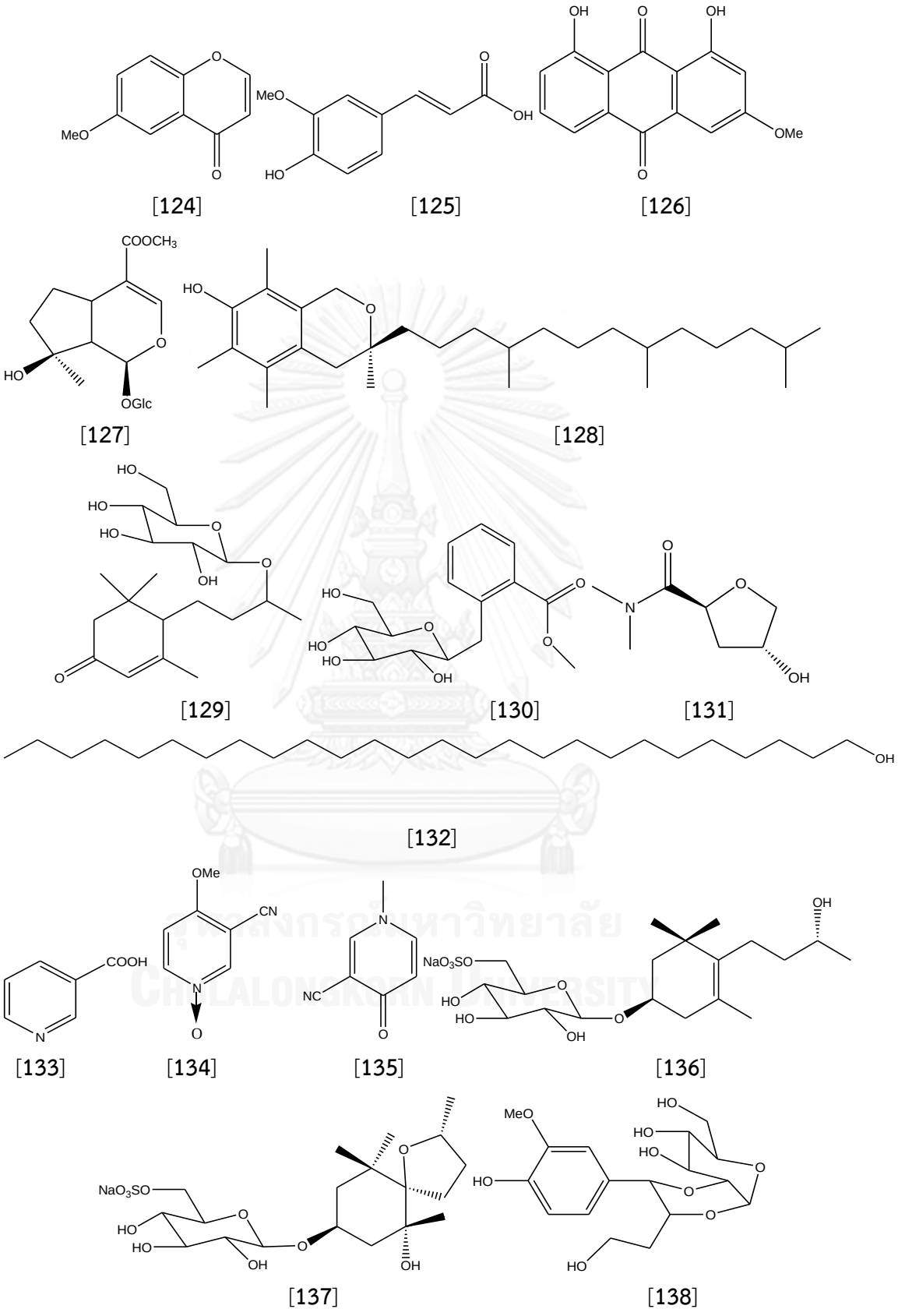

Figure 10 Miscellaneous compounds from *Mallotus* species

2. Biological activities of *Mallotus* species

2.1 Anti-inflammatory activity

A number of studies have revealed anti-inflammatory activity in some *Mallotus* species. The MeOH and BuOH extracts of *M. peltatus* leaves showed activity against carrageenan-induced (acute model) and dextran-induced (subacute model) rat paw edema and cotton pellet-induced granuloma formation in rats (chronic model), using indomethacin as the positive control. In both models, the MeOH extract at 200 and 400 mg/kg, and fractions A and B of the BuOH extract at 25 mg/kg showed significant activity in Albino rats (Chattopadhyay et al., 2002). The phytochemical investigation of both extracts showed that ursolic acid [**43**], *β*-sitosterol [**55**] and some fatty acids were responsible for their anti-inflammatory activities (Chattopadhyay et al., 2002). In addition, the MeOH extract of *M. peltatus* leaves from Bay islands showed similar results (Chattopadhyay et al., 2006). Three chalcones, mallotophilippens C [**84**, D [**85**] and E [**86**] isolated from fruits of *M. philippensis*, exhibited anti-inflammatory and immunomodulatory activities by inhibiting nitric oxide (NO) production and inducible NO synthase (iNOS) gene expression. They also downregulated cycloxygenase-2 gene, interleukin-6 gene and interleukin-1*β* gene expression (Daikonya et al., 2004). Similarly, the $CHCl_3$ extract of *M. scodocarpus* roots exhibited anti-inflammatory activities against ethyl phenylpropriolate (EPP)-induced ear edema, carrageenin-induced and arachidonic acid-induced hind paw edema (acute pain) and cotton pellet-induced granuloma formation in rats (chronic model) (Intahphuak et al., 2004).

2.2 Antifertility activity

The seed extract of *M. philippensis* exhibited antifertility activity on female rats (Thakur et al., 2005). It reduced serum FSH and LH levels, probably by affecting hypothalamic/pituitary axis. By reducing the levels of FSH and LH and estradiol, it affected the follicular development, quality of ovulated eggs, corpora lutea formation, estrus cycle establishment and maintenance of pregnancy in rats (Thakur

et al., 2005;Rivière et al., 2010). A subsequent chemical investigation showed that rottlerin [**93**] and acetylrottlerin, which were phloroglucinol derivatives, were responsible for this activity (Rivière et al., 2010).

2.3 Antimicrobial activity

Many compounds from the genus *Mallotus* exhibited antimicrobial activity. A benzopyran derivative [**108**] from *M. apelta* showed moderate antimicrobial activity against *Micrococcus lutens* (MIC of 7.34 µg/ml) as compared with the positive control tricolsan (An et al., 2001). Three triterpenoids, erythrodiol-3-acetate [**39**], 3*β*,29-dihydroxylupane [**24**] and ursolic acid acetate [**44**], and the steroid *β*-sitosterol [**55**] from *M. apelta* roots, exhibited bacteriostatic activities on some microbial pathogens including *Staphylococcus aureus*, *Bacillus subtilis*, *Escherichia coli* and *Bacillus pyocyaneum* (Rivière et al., 2010). In the screening of 61 Indian medicinal plants for their antimicrobial activities, an extract from the glandular hairs of *M. philippensis* fruit demonstrated antimicrobial activity against *Bacillus cereus* var mycoides (ATCC 11778), *Bacillus pumilus* (ATCC 14884), *B. subtilis* (ATCC 6633), *Bordetella bronchiseptica* (ATCC 4617), *M. luteus* (ATCC 9341), *S. aureus* (ATCC 29737), *Staphylococcus epidermidis* (ATCC 12228), *Klebsiella pneumoniae* (ATCC 10031) and *Streptococcus faecalis* (MTCC 8043) (Kumar et al., 2006). In addition, the *M. philippensis* bark extract had antibacterial activity against *E. coli*, *K. pneumoniae*, *P. aeruginosa*, *Salmonella typhi* and *B. subtilis* (Moorty et al., 2007). The EtOH extract of *M. philippensis* leaves showed potent bactericidal activity with minimum bactericidal concentrations (MBC) of 15.6-31.2 mg/L against 8 strains of *Helicobacter pylori*. The subsequent phytochemical investigation of this plant showed that rottlerin [**93**] possessed the most potent bactericidal activity (3.12-6.25 mg/L) against several types of *H. pylori* isolates, including Japanese and Pakistani strains, as well as clarithromycin-resistant and metronidazole-resistant strains (Zaidi et al., 2009).

2.4 Antioxidant and antiradical activities

Several studies have shown antioxidant and antiradical activities of *Mallotus* plants. The EtOAc and aqueous (50% MeOH) fractions obtained from *M. metcalfianus* bark possessed antiradical activity against DPPH free radicals. It could be concluded that tannins were responsible for their antiradical activity because the reduction of the activity was observed after elimination of the tannins. In addition, the flavonoids quercitrin [**69**], kaempferol 3-*O*-***α***-L-rhamnoside [**70**], and quercetin 3-*O*-***β***-neohesperidoside [**71**] were also isolated and showed antiradical activity (Rivière et al., 2009). The extracts from the fruit and bark of *M. philippensis* exhibited activity against DPPH (Afran et al., 2007). In another study, the extracts of roots and stems of *M. repandus* were evaluated for superoxide and hydroxyl scavenging activities. The result showed that the EtOAc fraction of the roots possessed the most potent superoxide-scavenging activity, and the hexane fraction of stems and roots showed the greatest hydroxyl-scavenging activity. (Lin et al., 1995)

2.5 Antiulcerogenic activity

A MeOH extract of *M. repandus* was found to have antiulcerogenic activity in mice. A bioassay-guide separation of this extract showed that bergenin [**123**] was the active principle, inhibiting the stress induced gastric ulcers formation (Hikino et al., 1978).

2.6 Antiviral activity

Some *Mallotus* species contain chemical constituents that possessed antiviral activity. *M. apelta* extract was found to weakly inhibit the reverse transcriptase of Rauscher leukemia virus (RLV) (IC_{50} 0.4-0.5 μg/mL). The Investigation for the mode of action disclosed that this extract was competitive with respect to the template-primer [poly (rA)-oligo(dT)] and noncompetitive with respect to dTTP substrate (Ono et al., 1989). Furthermore, the chemical constituents of *M. apelta* were tested for their antiviral activity against Human immunodeficiency virus (HIV). The result showed that the coumarinolignoid cerebroside was the most active compound. The root

extract of the same plant could also inhibit the duplication of duck hepatitis B virus (D-HBV) *in vivo* (Rivière et al., 2010). Five isolated compounds of *M. pallidus* were evaluated for the inhibitory activity against human immunodeficiency virus-1 (HIV-1) and herpes simplex virus (HSV-1 and HSV-2). All of them were characterized as phloroglucinol derivatives. Three of them, pallidol [**89**], mallopallidol [**90**] and homomallopallidol [**91**], were active. However, mallopallidol and homomallopallidol also showed cytotoxic effect against Vero cells and PMB cells. From the result of structure-activity relationship (SAR) study, it was suggested that the bis-hydroxy-phenyl structure was necessary for the antiviral activity (Likhitwitayawuid et al., 2005).

2.7 Cytotoxic and antitumor activities

Two phloroglucinol derivatives [**107** and **108**] isolated from *M. apelta* leaves possessed cytotoxic activity. Compound [**107**] showed strong cytotoxic activity against two types of human cancer cell line, human hepatocellular carcinoma (Hep-2, IC_{50} = 0.49 µg/mL) and rhabdosarcoma (RD, IC_{50} = 0.54 µg/mL). Compound [**108**] exhibited moderate activity against the Hep-2 cell line (IC_{50} = 4.22 µg/mL) (Kiem et al., 2005). Moreover, another study reported that malloapelta B [**103**], isolated from *M. apelta*, was cytotoxic against three human cancer cell lines, KB (human epidermoid carcinoma), FL (fibrillary sarcoma of the uterus) and Hep-2 (Rivière et al., 2010). In addition, scopoletin [**59**] from the root of *M. resinosus* was responsible for DNA strand cleavage activity of its root extract (Ma et al., 2004). This result showed that scopoletin could be used as an antitumor agent.

2.8 Hepatoprotective activity

Some studies have revealed the hepatoprotective activity of *Mallotus* species. It was reported that root extract of *M. apelta* could reduce the progression of liver fibrosis (Rivière et al., 2010). In addition, a coumarinolignoid isolated from *M. apelta*, malloapelin C [**66**], possessed protective effect against D-galactosamine-induced hepatotoxicity in WB-F344 rat hepatic epithelial stem-like cells (Xu et al., 2008). The rhizome extract of *M. repandus* could also inhibit liver toxicity induced by

toxic agents such as carbon tetrachloride and D-galactosamine with more than 50% inhibition (Yang et al., 1987).

CHAPTER III

EXPERIMENTAL

1. Source of plant materials

The stem bark of *Mallotus plicatus* was collected from the botanical garden of Faculty of Pharmaceutical Sciences, Chulalongkorn University, Bangkok, Thailand. Botanical identification was done by Professor Dr. Thawatchai Santisuk through comparison of the specimens with authentic samples (BKF No. 139376) at the Department of National Park, Wildlife and Plant Conservation, Ministry of Natural Resources and Environment. The voucher specimens of the plant have been deposited at the herbarium of Faculty of Pharmaceutical Sciences, Chulalongkorn University.

2. General techniques

2.1 Solvents

All organic solvents used in this work were of commercial grade and were redistilled before use.

2.2 Analytical thin-layer chromatography

Technique:	One dimension, ascending
Adsorbent:	Silica gel 60 F_{254} (E. MERCK) pre-coated plates
	Silica gel 60 RP-18 F_{254} (E. MERCK) pre-coated plates
Layer thickness:	0.2 mm
Distance:	5.0 cm
Temperature:	Room temperature (30-35 °C)
Detection:	1. Ultraviolet light (254 and 365 nm)
	2. 10% Sulfuric acid and heating at 130 °C for 5 minutes

2.3 Preparative thin-layer chromatography

Technique:	One dimension, ascending

Adsorbent: Silica gel 60 F_{254} (E. MERCK) pre-coated plates

Layer thickness: 0.2 mm

Sample loading: The sample was dissolved in a small volume of organic solvent, and then applied on the surface of the TLC plate.

Detection: All fractions collected from preparative TLC were examined by TLC as described in section 2.2

2.4 Column chromatography

2.4.1 Conventional column chromatography

Gel filter: Silica gel 60 number 9385 (particle size 0.040-0.063 mm) and number 7734 (particle size 0.063-0.200 mm) (E. Merck)

Packing method: Wet packing: The adsorbent was mixed with an organic solvent to form a slurry and poured into a column, and then left for settlement.

Dry packing: The adsorbent was packed in the column, and then the eluent was poured into the column.

Sample loading: The sample was dissolved in a small volume of organic solvent, and then applied on top of the column.

Detection: All fractions collected from column chromatography were examined by TLC as described in section 2.2

2.4.2 Preparative reverse phase high performance liquid chromatography

Adsorbent: Shim Pack preparative octadecylsilane (ODS) column No. 2025820 (Shimadzu)

Sample loading: The sample was dissolved in a small volume of the mobile phase and then loaded into the injection port using a syringe.

Detection: All eluates collected from the HPLC column were examined using an SPP-10A Shimadzu UV-VIS detector at the wavelength 254 nm and by TLC as described in section 2.2.

2.4.3 MCI gel chromatography

Gel filter: MCI gel CHP 20P Lot: 40058 (Supelco analytical)

Sample loading: The same as conventional column chromatography

Detection: All fractions collected from column chromatography were examined by TLC as described in section 2.2.

2.5 Spectroscopy

2.5.1 Ultraviolet (UV) spectra

UV spectra were obtained on a Shimadzu UV-160A spectrophotometer (Pharmaceutical Research Instrument Center, Faculty of Pharmaceutical Sciences, Chulalongkorn University)

2.5.2 Infrared (IR) spectra

IR spectra (KBr disc) were recorded on a Perkin Elmer FT-IR 1760X spectrometer (Scientific and Technological Research Equipment Center, Chulalongkorn University)

2.5.3 Mass spectra

Electrospray Ionization (ESI) mass spectra were obtained on a Bruker microOTOF mass spectrometer (National Center for Genetic Engineering and Biotechnology, BIOTEC, Thailand and the Department of Chemistry, Faculty of Science, Mahidol University)

2.5.4 Proton and carbon-13 nuclear magnetic resonance (^{1}H and ^{13}C) spectra

^{1}H (300 MHz) and ^{13}C (75 MHz) NMR spectra were recorded on a Bruker DPX-300 FT-NMR spectrometer (Pharmaceutical Research Instrument Center, Faculty of Pharmaceutical Sciences, Chulalongkorn University).

^{1}H (500 MHz) and ^{13}C (100 MHz) NMR spectra were obtained on a JEOL JMN-A500, Varian Unity INOVA (Scientific and Technological Research Equipment Center, Chulalongkorn University).

2.6 Physical properties

2.6.1 Melting points

Melting points were measured on a Fisher-Johns melting point apparatus (The Department of Pharmacognosy and Pharmaceutical Botany, Faculty of Pharmaceutical Sciences, Chulalongkorn University).

2.6.2 Optical rotations

Optical rotations were obtained on a Perkin-Elmer 314 polarimeter using sodium lamp operating at 589 nm (Pharmaceutical Research Instrument Center, Faculty of Pharmaceutical Sciences, Chulalongkorn University).

2.6.3 Circular dichroism spectra

Circular dichroism (CD) spectra were obtained on a Jasco J-715 spectropolarimeter. (Pharmaceutical Research Instrument Center, Faculty of Pharmaceutical Sciences, Chulalongkorn University).

3. Extraction and isolation of compounds from stem bark of *M. plicatus*

3.1 Extraction of stem bark of *M. plicatus*

The dried stem bark of *M. plicatus* (7.5 kg) was chopped into pieces, ground into powder and then macerated with EtOAc and MeOH. After removal of the solvents, a crude EtOAc extract (55.78 g, 0.74 % yield) and a crude MeOH extract (890.6 g, 11.87 % yield), were obtained respectively (Scheme 1).

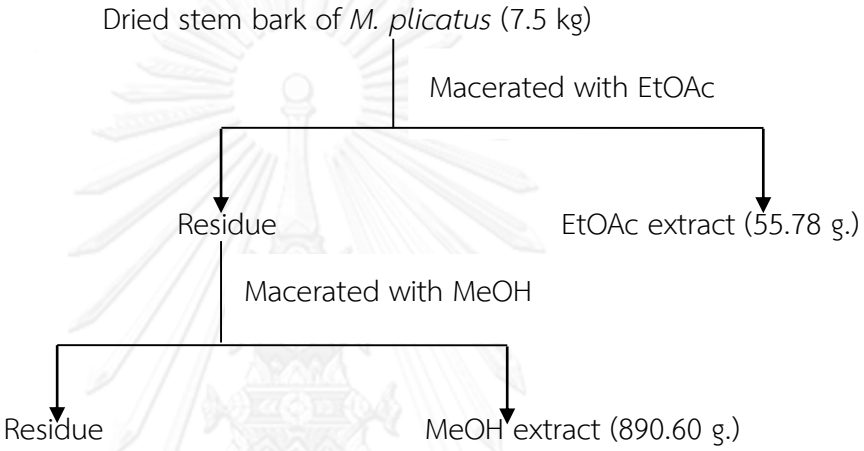

Scheme 1 Extraction of *M. plicatus* stem bark

3.2 Separation of the EtOAc Extract of *M. plicatus* stem bark

The EtOAc extract (55.78 g) was mixed with a small amount of silica gel powder and packed on top of a silica gel column. Elution was conducted with a gradient mixture of *n*-hexane-CH_2Cl_2 (0:1 to 1:0). All fractions collected from the column were combined into 14 fractions (I - XIV) following their TLC profiles (SiO_2, *n*-hexane-CH_2Cl_2 = 1:1) as shown in Table 11. These fractions were further separated as shown in Scheme 2.

Table 11 Fractions separated from the EtOAc extract of *M. plicatus* stem bark

Fraction Code	Weight (g)
I	0.1760
II	0.0915
III	0.1066
IV	0.4486
V	2.5610
VI	5.9715
VII	0.8976
VIII	2.1948
IX	0.5123
X	0.8996
XI	0.4586
XII	3.0516
XIII	2.2874
XIV	0.5267

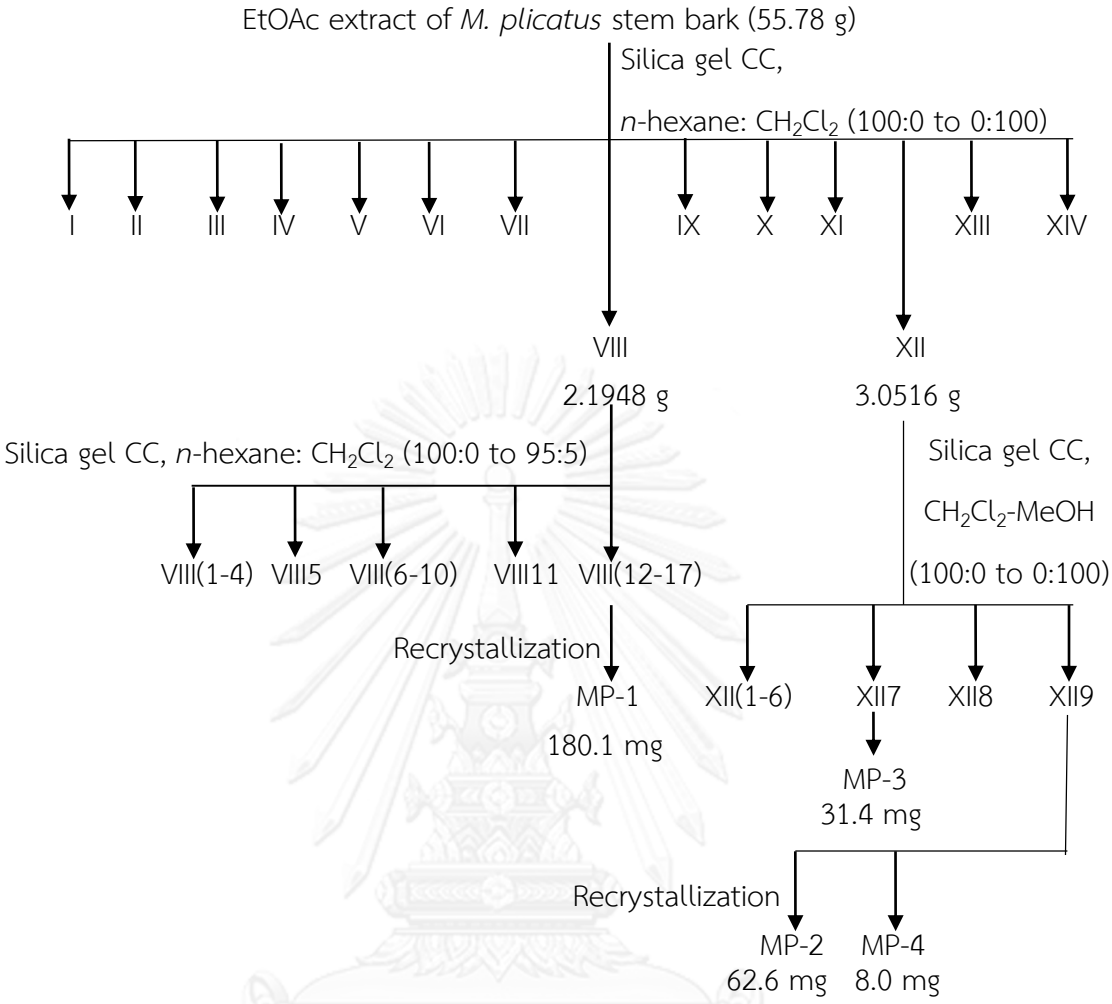

Scheme 2 Isolation of compounds from the EtOAc extract of *M. plicatus* stem bark

3.2.1 Isolation of compound MP-1 (aleuritolic acid 3-acetate)

Fraction VIII (2.1948 g) was further separated on a silica gel column (silica gel 60 No.9385, 83.97 g), and the mobile phase was a gradient mixture of *n*-hexane-CH_2Cl_2 (100:0 to 95:5). All fractions were collected and examined by TLC (SiO_2, *n*-hexane-CH_2Cl_2= 99.5:0.5). A total of 17 subfractions (VIII1 - VIII17) were obtained. Compound MP-1 was isolated by crystallization from subfractions VIII12 - VIII17 and further purified by washing with petroleum ether. It was obtained as colorless needles (188.1 mg, 0.0025 % yield).

3.2.2 Isolation of compound MP-2 (bergenin)

Fraction XII (3.0516 g) was further separated on a column using silica gel 60 (No.9385, 89.32 g.) as the stationary phase and a gradient mixture of CH_2Cl_2-MeOH (100:0 to 0:100) as the mobile phase. Nine subfractions (XII1 - XII9) were obtained. Compound MP-2 was then crystallized from subfraction XII9 and further purified by washing with acetone. It was obtained as colorless cubic crystals (62.6 mg, 0.0008 % yield).

3.2.3 Isolation of compound MP-3 (daucosterol)

Subfraction XII7 (0.6863 g) from section 3.2.2 was further purified by recrystallization from acetone to afford compound MP-3 as a white amorphous powder (31.4 mg, 0.00042 % yield).

3.2.4 Isolation of compound MP-4 (protocatechuic acid)

The residue from subfraction XII9 (332.8 mg) from section 3.2.2 was further separated using the preparative TLC method. A silica gel GF_{254} sheet was used as the stationary phase, and the mobile phase was a solvent system of CH_2Cl_2-acetone (4:6). After three-time development, compound MP-4 was extracted from the silica gel sheet with acetone and then purified by recrystallization from acetone to give yellow cubic crystals (8.0 mg, 0.00011 % yield).

3.3 Separation of the MeOH extract of *M. plicatus* stem bark

The crude MeOH extract (890.60 g) was partitioned between water and BuOH to yield a crude water extract (53.6 g, 0.71 % yield) and a crude BuOH extract (78.54 g, 1.05 % yield) after evaporation of the solvents.

3.3.1 Separation of the BuOH extract of *M. plicatus* stem bark

The crude BuOH extract (38.07 g) was mixed with small amounts of silica gel and placed on top of a silica gel column. The column was eluted with a gradient mixture of CH_2Cl_2-MeOH (100:0 to 0:100). All fractions were collected and combined into seven fractions (A - G) according to their TLC profiles (SiO_2, CH_2Cl_2-MeOH = 8:2) (Table 12 and Scheme 3).

Table 12 Fractions separated from the BuOH extract of *M. plicatus* stem bark

Fraction Code	Weight (g)
A	0.0468
B	0.8480
C	0.1653
D	6.0418
E	2.9823
F	4.5977
G	1.5073

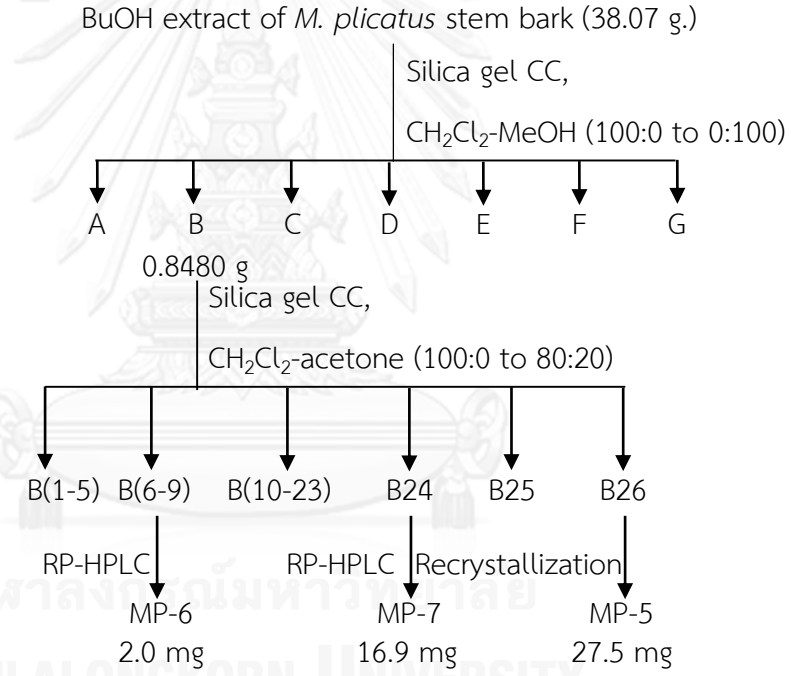

Scheme 3 Isolation of compounds from the BuOH extract of *M. plicatus* stem bark

3.3.1.1 Isolation of compound MP-5 (11-*O*-acetylbergenin)

Fraction B (0.8480 g) was chromatographed on a silica gel column, eluted with a gradient mixture of CH_2Cl_2-acetone (100:0 to 80:20). Twenty-six subfractions (B1 - B26) were collected, and subfraction 26 was purified by

recrystallization from CH_2Cl_2 to afford MP-5 as white needles (27.5 mg, 0.0004 % yield).

3.3.1.2 Isolation of compound MP-6 (scopoletin)

Subractions B6 - B9 (0.0126 g) from section 3.3.1.1 were pooled, dried and then purified by preparative HPLC using an ODS column as the stationary phase and a mixture of water-acetonitrile (6:4) as the mobile phase. Compound MP-6 was collected as colorless crystals (2.0 mg, 0.00003 % yield) after removal of the solvent.

3.3.1.3 Isolation of compound MP-7 (blumenol A)

Subfraction B24 (0.0416 g) from section 3.3.1.1 was further separated *via* preparative HPLC. An ODS column was used as the stationary phase, and a solvent system of water-acetonitrile (6:4) was used as the mobile phase. Compound MP-7 was obtained as yellow cubic crystals (16.9 mg, 0.0002 % yield).

3.3.2 Separation of the water extract of *M. plicatus* stem bark

The water extract (53.6 g) was redissolved in a small volume of water and then applied on top of an MCI column using the gradient solvent system of H_2O-MeOH (100:0 to 0:100) as the mobile phase. Five fractions (1 - 5) were collected and examined by TLC (SiO_2, CH_2Cl_2-MeOH-H_2O = 14:6:1) as shown in Table 13 and Scheme 4.

Table 13 Fractions separated from the water extract of *M. plicatus* stem bark

Fraction Code	Weight (g)
1	32.2204
2	3.9651
3	1.4174
4	5.8131
5	0.0580

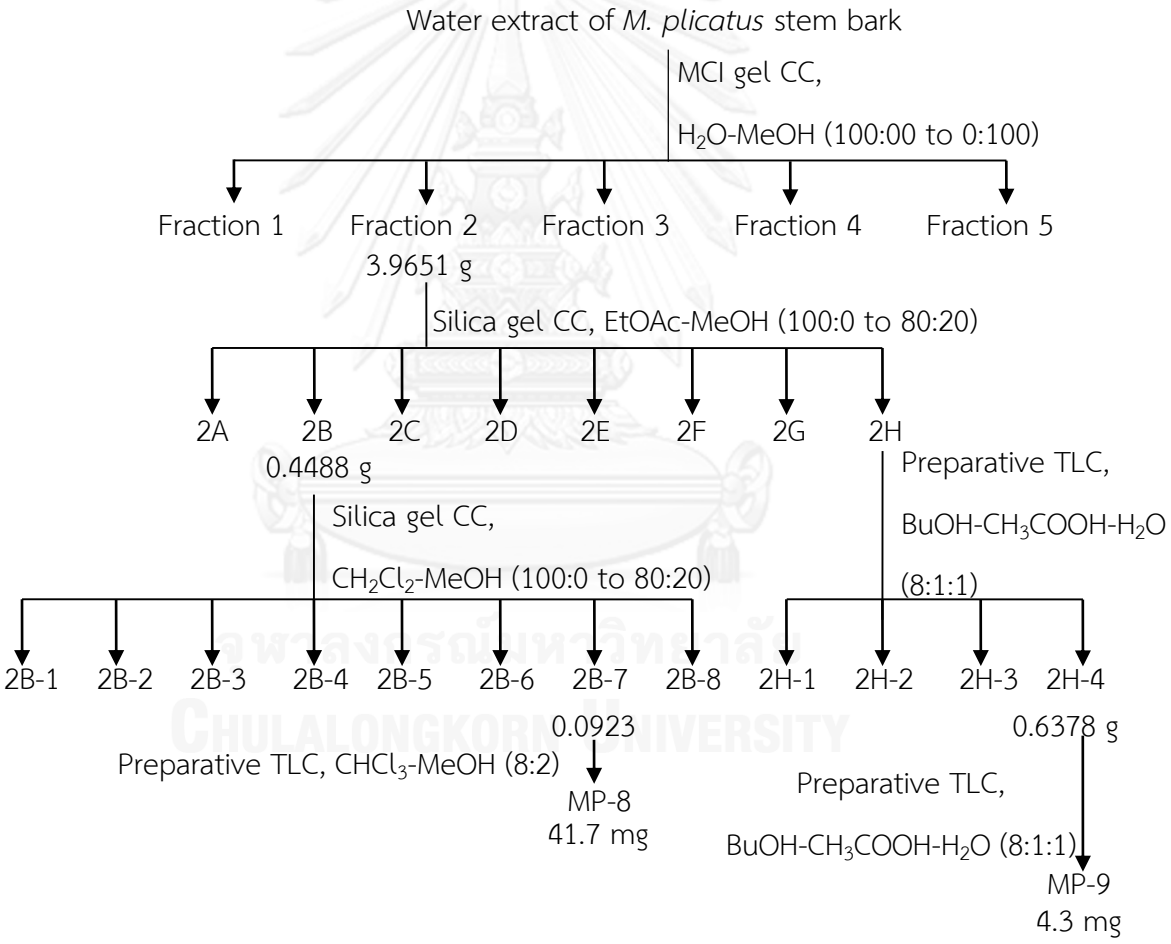

Scheme 4 Isolation of compounds from the water extract of *M. plicatus* stem bark

3.3.2.1 Isolation of compound MP-8 (bergenin-8-*O*-α-L-rhamnoside)

Fraction 2 (3.9651 g.) was further separated on a silica gel column, eluted with the solvent system EtOAc-MeOH (100:0 to 80:20). Eight fractions (2A - 2H) were collected. Fraction B (0.4488 g) was further separated on a silica gel column with a gradient mixture of CH_2Cl_2-MeOH (100:0 to 80:20) as the mobile phase to yield 8 subfractions (fractions 2B-1 - 2B-8). Compound MP-8 was isolated from subfraction 2B-7 (0.0923 g) by preparative TLC (SiO_2, CH_2Cl_2-MeOH = 8:2, double development). MP-8 was obtained as colorless needles (41.7 mg, 0.0006 % yield).

3.3.2.2 Isolation of compound MP-9 (*seco*-bergenin-8-*O*-α-L-rhamnoside)

Fraction 2H (0.6378 g) from section 3.3.2.1 was separated on a silica gel GF_{254} plate using the solvent system of BuOH-CH_3COOH-H_2O (8:1:1) as the mobile phase. Four subfractions (2H-1 - 2H-4) were obtained. Compound MP-9 was isolated from subfraction 2H-4 on a column using silica gel as the stationary phase and the solvent system, CH_2Cl_2-MeOH (1:1) as the mobile phase. MP-9 was obtained as colorless cubic crystals (4.3 mg, 0.00006 % yield).

4. Acid hydrolysis of compounds MP-8 and MP-9

Each compound (2 mg) was dissolved in 2 N HCl (2 mL) and refluxed at 100 ° C for 3 hrs. The solvent was removed from the hydrolysate, and H_2O (10 mL) was added to redissolved the residue. The solution was then partitioned with EtOAc (3 x 10 mL). Each fraction was evaporated to obtain the residue. The residue was redissolved in MeOH to yield a sample solution. The hydrolysis products and authentic samples of L-rhamnose, MP-2, MP-8 and MP-9 were examined on a silica gel TLC plate using $CHCl_3$-MeOH-H_2O (5:4:1) as the mobile phase. This TLC plate was sprayed with 10 % sulfuric acid and then heated at 130°C for 5 minutes to visualize the spots. The R_f values for L-rhamnose, compound MP-2 (bergenin), MP-8 (bergenin-

8-*O*-**α**-L-rhamnoside) and MP-9 (*seco*-bergenin-8-*O*-**α**-L-rhamnoside) were found to be 0.55, 0.70, 0.58 and 0.25, respectively.

5. Physical and spectral data of isolated compounds

5.1 Compound MP-1 (aleuritolic acid 3-acetate)

Compound MP-1 was obtained as colorless needles (188.1 mg, 0.0025 % yield based on dried weight of *M. plicatus* stem bark). The compound is soluble in CH_2Cl_2.

$[\alpha]^{20}_D$: +22.1° (*c* 0.01, $CHCl_3$)

ESI-MS: *m/z* (% rel. int.): 498 $[M]^+$ (98); Figure 15

^{1}H-NMR: **δ** ppm, 300 MHz, in $CDCl_3$; Table 14 and Figure 16

^{13}C-NMR: **δ** ppm, 75 MHz, in $CDCl_3$; Table 14 and Figure 17

5.2 Compound MP-2 (bergenin)

Compound MP-2 was obtained as colorless crystals (62.6 mg, 0.0008 % yield based on dried weight of *M. plicatus* stem bark). The compound is soluble in MeOH.

$[\alpha]^{20}_D$: -207.6° (*c* 0.001, MeOH)

UV: λ_{max} (MeOH) nm (log **ε**): 223 (4.58), 275 (4.10); Figure 22

ESI-MS: *m/z* (% rel. int.): 329 $[M+H]^+$ (74) ; Figure 23

^{1}H-NMR: **δ** ppm, 300 MHz, in DMSO-d_6; Table 15and Figure 24

^{13}C-NMR: **δ** ppm, 75 MHz, in DMSO-d_6; Table 15 and Figure 26

5.3 Compound MP-3 (daucosterol)

Compound MP-3 was obtained as white amorphous powder (31.4 mg, 0.0004 % yield based on dried weight of *M. plicatus* stem bark). This compound is soluble in DMSO.

ESI-MS: *m/z* (% rel. int.): 599 $[M+Na]^+$; Figure 29

^{1}H-NMR: **δ** ppm, 300 MHz, in DMSO-d_6; Table 16 and Figure 30

^{13}C-NMR: **δ** ppm, 75 MHz, in DMSO-d_6; Table 16 and Figure 31

5.4 Compound MP-4 (protocatechuic acid)

Compound MP-4 was obtained as yellow crystals (8.0 mg, 0.00011 % yield based on dried weight of *M. plicatus* stem bark). This compound is soluble in MeOH

UV: λ_{max} (MeOH) nm (log ε): 221 (4.52), 259 (4.23), 296 (3.96); Figure 36

HR-ESI-MS: *m/z* (% rel. int.): 153 $[M-H]^-$ (100); Figure 37

^{1}H-NMR: δ ppm, 300 MHz, in acetone-d_6; Table 17 and Figure 38

^{13}C-NMR: δ ppm, 75 MHz, in acetone-d_6; Table 17 and Figure 39

5.5 Compound MP-5 (11-*O*-acetylbergenin)

Compound MP-5 was obtained as white needles (27.5 mg, 0.0004 % yield based on dried weight of *M. plicatus* stem bark). This compound is soluble in acetone.

$[\alpha]^{20}_D$: -96.2° (*c* 0.001, MeOH)

UV: λ_{max} (MeOH) nm (log ε): 223 (4.56), 275 (4.00); Figure 40

HR-ESI-MS: *m/z* (% rel. int.): 393 $[M+Na]^+$ (100); Figure 41

^{1}H-NMR: δ ppm, 300 MHz, in acetone-d_6; Table 19 and Figures 42 and 43

^{13}C-NMR: δ ppm, 75 MHz, in acetone-d_6; Table 19 and Figure 45

5.6 Compound MP-6 (scopoletin)

Compound MP-6 was obtained as colorless crystals (2.0 mg, 0.00003 % yield based on dried weight of *M. plicatus* stem bark). This compound is soluble in CH_2Cl_2.

^{1}H-NMR: δ ppm, 300 MHz, in $CDCl_3$; Table 20 and Figure 48

^{13}C-NMR: δ ppm, 75 MHz, in $CDCl_3$; Table 20 and Figure 49

5.7 Compound MP-7 (blumenol A)

Compound MP-7 was obtained as yellow gum (16.9 mg, 0.0002 % yield % yield based on dried weight of *M. plicatus* stem bark). This compound is soluble in acetone.

$[\alpha]^{20}_D$: 204.1° (*c* 0.003, $CHCl_3$)

UV: λ_{max} (MeOH) nm (log ε): 271 (3.86); Figure 50

HR-ESI-MS: *m/z* (% rel. int.): 247 $[M+Na]^+$ (100); Figure 51

^{1}H-NMR: δ ppm, 500 MHz, in acetone-d_6; Table 21 and Figure 52

^{13}C-NMR: δ ppm, 125 MHz, in acetone-d_6; Table 21 and Figure 53

CD: λ (*c* 0.003, $CHCl_3$) nm [θ]: 262 (10.7), 328 (-2.1); Figure 56

5.8 Compound MP-8 (bergenin-8-*O*-α-L-rhamnoside)

Compound MP-8 obtained as white crystals (41.7 mg, 0.0006 % yield based on dried weight of *M. plicatus* stem bark). This compound is soluble in MeOH.

mp: 198-203 °C

$[\alpha]^{20}_{D}$: -62.3° (*c* 0.001, MeOH)

UV: λ_{max} (MeOH) nm (log ε): 222 (4.42), 274 (3.67); Figure 57

FT-IR: ν_{max} (KBr) cm^{-1}: 3400, 1722, 1612, 1510, 1460, 1374, 1337, 1093; Figure 58

HR-ESI-MS: *m/z* (% rel. int.): 497.1287 $[M+Na]^+$ (100), calcd. for $C_{20}H_{26}NaO_{14}$, 497.1271; Figure 59

^{1}H-NMR: δ ppm, 300 MHz, in DMSO-d_6; Table 22 and Figure 60

^{13}C-NMR: δ ppm, 75 MHz, in DMSO-d_6; Table 22 and Figure 63

5.9 Compound MP-9 (*seco*-bergenin-8-*O*-α-L-rhamnoside)

Compound MP-9 was obtained as colorless cubic crystals (4.3 mg, 0.00006 % yield based on dried weight of *M. plicatus* stem bark). This compound was soluble in MeOH.

mp: 146-149 °C

$[\alpha]^{20}_{D}$: -10.4° (*c* 0.0003, MeOH)

UV: λ_{max} (MeOH) nm (log ε): 219 (3.12); Figure 77

FT-IR: ν_{max} (KBr) cm^{-1}: 3434, 1623, 1574, 1403, 1396; Figure 78

HR-ESI-MS: *m/z* (% rel. int.): 491.1399 $[M-H]^-$ (100), calcd. for $C_{20}H_{27}O_{14}$, 491.1406; Figure 79

^{1}H-NMR: δ ppm, 300 MHz, in CD_3OD; Table 23 and Figure 80

^{13}C-NMR: δ ppm, 75 MHz, in CD_3OD; Table 23 and Figure 83

6. Evaluation of biological activities

6.1 Evaluation of anti-HSV activity

The anti-HSV activity evaluation was performed by plaque reduction assay (Sritularak et al., 2013). This bioassay was conducted at the Department of Biochemistry and Microbiology, Faculty of Pharmaceutical Sciences, Chulalongkorn University. Vero cells (African green monkey kidney cell ATCC CCL81) were cultivated in Minimum Essential Medium (MEM) with Fetal Bovine Serum (FBS) 10% and antibiotics containing penicillin G 60 µg/ml and streptomycin 100 µg/mL, and incubated at 37 °C in humidified atmosphere of 5% CO_2. Acyclovir was used as the positive control, and the negative control was DMSO 1.0 % (v/v). Each test compound was diluted to 100 µg/mL for maximum final concentration.

Cells were seeded in 96-well plate as a confluent monolayer. HSV-1(KOS) or HSV-2 (Baylor 186) was added into each well. The plate was incubated at 37 °C in humidified atmosphere of 5% CO_2 for 1 hr. Then, the sample at various concentrations was added, and the plate was incubated again at 37 °C in humidified atmosphere of 5% CO_2 for 48 hrs. Formalin was added to fix cells, followed with methylene blue for staining cells. Plaques in the well containing samples were counted and compared with the number of plagues of the negative control to calculate the percentage of the inhibitory activity for each sample.

The compounds that showed more than 50 % inhibition at 100 µg/mL were further analyzed for the IC_{50} value (50% inhibitory concentration). This was done by plotting a dose response curve of 5 concentrations (µg/mL) of each sample against their percentage of the inhibitory activity. This curve was used to calculate the IC_{50} value. The experiment was repeated 2 times, and the mean IC_{50} value was calculated.

6.2 Evaluation of cytotoxicity against KB cells

The assay for cytotoxicity was provided by the Bioassay Laboratory, National Center for Genetic Engineering and Biotechnology (BIOTEC).

The cytotoxicity determination against KB (oral epidermal carcinoma) cell was done using resazurin microplate assay method (REMA) (O'Brien et al., 2000). Doxorubicin and elipticine were used as positive controls whereas 0.5 % DMSO was used as the negative control. Each test compound was diluted to 50 µg/mL for maximum final concentration.

KB cells at a logarithmic growth phase were seeded and diluted to 7×10^4 cells/mL in fresh medium. The cell suspension was drained about 45 µL to mix with 5 µL of each test compound diluted in 5 % DMSO in 384-well plate and then incubated at 37 °C in humidified atmosphere of 5% CO_2 for 3 days. After that, 12.5 µL of 62.5 µg/mL of resazurin solution was added to each well, and the plate was further incubated at 37 °C for 4 hrs. Each well was measured its fluoresce signal using a Spectramax M5 microplate reader (Molecular Device, USA) in the bottom reading mode with excitation and emission wavelengths at 485 and 535 nm, respectively. The fluorescent signal at day 4 was subtracted with the background fluoresce at day 0. The percentage of the cytotoxicity was calculated using the equation which is shown below. FU_T and FU_C represent the fluoresce units of cells treated with the sample and untreated cells, respectively.

$$\% \text{ cytotoxicity} = [1-(FU_T/FU_C)] \times 100$$

The compounds that showed more than 50 % inhibition at 50 µg/mL were further studied to determine the IC_{50} value (50% inhibitory concentration).

Six concentrations of 2-fold serially diluted test compound were used to plot dose-response curve in order to calculate the concentration that inhibited the cell growth by 50 % (IC_{50} value). This process was done using SOFTmax pro software (Molecular Device, USA).

6.3 Evaluation of scavenging activity against DPPH free radicals

The antiradical activity evaluation was performed using DPPH as the free radical. Vitamin C and MeOH were used as the positive and negative control,

respectively. Each test compound was diluted to 100 µg/mL for maximum final concentration.

The assay was carried out by adding 180 µL of DPPH (50 µM) in each well of the 96-well plate, followed by 20 µL of the test compound. The plate was incubated at 37 °C without the light for 30 minutes. Absorbance at 510 nm was measured in order to calculate % free radical scavenging activity using the equation shown below.

$$\% \text{ DPPH reduction} = (A-B)/A \times 100$$

A = the absorbance of the negative control at 510 nm

B = the absorbance of the test compound at 510 nm

CHAPTER IV

RESULTS AND DISCUSSION

1. Structural characterization of isolated compounds

Maceration of *M. plicatus* stem bark yielded 2 extracts: an EtOAc extract and a MeOH extract. The results from anti-HSV activity assays showed that both extracts were active. The EtOAc extract exhibited IC_{50} values of 87.5 and 68.8 µg/mL against HSV-1 and HSV-2, respectively, whereas the respective IC_{50} values of MeOH extract were 43.8 and 31.3 µg/mL. Separation of the EtOAc extract using several chromatographic methods led to the isolation of 4 compounds (MP-1 to MP-4). The MeOH extract was first partitioned between BuOH and water to obtain BuOH and water extracts. The BuOH extract was then subjected to chromatographic separation to yield 3 pure compounds, MP-5, MP-6 and MP-7, while the water extract gave two pure compounds (MP-8 and MP-9) after extensive repeated chromatography The structures of all the isolated compounds were determined using several spectroscopic techniques including UV, IR, MS and NMR.

1.1 Identification of compound MP-1 (aleuritolic acid 3-acetate)

Compound MP-1 [**40**] was obtained as white needles (188.1 mg, 0.0025 % yield). It did not absorb UV light, but gave a purple spot on a TLC chromatogram upon spraying with 10% sulfuric acid followed by heating. The ESI mass spectrum (Figure 15) presented its molecular ion $[M]^+$ at *m/z* 498, suggesting that the molecular formula was $C_{32}H_{50}O_4$.

The ^{1}H-NMR spectrum of compound MP-1 (Figure 16, Table 14) showed resonances in the aliphatic region, suggesting that the compound does not have an aromatic ring. There are six methyl singlets appearing at δ_H 0.87 (s, H-23) 0.90 (s, H-24), 0.93 (s, H-27, 30), 0.96 (s, H-29), 0.97 (s, H-25, 26), and 2.06 (s, C$\underline{H}_3$COO-3) ppm.

The peak at δ_H 4.47 (dd, *J* = 6.0, 9.3 Hz, H-3) ppm belonged to the proton which was attached to an oxygenated carbon. The most downfield resonance at δ_H 5.53 ppm (d, *J* = 4.8 Hz, H-15) was due to an olefenic proton.

The ^{13}C-NMR spectrum (Figure 17, Table 14) displayed 32 carbon signals. The HSQC spectrum (Figures 19-21) showed thirty signals assumed to be signals of a triterpenoid skeleton, including seven signals of methyl carbons at δ_C 15.6 (C-25), 16.5 (C-24), 22.5 (C-27), 26.2 (C-26), 28.0 (C-23), 28.6 (C-30) and 31.9 (C-29) ppm, ten methylenes at δ_C 17.3 (C-11), 18.7 (C-6), 23.4 (C-2), 30.7 (C-22), 31.3 (C-16), 33.3 (C-12), 33.7 (C-21), 35.4 (C-19), 37.4 (C-1) and 40.8 (C-7) ppm, five methines at δ_C 41.4 (C-18), 49.1 (C-9), 55.6 (C-5), 80.9 (C-3) and 116.9 (C-15) ppm, seven quaternaries at δ_C 29.3 (C-20), 37.3 (C-13), 37.7 (C-4), 37.9 (C-10), 39.0 (C-8), 51.5 (C-17) and 160.6 (C-14) ppm and a signal for carboxylic group at 184.2 (C-28) ppm. Two additional peaks at δ_C 170.9 ($CH_3\underline{C}OO$-3) and 21.2 ($\underline{C}H_3COO$-3) ppm were suggested as an acetyl group.

Comparison of the NMR data of compound MP-1 with previous reports (Table 14) revealed that compound MP-1 were identical with aleuritolic acid 3-acetate [**40**]. Aleuritolic acid 3-acetate (also known as maprounic acid acetate) is a triterpenoid found in many plants, particularly in the family Euphorbiaceae (Chaudhuri et al., 1995). In the genus *Mallotus*, this compound has been isolated from the stem of *M. apelta* and the bark of *M. philippensis* (Rivière et al., 2010). It possessed weak antimicrobial activity against *Staphylococcus. aureus* and *Salmonella. typhimurium* (Prachayasittikul et al., 2009), and cytotoxic activity against some types of cancer cells such as U251 neuroblastoma cells with a 50 % inhibitory concentration (IC_{50}) of 8.4 μM (Reyes et al., 2010) and human lung carcinoma A549 cells with an IC_{50} value of 13.84 μM (Wada and Tanaka, 2006).

Table 14 NMR Spectral data of compound MP-1 [**40**] ($CDCl_3$) and aleuritolic acid 3-acetate ($CDCl_3$)

Position	Compound MP-1		Aleuritolic acid 3-acetate*	
	δ_C	δ_H	δ_C	δ_H
1	37.4	1.04 (1H, m), 1.61 (1H, m)	37.4	1.04 (1H, m), 1.61 (1H, m)
2	23.4	1.61 (1H, m), 1.66 (1H, m)	23.4	1.61 (1H, m), 1.66 (1H, m)
3	80.9	4.47 (1H, dd, *J* = 6.0, 9.3 Hz)	80.8	4.47 (1H, dd, *J* = 6.0, 10.0 Hz)
4	37.7	-	37.6	-
5	55.6	-	55.5	0.88 (1H, m)
6	18.7	1.52 (1H, m), 1.64 (1H, m)	18.7	1.49 (1H, m), 1.62 (1H, m)
7	40.8	1.31 (1H, m), 1.97 (1H, m)	40.6	1.30 (1H, m), 1.97 (1H, m)
8	39.0	-	39.0	-
9	49.1	1.41 (1H, m)	49.0	1.42 (1H, m)
10	37.9	-	37.8	-
11	17.3	1.48 (1H, m) 1.64 (1H, m)	17.2	1.48 (1H, m), 1.69 (1H, m)
12	33.3	1.64 (1H, m), 1.78 (1H, m)	33.2	1.60 (1H, m), 1.78 (1H, m)
13	37.3	-	37.2	-
14	160.6	-	160.5	-
15	116.9	5.53 (1H, d, *J* = 4.8 Hz)	116.8	5.52 (1H, dd, *J* = 4.0, 8.0 Hz)
16	31.3	1.92 (1H, m), 2.38 (1H, m)	31.2	1.93 (1H, m), 2.37 (1H, m)
17	51.5	-	51.4	-
18	41.4	2.27 (1H, m)	41.3	2.28 (1H, m)
19	35.4	1.10 (1H, m), 1.22 (1H, m)	35.2	1.09 (1H, m), 1.24 (1H, m)
20	29.3	-	29.2	-
21	33.7	1.08 (1H, m), 1.13 (1H, m)	33.6	1.05 (1H, m), 1.16 (1H, m)

Table 14 NMR Spectral data of compound MP-1 [**40**] ($CDCl_3$) and aleuritolic acid 3-acetate ($CDCl_3$) (continued)

Position	Compound MP-1		Aleuritolic acid 3-acetate *	
	δ_C	δ_H	δ_C	δ_H
22	30.7	1.46 (1H, m), 1.71 (1H, m)	30.6	1.44 (1H, m), 1.69 (1H, m)
23	28.0	0.87 (3H, s)	27.9	0.85 (3H, s)
24	16.5	0.90 (3H, s)	16.5	0.89 (3H, s)
25	15.6	0.97 (3H, s)	15.6	0.95 (3H, s)
26	26.2	0.97 (3H, s)	26.1	0.95 (3H, s)
27	22.5	0.93 (3H, s)	22.4	0.92 (3H, s)
28	184.2	-	184.2	-
29	31.9	0.96 (3H, s)	31.8	0.94 (3H, s)
30	28.6	0.93 (3H, s)	28.6	0.91 (3H, s)
$CH_3\underline{C}OO$-3	170.9	-	170.9	-
$\underline{C}H_3COO$-3	21.2	2.06 (3H, s)	21.2	2.03 (3H, s)

* NMR data from the reference (Rahman and Ahmad, 1994).

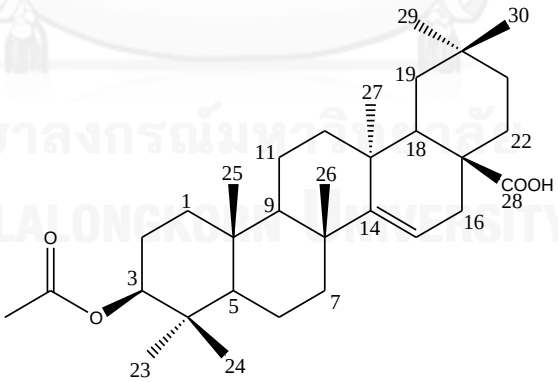

Aleuritolic acid 3-acetate [**40**]

1.2 Identification of compound MP-2 (bergenin)

Compound MP-2 [**123**] was obtained as white crystals (62.6 mg, 0.0008 % yield). It appeared as a dark spot on the TLC plate under UV light at 254 nm. Its UV absorption maxima were at 223 and 275 nm (Figure 22). From its protonated molecular ion $[M+H]^+$ at *m/z* 329 in the mass spectrum, its molecular weight was deduced to be 328 (Figure 23), and its molecular formula was characterized as $C_{14}H_{16}O_9$.

The ^{1}H-NMR and COSY spectra (Figures 24 and 25, Table 15) suggested that MP-2 has an aromatic ring with a methoxyl group and a sugar moiety. It showed methoxyl protons as a singlet signal at δ_H 3.76 (s, CH_3O-9) ppm. An aromatic proton signal was observed at δ_H 6.98 (s, H-7), together with two phenolic protons at, 8.43 (s, OH-10) and 9.75 (s, OH-8) ppm. The sugar moiety showed five methine protons at δ_H 3.56 (t, *J* = 9.0 Hz, H-2), 3.19 (m, H-3), 3.63 (m, H-4), 3.98 (t, *J* = 10.0 Hz, H-4a) and 4.96 (d, *J* = 10.0 Hz, H-10b) and two methylene protons at δ_H 3.43 (m, H-11) and 3.81 (td, *J* = 9.0, 4.8 Hz, H-11) ppm.

The ^{13}C-NMR (Figure 26, Table 15) and HSQC (Figure 27) spectra confirmed the existence of the aromatic ring by carbon signals at δ_C 118.1 (C-6a), 116.0 (C-10a), 109.5 (C-7), 151.0 (C-8), 140.7 (C-9) and 148.1 (C-10) ppm. The peak at δ_C 163.4 (C-6) ppm indicated the presence of a lactone ring. The carbon signals of the sugar moiety were observed at δ_C 81.8 (C-2), 70.8 (C-3), 73.8 (C-4), 79.9 (C-4a), 72.2 (C-10b) and 61.2 (C-11) ppm. The methoxyl carbon resonated at δ_C 59.9 (CH_3O-9) ppm.

The NMR data of compound MP-2 were found to be superimposable with those of bergenin [**123**] (Nasser et al., 2009) as shown in Table 15. The HMBC spectrum (Figure 28) showed correlations in support of this conclusion. The specific rotation $[\alpha]^{20}_D$ of MP-2 is consistent with the previously reported value (Wang et al., 2008). Bergenin is a gallic acid *C*-glucoside firstly found in the genus *Bergenia* of the family Saxifragaceae (Taneyama and Yoshida, 1978). It was also found in *Mallotus* species. It has been isolated from the heartwood, bark, and leaves of *M. philippensis*.

In addition, it was obtained from *M. repandus* (Rivière et al., 2010) and *M. roxburghianus* (Rana et al., 2005). Bergenin exhibited various biological activities, for instance, anti-arthritic activity *via* the modulation of Th1/Th2 cytokine balance (Patel et al., 2012), antifungal activity against *Candida sp.*(Silva et al., 2009;Patel et al., 2012), antidiabetic activity, antiulcerogenic activity, anti-inflammatory by inhibition of COX-1, COX-2 and phospholipase A2 (Patel et al., 2012), and antioxidant activity against DPPH free radical, ABTS radical cation, hydrogen peroxide, nitric oxide and lipid peroxidation *in vitro* (Rana et al., 2005;Patel et al., 2012). Bergenin also showed antioxidant activity *in vivo* by increasing the level of catalase (CAT) and superoxide dismutase (SOD) and decreasing the level of lipidperoxidation (LPO) in the rat serum (Patel et al., 2012).

Table 15 NMR Spectral data of compound MP-2 [**123**] (DMSO-d_6) and bergenin (DMSO-d_6)

Position	Compound MP-2		Bergenin	
	δ_C	δ_H	δ_C [a]	δ_H [b]
2	81.8	3.56 (1H, t, *J* = 9.0 Hz)	81.8	3.56 (1H, dd)
3	70.8	3.19 (1H, m)	70.7	-
4	73.8	3.63 (1H, m)	73.7	3.65 (1H, m)
4a	79.9	3.98 (1H, t, *J* = 10.0 Hz)	79.8	3.98 (1H, m)
6	163.4	-	163.3	-
6a	118.1	-	118.0	-
7	109.5	6.98 (1H, s)	109.5	6.98 (1H, s)
8	151.0	-	150.9	-
9	140.7	-	140.6	-
10	148.1	-	148.0	-
10a	116.0	-	115.9	-
10b	72.2	4.96 (1H, d, *J* = 10.0 Hz)	72.2	4.98 (1H, dd)
11	61.2	3.43 (1H, m)	61.2	3.86 (2H, d)
		3.81 (1H, td, *J* = 9.0, 4.8 Hz)		-
OH-3	-	5.42 (1H, d, *J* = 5.7 Hz)	-	-
OH-4	-	5.64 (1H, d, *J* = 5.4 Hz)	-	5.62 (1H, s)
OH-8	-	9.75 (1H, s)	-	-
OH-10	-	8.43 (1H, s)	-	-
OH-11	-	4.90 (1H, t, *J* = 5.1 Hz)	-	-
CH_3O-9	59.9	3.76 (3H, s)	60.0	3.77 (3H, s)

[a] NMR data from the reference (Taneyama et al., 1983).

[b] NMR data from the reference (Deng et al., 2010).

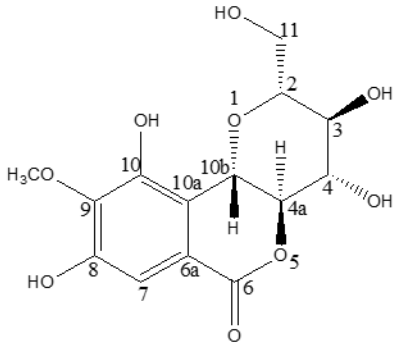

Bergenin [**123**]

1.3 Identification of compound MP-3 (daucosterol)

Compound MP-3 [**56**], a white powder (31.4 mg, 0.0004 %), did not absorb UV light but appeared as a purple spot on the TLC plate upon spraying with 10 % sulfuric acid followed by heating. The ESI Mass spectrum (Figure 29) displayed a sodium-adduct molecular ion $[M+Na]^+$ at *m/z* 599, suggesting that its molecular formula was $C_{35}H_{60}O_6$.

The ^{1}H-NMR spectrum (Figure 30, Table 16) exhibited resonances in the upfield region, suggesting that this compound might be a terpenoid or a steroid. MP-3 showed two singlets for methyl protons at δ_H 0.83 (s, H-18) and 0.97 (br s, H-19) ppm and a doublet for methyl protons at δ_H 0.80 (d, *J* = 5.6 Hz, H-27) ppm. It also displayed a doublet at δ_H 4.20 (d, *J* = 7.6 Hz, H-1′) ppm and an olefinic proton at δ_H 5.31 (br s, H-6) ppm.

The ^{13}C-NMR, DEPT and HSQC spectra (Figures 31-35, Table 16) displayed 35 carbon signals. Twenty-nine signals were similar to those of *β*-sitosterol including six methyl carbons at δ_C 11.7 (C-29), 11.9 (C-18), 18.7 (C-21), 19.2 (C-19), 19.0 (C-27) and 19.8 (C-26) ppm, eleven methylenes at δ_C 20.7 (C-11), 22.7 (C-28), 23.9 (C-15), 25.6 (C-23), 27.9 (C-16), 29.4 (C-2), 33.4 (C-7), 35.6 (C-22), 36.9 (C-1), 38.4 (C-12) and 40.4 (C-4) ppm, nine methines at δ_C 28.8 (C-25), 31.5 (C-8), 36.3 (C-20), 45.2 (C-24), 49.7 (C-9), 56.3 (C-14), 55.5 (C-17), 77.0 (C-3) and 121.3 (C-6) ppm and quaternaries at δ_C 36.3 (C-10), 41.9 (C-13) and 140.5 (C-5) ppm. There were also six signals for a glucose moiety,

including δ_C 100.9 (C-1′), 76.8 (C-2′), 73.5 (C-3′), 70.2 (C-4′), 76.9 (C-5′) and 61.2 (C-6′) ppm. Based on these spectroscopic data, it could be proposed that MP-3 was a steroidal glucoside.

The ^{13}C-NMR data of compound MP-3 were found to be identical with those of daucosterol [**56**], as shown in Table 16 (Akhtar et al., 2010). However, it should be noted that the ^{1}H-NMR assignments reported in this reference should be revised on the basis of C-H direct couplings observed in the HSQC spectrum (Figures 33-35) in this study. Table 16 summarizes our ^{1}H-NMR assignments in comparison with the earlier described values (Akhtar et al., 2010). Daucosterol or sitosteryl ***β***-D-glucose is a steroid glucoside found in plants. In *Mallotus* species, daucosterol has been isolated from the stems and leaves of *M. apelta* and from the ether extract of *M. philippinensis*'s bark (Rivière et al., 2010). This compound showed immunomodulatory activity by inducing the protective effect of Th1 immune response against candidiasis in mice (Lee et al., 2007).

Table 16 NMR Spectral data of compound MP-3 [**56**] (DMSO-d_6) and daucosterol (DMSO-d_6)

Position	Compound MP-3		Daucosterol*	
	δ_C	δ_H	δ_C	δ_H
1	36.9	1.01 (1H, m), 1.80 (1H, m)	36.86	1.38 (1H, m), 2.50 (1H, m)
2	29.4	1.50 (1H, m), 1.83 (1H, m)	29.28	1.80 (1H, m), 1.78 (1H, m)
3	77.0	3.52 (1H, br s)	77.00	4.43 (1H, br m)
4	40.4	1.14 (1H, m), 1.95 (1H, m)	40.33	2.50 (1H, m), 2.34 (1H, m)
5	140.5	-	140.46	-
6	121.3	5.31 (1H, br s)	121.18	5.31 (1H, d, *J* = 5.2 Hz)
7	33.4	1.31 (1H, m), 1.03 (1H, m)	33.38	1.93 (1H, m), 2.08 (1H, m)
8	31.5	1.39 (1H, m)	31.38	1.13 (1H, m)
9	49.7	0.91 (1H, m)	49.64	1.45 (1H, m)
10	36.3	-	36.22	-
11	20.7	1.53 (2H, m)	20.62	1.93 (1H, m), 1.50 (1H, m)
12	38.4	2.14 (1H, m), 2.38 (1H, m)	38.34	1.13 (1H, m), 1.80 (1H, m)
13	41.9	-	42.11	-
14	56.3	1.01 (1H, m)	56.21	1.15 (1H, m)
15	23.9	1.05 (1H, m), 1.58 (1H, m)	23.88	1.06 (1H, m), 1.80 (1H, m)
16	27.9	1.24 (1H, m), 1.85 (1H, m)	28.74	1.61 (1H, m), 1.36 (1H, m)
17	55.5	1.11 (1H, m)	55.47	1.45 (1H, m)
18	11.9	0.83 (3H, s)	11.74	0.64 (3H, br s)
19	19.2	0.97 (3H, br s)	19.10	0.95 (3H, br s)
20	36.3	1.32 (1H, m)	36.22	2.34 (1H, m)
21	18.7	0.91 (3H, m)	18.63	0.90 (3H, d, *J* = 6.0 Hz)

Table 16 NMR Spectral data of compound MP-3 [**56**] (DMSO-d_6) and daucosterol (DMSO-d_6) (continued)

Position	Compound MP-3		Daucosterol*	
	δ_C	δ_H	δ_C	δ_H
22	35.6	1.33 , (2H, m)	35.51	1.78 (1H, m), 1.10 (1H, m)
23	25.6	1.16 (2H, m)	25.49	1.25 (1H, m), 1.80 (1H, m)
24	45.2	0.92 (1H, m)	44.66	1.30 (1H, m), 1.55 (1H, m)
25	27.9	1.66 (1H, m)	27.81	1.73 (1H, m)
26	19.8	0.82 (3H. br s)	19.62	0.92 (3H, d, *J* = 6.1 Hz)
27	19.0	0.80 (3H, d, *J* = 5.6 Hz)	18.95	0.80 (3H, d, *J* = 6.6 Hz)
28	22.7	1.21 (2H, m)	22.63	1.15 (1H, m), 1.42 (1H, m)
29	11.7	0.65 (3H. br s)	11.67	0.82 (3H, d, *J* = 7.3 Hz)
1′	100.9	4.20 (1H, br s)	100.84	4.90 (1H, br s)
2′	76.8	3.13 (1H, m)	76.74	3.62 (1H, m)
3′	73.5	3.03 (1H, m)	73.47	3.08 (1H, m)
4′	70.2	3.07 (1H, br s)	70.09	3.04 (1H, m)
5′	76.9	3.13 (1H, m)	76.74	4.22 (1H, d, *J* = 5.6 Hz)
6′	61.2	3.41 (1H, br s), 3.63 (1H, br s)	62.10	4.88 (1H, br s), 4.66 (1H, br s)

* NMR data from the reference (Akhtar et al., 2010), which need revision (see text).

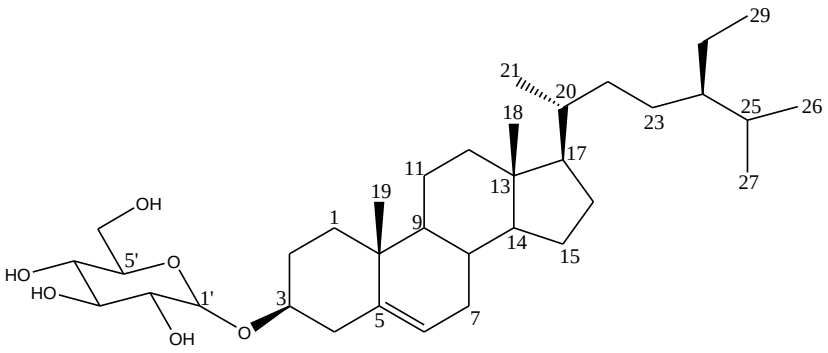

Daucosterol [**56**]

1.4 Identification of compound MP-4 (protocatechuic acid)

Compound MP-4 [**139**] was obtained as yellow crystals (8.0 mg, 0.00011 % yield). It appeared as a dark spot on the TLC plate under 254 nm UV light. The UV spectrum (Figure 36) exhibited absorption maxima at 221, 259 and 296 nm. The HR-ESI mass spectrum (Figure 37) showed its deprotonated molecular ion $[M-H]^-$ at *m/z* 153, suggesting a molecular formula of $C_6H_7O_4$.

The ^{1}H-NMR spectrum (Figure 38, Table 17) of compound MP-4 showed peaks for three aromatic protons at δ_H 7.50 (d, *J* = 1.8 Hz, H-2), 7.45 (dd, *J* = 8.2, 1.8 Hz, H-6) and 6.86 (d, *J* = 8.2 Hz, H-5) ppm, suggesting that MP-4 has a trisubstituted aromatic ring.

The ^{13}C-NMR spectrum (Figure 39, Table 17) supported the existence of the phenolic ring with carbons resonating at δ_C 123.0 (C-1), 117.3 (C-2), 145.3 (C-3), 150.5 (C-4), 115.5 (C-5) and 123.4 (C-6) ppm. MP-4 has a carboxylic carbon signal at δ_C 167.5 ppm (COOH-1). The compound appeared to be a derivative of phenolic acid.

By comparison of the NMR data of compound MP-4 with previously reported values (Table 17), compound MP-4 was identified as protocatechuic acid [**139**] (Keawsa-ard et al., 2012). Protocatechuic acid is a phenolic acid derivative found in green tea (Yen and Hsieh, 2000). In the genus *Mallotus*, it has been reported in the leaves of *M. bartatus* (Giang et al., 2013). A water extract of *Eucommia ulmoides* Oliv. exhibited ROS scavenging activity, and the effect was correlated to the content of protocatechuic acid (Yen and Hsieh, 2000). Protocatechuic acid isolated from *Hibiscus sabdariffa* was reported for its protective activity against chemically induced liver toxicity (Liu et al., 2002). Furthermore, it prevented the metastatis of B16/F10 melanoma cells to the liver in mice (Lin et al., 2011). However, it was inactive against human oral carcinoma (KB), human breast cancer (MCF-7) and human small cell lung cancer (NCI-H187) (Keawsa-ard et al., 2012). There was a report about its inactivity against HSV (Alvarez et al., 2012).

Table 17 NMR Spectral data of compound MP-4 [**139**] (acetone-d_6) and protocatechuic acid (acetone-d_6)

Position	Compound MP-4		Protocatechuic acid*	
	δ_C	δ_H	δ_C	δ_H
1	123.0	-	121.7	-
2	117.3	7.50 (1H, d, *J* = 1.8 Hz)	116.3	7.44 (1H, d, *J* = 1.2 Hz)
3	145.3	-	144.6	-
4	150.5	-	150.1	-
5	115.5	6.86 (1H, d, *J* = 8.2 Hz)	114.3	6.79 (1H, d, *J* = 7.8 Hz)
6	123.4	7.45 (1H, dd, *J* = 8.2, 1.8 Hz)	122.5	7.41 (1H, dd, *J* = 7.8, 1.2 Hz)
COOH-1	167.5	-	168.9	-

* NMR data from the reference (Keawsa-ard et al., 2012).

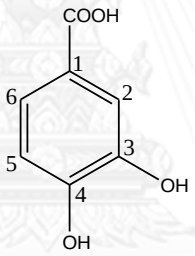

Protocatechuic acid [**139**]

1.5 Identification of compound MP-5 (11-*O*-acetylbergenin)

Compound MP-5 [**140**], a white powder (27.5 mg, 0.0004 % yield), appeared as a dark spot on the TLC plate under UV light at 254 nm. The UV spectrum (Figure 40) was similar to that of compound MP-2, showing absorption maxima at 223 and 275 nm. Its molecular formula, $C_{16}H_{18}O_{10}$, was deduced from with its sodium-adduct molecular ion $[M+Na]^+$ at *m/z* 393 (Figure 41).

The ^{1}H-NMR and COSY spectra of compound MP-5 (Figures 42-44, Table 19) were similar to that of MP-2, even though different NMR solvents were employed. It exhibited the resonances of a methyl group at δ_H 2.07 (s, C$\underline{H}_3$COO-11) ppm, a methoxyl group at δ_H 3.89 (s, CH_3O-9) ppm and aromatic protons at δ_H at 7.09 (s, H-7)

ppm, 8.49 (s, OH-8) and 8.17 (s, OH-10) ppm, which were similar to those of bergenin [**123**]. Moreover, the ^{1}H-NMR spectrum showed signals for a glucose moiety, including a hydroxyl proton at δ_H 4.98 (br s, OH-3) ppm, peaks for methine protons at δ_H 4.01 (m, H-2), 3.57 (br t, *J* = 8.3 Hz, H-3), 4.12 (t, *J* = 10.0 Hz, H-4a), 3.98 (m, H-4) and 5.10 (d, *J* = 10.0 Hz, H-10b) ppm and for methylene protons at δ_H 4.23 (dd, *J* = 7.1, 12.2 Hz, H-11) and 4.70 (dd, *J* = 2.1, 12.2, H-11) ppm. Based on the chemical shifts and splitting patterns of these protons, compound MP-5 appeared to be a derivative of bergenin with an additional acetyl group.

The ^{13}C-NMR spectrum of compound MP-5 (Figure 45, Table 19) was similar to that of bergenin. The HSQC (Figure 46) and HMBC (Figure 47) spectra displayed signals of the gallic acid moiety at δ_C 163.5 (C-6), 119.4 (C-6a), 110.2 (C-7), 151.7 (C-8), 141.2 (C-9), 148.9 (C-10) and 116.2 (C-10a) ppm. Six carbon signals of the glucose moiety were observed at δ_C 79.7 (C-2), 71.5 (C-3), 75.1 (C-4), 80.5 (C-4a), 73.8 (C-10b) and 64.0 (C-11) ppm. MP-5 also presented a signal for a methoxy group at δ_C 60.5 (CH_3O-9) ppm and signals for an acetyl group at 170.9 ($CH_3\underline{C}OO$-11) and 20.5 ($\underline{C}H_3COO$-11) ppm. The location of the acetyl group was determined by comparing the spectra of compound MP-2 and MP-5 (Table 18). The downfiled shift of C-11 and the upfield shift of C-2 were clearly observed. This phenomenon implied that the acetyl group was attached to C-11 of compound MP-5. This was further supported by the HMBC correlation from the acetyl carbonyl carbon to the C-11 methylene protons (Figure 48). Comparison of its NMR data and those of 11-*O*-acetylbergenin (Wang et al., 2008) revealed that they were identical (Table 20). Therefore, compound MP-5 was identified as 11-*O*-acetylbergenin. The specific rotation $[\alpha]^{20}_{D}$ is -96.2° (*c* 0.001, MeOH) agreed with the earlier reported value (Wang et al., 2008).

11-*O*-acetylbergenin [**140**] was earlier found in the twigs and leaves of *Flueggea virosa*. (Euphorbiaceae) (Wang et al., 2008). This is the first time that this compound was isolated from the genus *Mallotus*.

Table 18 ^{13}C-NMR Spectral data for compound MP-2 [**123**] and MP-5 [**140**]

Position	Compound MP-5	Compound MP-2	**Δδ**
	δ_C	δ_C	
2	79.7	81.8	-2.1
3	71.5	70.7	0.8
4	75.1	73.8	1.3
4a	80.5	79.8	0.7
6	163.5	163.4	0.1
6a	119.4	118.1	1.3
7	110.2	109.5	0.7
8	151.7	151.0	0.7
9	141.2	140.7	0.5
10	148.9	148.1	0.8
10a	116.2	116	0.2
10b	73.8	72.2	1.6
11	64.0	61.2	2.8
CH_3O-9	60.5	59.9	0.6
$CH_3\underline{C}OO$-11	170.9	-	-
$\underline{C}H_3COO$-11	20.5	-	-

Table 19 NMR Spectral data of compound MP-5 [**140**] (acetone-d_6) and 11-*O*-acetylbergenin (acetone-d_6)

Position	Compound MP-5		11-*O*-acetlybergenin*	
	δ_C	δ_H	δ_C	δ_H
2	79.7	4.01 (1H, m)	80.3	3.81 (1H, m)
3	71.5	3.57 (1H, br t, *J* = 8.3 Hz)	71.8	3.48 (1H, m)
4	75.1	3.98 (1H, m)	75.4	3.85 (1H, m)
4a	80.5	4.12 (1H, t, *J* = 10.0 Hz)	81.2	4.08 (1H, t, *J* = 9.9 Hz)
6	163.5	-	165.6	-
6a	119.4	-	119.4	-
7	110.2	7.09 (1H, s)	111.2	7.11 (1H, s)
8	151.7	-	152.4	-
9	141.2	-	142.3	-
10	148.9	-	149.3	-
10a	116.2	-	117.0	-
10b	73.8	5.10 (1H, d, *J* = 10.0 Hz)	74.3	4.98 (1H, d, *J* = 10.4 Hz)
11	64.0	4.70 (1H, dd, *J* = 2.1, 12.2 Hz), 4.23 (1H, dd, *J* = 7.1, 12.2 Hz)	64.6	4.26 and 4.65 (2H, m)
OH-3	-	4.98 (1H, br s)	-	-
OH-8	-	8.49 (1H, s)	-	-
OH-10	-	8.17 (1H, s)	-	-
CH_3O-9	60.5	3.89 (3H, s)	60.9	3.92 (3H, s)
$CH_3\underline{C}OO$-11	170.9	-	172.6	-
$\underline{C}H_3COO$-11	20.5	2.07 (3H, s)	20.9	2.13 (3H, s)

* NMR data from the reference (Wang et al., 2008).

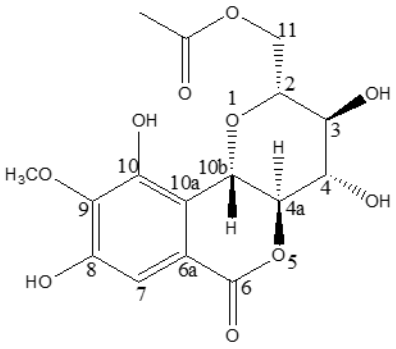

11-*O*-acetylbergenin [**140**]

1.6 Identification of compound MP-6 (scopoletin)

Compound MP-6 [**59**] was obtained as white needles (2.0 mg, 0.00003 % yield). It appeared as a blue fluorescent spot on the TLC plate under UV light at 254 nm and 365 nm. The ^{1}H-NMR spectrum of compound MP-6 (Figure 48, Table 20) showed a singlet for a methoxyl group at δ_H 3.96 (s, CH_3O-6) ppm, a singlet signal for a hydroxy group at δ_H 6.17 (s, OH-7) ppm, two signals of aromatic protons at δ_H 6.85 (s, H-5) and 6.92 (s, H-8) ppm and two doublets of olefinic protons at δ_H 6.28 (d, J = 9.5 Hz, H-3) and δ_H 7.60 (d, J = 9.5 Hz, H-4) ppm. The ^{13}C-NMR spectrum (Figure 49, Table 20) indicated the presence of the methoxyl group at δ_C 56.4 ppm (CH_3O-6), and exhibited two carbon signals of the double bond attached to ketone at δ_C 113.5 (C-3) and 143.3 ppm (C-4) and five aromatic carbon signals at δ_C 107.5 (C-5), 144.0 (C-6), 149.7 (C-7), 103.2 (C-8), 150.7 (C-9) and 111.5 ppm (C-10). Comparison of NMR data of compound MP-6 with previously reported values (Table 20) (Vasconcelos et al., 1998) indicated that compound MP-6 was identical with scopoletin. The ^{13}C-NMR spectrum did not show the signal of C-2 because of insufficient amounts of the sample.

Scopoletin [**59**] is a coumarin widely found in plants. It was previously found in *M. resinosus* (Rivière et al., 2010). Scopoletin isolated from roots of this plant exhibited DNA cleavage activity (Ma et al., 2004;Rivière et al., 2010). It also had acetylcholinesterase inhibitory activity and displayed antitumor activity against HL-60 promyelocytic cell by the activation of the signal cascade pathways including the

caspase-3 and the hetereodimeric redox-sensitive transcription factor nuclear factor kappa B. These led to the apoptosis of the tumor cells (Kim et al., 2005).

Table 20 NMR Spectral data of compound MP-6 [**59**] ($CDCl_3$) and scopoletin ($CDCl_3$)

Position	Compound MP-6		Scopoletin*	
	δ_C	δ_H	δ_C	δ_H
2	-	-	161.5	-
3	113.5	6.28 (1H, d, *J* = 9.5 Hz)	113.4	6.28 (1H, d, *J* = 9.5 Hz)
4	143.3	7.60 (1H, d, *J* = 9.5 Hz)	143.3	7.60 (1H, d, *J* = 9.5 Hz)
5	107.5	6.85 (1H, s)	107.4	6.85 (1H, s)
6	144.0	-	144.0	-
7	149.7	-	150.2	-
8	103.2	6.92 (1H, s)	103.2	6.91 (3H, s)
9	150.7	-	150.2	-
10	111.5	-	111.5	-
OH-7	-	6.17 (1H, s)		6.15 (1H, s)
CH_3O-6	56.4	3.96 (3H, s)	56.4	3.97 (3H, s)

* NMR data from the reference (Vasconcelos et al., 1998).

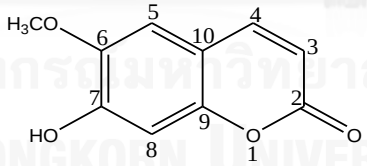

Scopoletin [**59**]

1.7 Identification of compound MP-7 (blumenol A)

Compound MP-7 [**141**] was obtained as yellow crystals (16.9 mg, 0.0002 % yield). It absorbed UV light at 254 nm. Its UV absorption maximum was at 271 nm (Figure 50). The HR-ESI mass spectrum (Figure 51) showed its sodium-adduct molecular ion $[M+Na]^+$ at *m/z* 247, indicating a molecular formula of $C_{13}H_{20}O_3$.

The ^{1}H-NMR spectrum of compound MP-7 (Figure 52, Table 21) showed three singlets of methyl protons at δ_H 0.98 (s, H-12), 1.03 (s, H-11) ppm and 1.87 (s, H-13) ppm and one doublets of methyl protons at δ_H 1.19 (d, *J* = 1.2 Hz, H-10) ppm. It also displayed two doublets at δ_H 2.08 (d, *J* = 16.9 Hz, H-2b) and 2.44 (d, *J* = 16.9 Hz, H-2a) ppm, indicating two geminally coupled methylene protons. Two proton signals at δ_H 5.83 (d, *J* = 15.4 Hz, H-7) and 5.84 (dd, *J* = 6.6, 15.4 Hz, H-8) ppm indicated the presence of *trans* olefinic protons.

The ^{13}C-NMR, DEPT and HSQC spectra (Figures 53-54, Table 21) displayed 13 carbon signals. The peaks at δ_C 126.8 (C-4), 164.3 (C-5) and 197.6 (C-3) ppm belonged to carbons of α,β-unsaturated ketone. Two peaks appearing at δ_C 129.4 (C-8) and 137.0 ppm (C-7) were due to an olefinic partial structure. The peak at δ_C 50.4 ppm (C-2) came from a methylene carbon. Four peaks observed at δ_C 19.2 (C-13), 23.4 (C-10), 24.2 (C-11) and 24.4 (C-12) ppm belonged to four methyl carbons, and the peak at δ_C 41.8 (C-1) ppm represented a quaternary carbon. Two resonances at δ_C 67.9 (C-9) and 79.4 (C-6) ppm belonged to two carbons that each contained a hydroxyl group. Compound MP-7 was identified as blumenol A by comparison of its NMR data and those of blumenol A (Table 21) (Liu et al., 1999). The HMBC correlations confirmed the structure (Figure 55) The CD spectrum (Figure 56) of compound MP-7 showed a positive cotton effect at 262 nm and a negative cotton effect at 328 nm, which were the same as that of blumenol A, which had C-6 and C-9 in *S* and *R* configuration, respectively. Therefore, the respective absolute configulations of C-6 and C-9 should be *S* and *R*.

Blumenol A [**141**] is a norisoprenoid with wide distribution. However, prior to this study there was no report of this compound from the genus *Mallotus*. The compound showed phytotoxic activity by inhibiting the growth of roots and shoots of other plants (Kato-Noguchi et al., 2012) and weak cytotoxic activity against cancer cells (Liu et al., 1999). Nevertheless, it was reported to be inactive against human

oral carcinoma (KB), human breast cancer (BC) and human small cell lung cancer (NCI-H187) cells (Phommart et al., 2005).

Table 21 NMR Spectral data of compound MP-7 [**141**] (acetone-d_6) and blumenol A (acetone-d_6)

Position	Compound MP-7		Blumenol A*	
	δ_C	δ_H	δ_C	δ_H
1	41.8	-	41.1	-
2	50.4	2.44 (1H, d, *J* = 16.9 Hz)	49.7	2.45 (1H, d, *J* = 17.0 Hz)
		2.08 (1H, d, *J* = 16.9 Hz)		2.25 (1H, d, *J* = 17.0 Hz)
3	197.6	-	197.9	-
4	126.8	5.78 (1H, m)	127	5.91 (1H, br s)
5	164.3	-	162.6	-
6	79.4	-	79.1	-
7	137.0	5.83 (1H, d, *J* = 15.4 Hz)	135.7	5.79 (1H, d, *J* = 15.5 Hz)
8	129.4	5.84 (1H, dd, *J* = 15.4, 6.6 Hz)	129.0	5.86 (1H, dd, *J* = 15.5, 6.0 Hz)
9	67.9	4.32 (1H, m)	68.1	4.42 (1H, m)
10	23.4	1.19 (3H, d, *J* = 1.2 Hz)	23.8	1.30 (3H, d, *J* = 1.5 Hz)
11	24.2	1.03 (3H, s)	22.9	1.02 (3H, s)
12	24.4	0.98 (3H, s)	24.0	1.09 (3H, s)
13	19.2	1.87 (3H, s)	18.9	1.90 (3H, br s)

* NMR data from the reference (Liu et al., 1999).

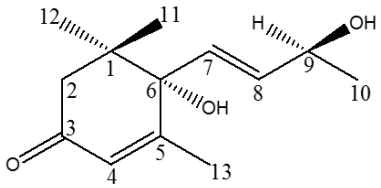

Blumenol A [**141**]

1.8 Structure elucidation of compound MP-8 (bergenin-8-*O*-α-L-rhamnoside)

Compound MP-8 [**142**] was obtained as colorless needles (41.7 mg, 0.0006 % yield). The UV spectrum (Figure 57) showed absorption maxima at 222 and 274 nm, which were similar to those of compounds MP-2 [**123**] and MP-5 [**140**]. The IR spectrum (Figure 58) showed absorption bands for hydroxyl groups at 3400 cm^{-1}, C=O stretching at 1722 cm^{-1}, C-O stretching at 1374, 1337 and 1093 cm^{-1}, and bands for an aromatic ring (=C-H stretching) at 3,000-3,200 cm^{-1}. Its molecular formula was $C_{20}H_{26}O_{14}$ as deduced from $[M+Na]^+$ 497.1287 in the mass spectrum (Figure 59). When it was exposed to heat (approximately 40 °C) during rotatory evaporation, the compound degraded to yield bergenin [**123**], as detected by TLC examination.

The ^{1}H-NMR and COSY spectra (Figures 60-62, Table 22) showed signals similar to those of compound MP-2, including the signals for the pentasubstituted gallic structure at δ_H 7.24 (s, H-7) and 8.59 (s, OH-10) ppm, methoxyl protons at δ_H 3.83 (s, CH_3O-9) and the glucose moiety at δ_H 3.59 (m, H-2), 3.21 (t, *J* = 9.0 Hz, H-3), 3.44 (m, H-11a), 3.67 (m, H-4), 3.85 (m, H-11b), 4.07 (t, *J* = 10.1 Hz, H-4a) and 5.04 (d, *J* = 10.1 Hz, H-10b) ppm. In addition, the spectrum exhibited proton signals for a rhamnose unit at δ_H 5.33 (br s, H-1′), 3.87 (m, H-2′), 3.64 (m, H-3′), 3.30 (t, *J* = 9.2 Hz, H-4′), 3.53 (m, H-5′) and 1.11 (d, *J* = 6.0 Hz, H-6′) ppm. This indicated that MP-8 was a derivative of bergenin [**123**] with rhamnose as an additional sugar moiety.

The ^{13}C-NMR and DEPT spectra of compound MP-8 (Figures 63-64, Table 22) displayed 20 signals. Fourteen signals belonged to the bergenin moiety, including δ_C 81.9 (C-2), 70.7 (C-3), 73.7 (C-4), 79.7 (C-4a), 163.3 (C-6), 119.2 (C-6a), 110.0 (C-7), 149.8 (C-8), 142.8 (C-9), 148.3 (C-10), 118.3 (C-10a), 72.1 (C-10b), 61.2 (C-11) and 60.4 (CH_3O-9) ppm. Additional six signals, including δ_C 99.7 (C-1′), 70.2 (C-2′), 70.5 (C-3′), 71.7 (C-4′), 70.1 (C-5′) and 18.0 (C-6′) ppm, were assignable to the rhamnose unit as interpreted from the correlation peaks in the HSQC spectra (Figures 65-69).

To determine the position of the rhamnose, HMBC (Figures 70-74) and NOESY (Figures 75-76) experiments were performed. The HMBC spectrum showed a correlation peak between H-1′ (*δ* 5.33 ppm, br s) and C-8 (*δ* 149.8 ppm) (Figure 72), indicating that the rhamnose was attached to C-8 of the bergenin structure through a (C-1′)-*O*-(C-8) ether bond. In addition, the absence of the resonance of OH-8 supported this proposed structure. The NOESY spectrum further confirmed the proposed structure by exhibiting a correlation peak between H-7 (*δ* 7.24 ppm, s) and H-1′ (*δ* 5.33 ppm, br s). Furthermore, the NOESY correlation peak observed between H-1′ (*δ* 5.33 ppm, br s) and H-2′ (*δ* 3.87 ppm, m) (Figure 76) confirmed the 1, 2 –di-equatorial relation in the *α*-rhamnopyranoside. The structure of compound MP-8 was then verified by an acid hydrolysis experiment (Figure 11). The TLC chromatograms in Figure 12 show that compound MP-8 consisted of two parts: the aglycone bergenin [**123**] and the sugar rhamnose. Therefore, compound MP-8 was characterized as bergenin-8-*O*-*α*-L-rhamnoside [**142**]. It should be noted that the structure of the aglycone bergenin was still intact after the hydrolysis reaction. This indicated that both the *C*-glycosidic bond and the lactone ring of bergenin were resistant to acid hydrolysis.

Table 22 NMR Spectral data of compound MP-8 [**142**] (DMSO-d_6)

Position	Compound MP-8		HMBC (H ⟶C)
	δ_H	δ_C	
2	3.59 (1H, m)	81.9	4
3	3.21 (1H, t, *J* = 9.0 Hz)	70.7	-
4	3.67 (1H, m)	73.7	10b
4a	4.07 (1H, t, *J* = 10.1 Hz)	79.7	10a, 10b
6	-	163.3	-
6a	-	119.2	-
7	7.24 (1H, s)	110.0	6, 8, 9, 10a
8	-	149.8	-
9	-	142.8	-
10	-	148.3	-
10a	-	118.3	
10b	5.04 (1H, d, *J* = 10.1 Hz)	72.1	4a, 10, 10a
11	3.44 (1H, m), 3.85 (1H, m)	61.2	2
OH-10	8.59 (1H, s)	-	9, 10, 10a
CH_3O-9	3.83 (3H, s)	60.4	9
1′	5.33 (1H, br s)	99.7	8, 2′, 3′
2′	3.87 (1H, m)	70.2	-
3′	3.64 (1H, m)	70.5	-
4′	3.30 (1H, t, *J* = 9.2 Hz)	71.7	-
5′	3.53 (1H, m)	70.1	1′, 3′, 6′
6′	1.11 (3H, d, *J* = 6.0 Hz)	18.0	4′, 5′

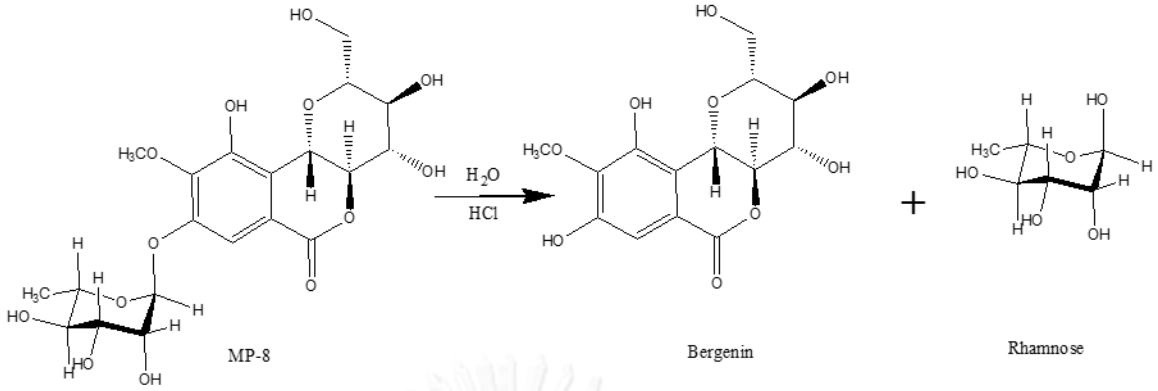

Figure 11 Acid hydrolysis of MP-8 [**142**]

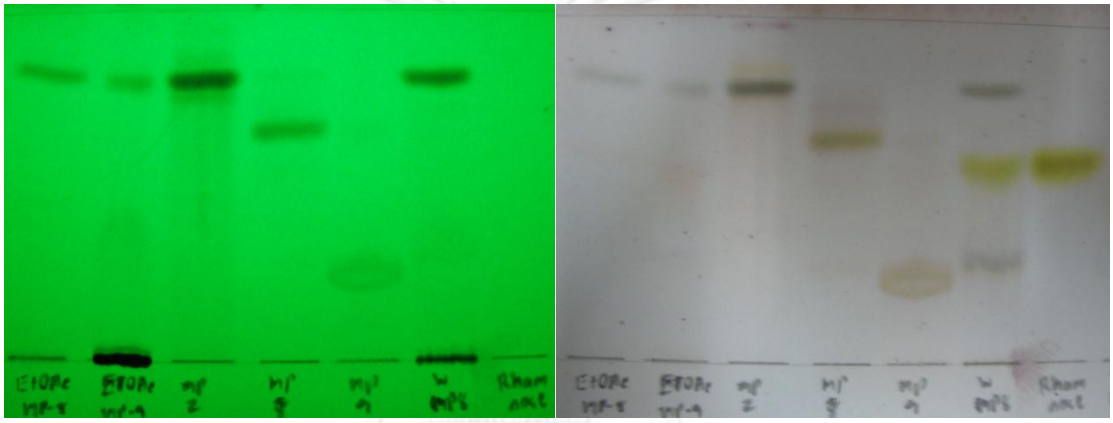

Figure 12 TLC chromatograms of acid hydrolysis products of compound MP-8 [**142**] under UV 254 nm (left) and spraying with 10 % sulfuric acid (right) [Stationary phase: silica gel 60 F_{254} plate; Mobile phase: $CHCl_3$-MeOH-H_2O (5:4:1); Lane 1: R_f 0.70 (EtOAc fraction of MP-8 hydrolysis product), Lane 2: R_f 0.70 (EtOAc fraction of MP-9 hydrolysis product), Lane 3: R_f 0.70 (bergenin), Lane 4: R_f 0.58 (MP-8), Lane 5: R_f 0.25 (MP-9), Lane 6: R_f 0.70, 0.55 (water fraction of MP-8 hydrolysis product), Lane 7: R_f 0.55 (rhamnose)].

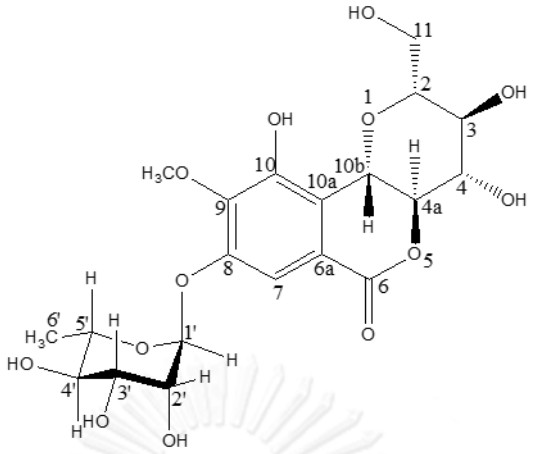

Bergenin-8-*O*-***α***-L-rhamnoside [**142**]

1.9 Structure elucidation of compound MP-9 (*seco*-bergenin-8-*O*-*α*-L-rhamnoside)

Compound MP-9 [**143**] was obtained as colorless cubic crystals (4.3 mg, 0.00006 % yield). It appeared as a dark spot on a TLC plate under UV light of 254 nm. Its UV absorption maximum appeared at 219 nm (Figure 77). The IR spectrum (Figure 78) showed absorption bands for hydroxyl groups at 3434 cm^{-1}, a carbonyl at 1623 $cm^{-1}$and an aromatic ring at 1574 cm^{-1}. The HR-ESI mass spectrum (Figure 79) showed a deprotonated molecular ion $[M-H]^-$ at *m/z* 491.1399, indicating that its molecular formula was $C_{20}H_{28}O_{14}$.

The ^{1}H-NMR and COSY spectra (Figures 80-82, Table 23) showed signals similar to those of compound MP-8 [**142**] (Table 23), including the signal of the pentasubstituted gallic moiety at δ_H 7.02 ppm (s, H-7), methoxyl protons at δ_H 3.83 (s, CH_3O-9) and the glucose moiety at δ_H 3.40 (m, H-2), 3.50 (t, *J* = 9.6 Hz, H-3), 3.43 (t, *J* = 9.6 Hz, H-4), 3.69 (m, H-4a), 3.83 (m, H-11) and 5.14 (d, *J* = 9.9 Hz, H-10b) ppm and signals of the rhamnose moiety at δ_H 5.48 (br s, H-1′), 4.06 (dd, *J* = 3.3, 1.7 Hz, H-2′), 3.90 (dd, *J* = 9.6, 3.3 Hz, H-3′), 3.54 (m, H-4′), 3.71 (m, H-5′) and 1.23 (d, *J* = 6.2 Hz, H-6′) ppm. However, H-4a and H-7 of MP-9, which appeared at δ_H 3.69 and 7.02 ppm, respectively, were shifted upfield as compared with those of compound MP-8. This suggested that compound MP-9 was a derivative of compound MP-8 [**142**].

The ^{13}C-NMR, DEPT and HSQC spectra of MP-9 exhibited 20 signals similar to those of compound MP-8 [**142**] (Figures 83-89, Table 23), including resonances for the gallic acid structure at δ_C 176.1 (C-6), 137.3 (C-6a), 109.3 (C-7), 150.4 (C-8, 10), 140.2 (C-9) and 117.8 (C-10a) ppm, the glucose moiety at δ_C 82.8 (C-2), 80.7 (C-3), 73.9 (C-4), 74.3 (C-4a), 80.1 (C-10b) and 62.1 (C-11) ppm and the rhamnose unit at δ_C 100.5 (C-1′), 72.2 (C-2′), 72.4 (C-3′), 71.1 (C-4′), 71.0 (C-5′) and 18.1 (C-6′) ppm, as well as a methoxyl carbon at 61.4 (CH_3O-9) ppm. However, the carbons that were part of the lactone ring, including C-4a, C-6, and C-6a, differed from those of compound MP-8. In MP-9, C-4a was shifted upfield to δ_C 74.3 ppm, whereas C-6 and C-6a of MP-9 were moved to δ_C 176.1 and 137.3 ppm, respectively. The downfield shift of C-6 could be caused by the opening of the lactone ring, which resulted in the formation of a free carboxyl and a hydroxyl group at C-6a and C-4a, respectively. In addition, the shift of the C=O IR band to a lower position at 1623 cm^{-1} in comparison to that of MP-8 further supported a free carboxylic acid in the place of the lactone functionality. These observations agreed with the fact that the molecular mass of compound MP-9 (as deduced from $[M-H]^-$ at 491.1399 calcd. for $C_{20}H_{27}O_{14}$, 491.1406) was 18 amu higher than that of compound MP-8. Therefore, the aglycone part of compound MP-9 should be *seco*-bergenin, not bergenin.

In order to confirm the position of the rhamnose unit, an HMBC experiment was performed (Figures 90-94, Table 23). In the HMBC spectrum there was a correlation peak between H-1′ (δ_H 5.48 ppm, br s) and C-8 (δ_C 150.4 ppm), which was similar to that of compound MP-8. This confirmed the linkage of C-1′ of the rhamnose to C-8 of the aglycone part. Furthermore, the NOESY correlation peak between H-7 (7.02 ppm, s) and H-1′ (5.48 ppm, br s), (Figures 95-96) further supported the location of the rhamnose. Compound MP-9 was determined as new naturally occurring compound, and named *seco*-bergenin-8-*O*-**α**-L-rhamnoside [**143**]. Finally, the proposed structure of compound MP-9 was verified by an acid hydrolysis reaction (Figure 13). The hydrolysis products were identified by TLC (Figure 14) to be

rhamnose and bergenin. This means that the free carboxylic acid group of the aglycone part was rapidly cyclized to form a lactone ring to give the bergenin structure during the acid hydrolysis reaction.

Table 23 NMR Spectral data of compound MP-9 [**143**] (CD_3OD)

Position	Compound MP-9		HMBC (H ⟶ C)
	δ_H	δ_C	
2	3.40 (1H, m)	82.8	-
3	3.50 (1H, t, *J* = 9.6 Hz)	80.7	-
4	3.43 (1H, t, *J* = 9.6 Hz)	73.9	-
4a	3.69 (1H, m)	74.3	3
6	-	176.1	-
6a	-	137.3	-
7	7.02 (1H, s)	109.3	6, 8, 9, 10a
8	-	150.4	-
9	-	140.2	-
10	-	150.4	-
10a	-	117.8	-
10b	5.14 (1H, d, *J* = 9.9 Hz)	80.1	4, 10, 10a
11	3.83 (2H, m)	62.1	-
CH_3O-9	3.83 (3H, s)	61.4	9
1′	5.48 (1H, br s)	100.5	8, 2′, 3′
2′	4.06 (1H, dd, *J* = 3.3, 1.7 Hz)	72.2	-
3′	3.90 (1H, dd, *J* = 9.6, 3.3 Hz)	72.4	-
4′	3.54 (1H, m)	71.1	-
5′	3.71 (1H, m)	71.0	-
6′	1.23 (3H, d, *J* = 6.2 Hz)	18.1	3′, 4′, 5′

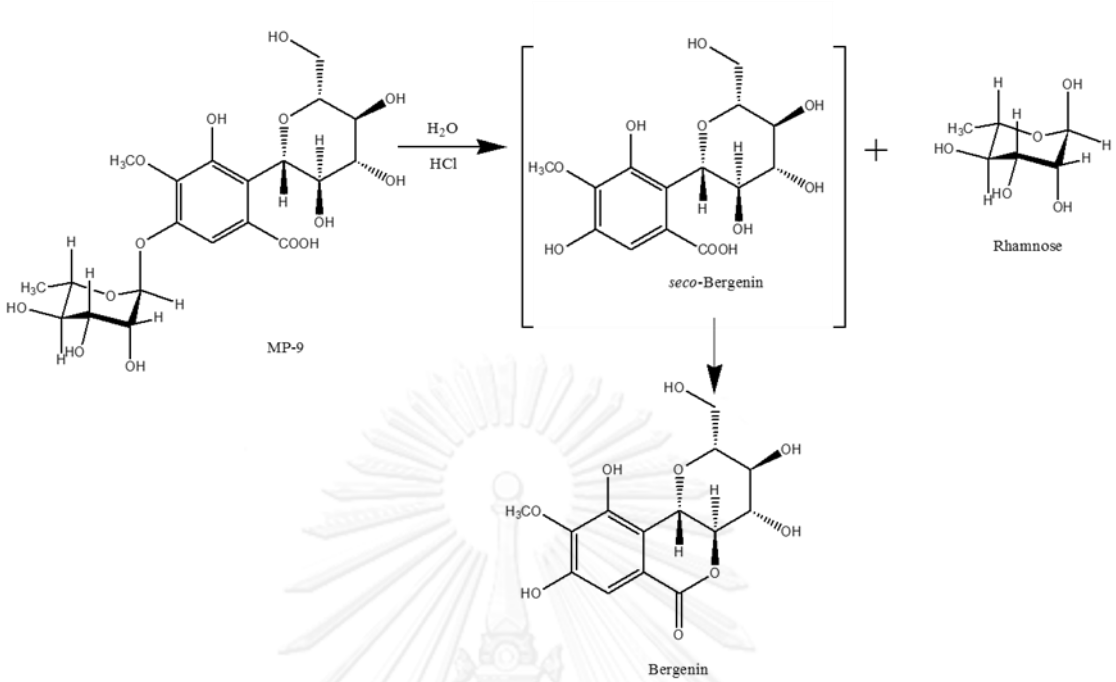

Figure 13 Acid hydrolysis of MP-9 [**143**]

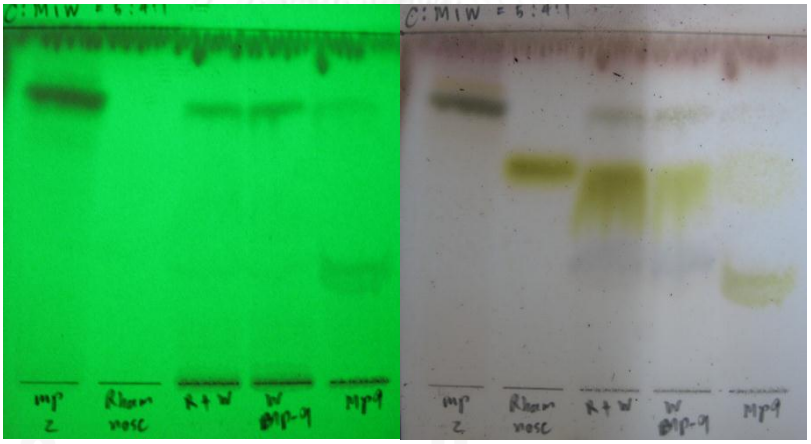

Figure 14 TLC chromatograms of acid hydrolysis products of compound MP-9 [**143**] under UV 254 nm (left) and spraying with 10 % sulfuric acid (right) [Stationary phase: silica gel 60 F_{254} plate; Mobile phase: $CHCl_3$-MeOH-H_2O (5:4:1); Lane 1: R_f 0.70 (bergenin), Lane 2: R_f 0.55 (rhamnose), Lane 3: R_f 0.70, 0.55 (rhamnose plus water fraction of MP-9 hydrolysis product), Lane 4: R_f 0.70, 0.55 (water fraction of MP-9 hydrolysis product), Lane 5: R_f 0.25 (MP-9)].

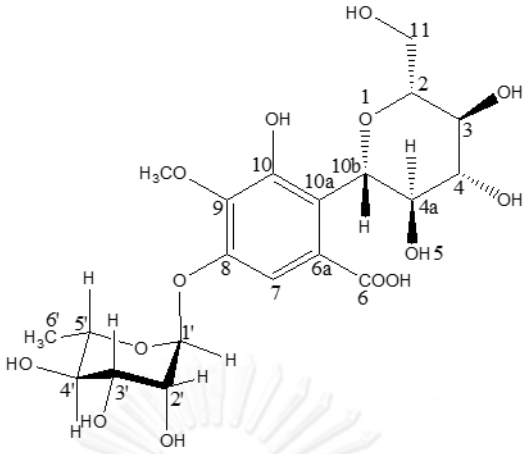

seco-Bergenin-8-*O*-**α**-L-rhamnoside [**143**]

Compounds **142** and **143** both are members of gallic acid *C*-glycosides, a very small group of secondary metabolites with limited distribution (Bao et al., 2012). Most of gallic acid glycosides occur in the form of galloyl esters. It should be noted that the structures of bergenin [**123**] and its derivatives [**140** and **142**] have an uncommon six-membered lactone ring which links the sugar to the aglycone. It could be proposed that this α-pyrone structure is constructed by the formation of a carbon-carbon bond between the aglycone (gallic acid) and the sugar (glucose), followed by the esterification of the carboxyl group of the gallic acid with a hydroxyl group of the glucose.

2. Evaluation of biological activities

2.1 Evaluation of anti-HSV activity

All of the compounds isolated from stem bark of *M. plicatus*, except for MP-6 due to insufficient amounts, were evaluated for antiviral activity against 2 types of HSV (HSV-1 and HSV-2), and the results are summarized in Table 24.

Table 24 Anti-herpetic activity of isolated compounds

Compounds	IC_{50} (μg/mL)		IC_{50} (μM)	
	HSV-1	HSV-2	HSV-1	HSV-2
Aleuritolic acid 3-acetate (MP-1) [**40**]	inactive	inactive	inactive	inactive
Bergenin (MP-2) [**123**]	inactive	inactive	inactive	inactive
Daucosterol (MP-3) [**56**]	inactive	inactive	inactive	inactive
Protocatechuic acid (MP-4) [**139**]	95.0	95.0	620.9	620.9
11-*O*-acetylbergenin (MP-5) [**140**]	inactive	inactive	inactive	inactive
Blumenol A (MP-7) [**141**]	inactive	inactive	inactive	inactive
Bergenin-8-*O*-**α**-L- rhamnoside (MP-8) [**142**]	inactive	inactive	inactive	inactive
seco-bergenin-8-*O*-**α**-L- rhamnoside (MP-9) [**143**]	95.0	95.0	193.1	193.1
acyclovir	0.63	-	2.8	-

Inactive = Less than 50 % inhibition at concentration of 100 μg/mL

ND = not determined

In this study, protocatechuic acid [**139**] and *seco*-bergenin-8-*O*-**α**-L-rhamnoside [**143**] exhibited weak antiviral potential against the two types of HSV. It could be noted that *seco*-bergenin-8-*O*-**α**-L- rhamnoside [**143**] was active whereas its 3 derivatives, including bergenin [**123**], 11-*O*-acetylbergenin [**140**] and bergenin-8-*O*-**α**-L- rhamnoside [**142**] were devoid of antiviral activity. However, bergenin [**123**] was earlier reported to posse anti-HSV activity (Patel et al., 2012). The differing result

observed in this study was probably due to the difference of the methods used in this and in the previous report. The antiviral potential of protocatechuic acid [**139**] and *seco*-bergenin-8-*O*-**α**-L- rhamnoside [**143**] suggested that a free carboxylic acid group might play an important role in the activity. However, both compounds possessed weak antiviral activity against the herpes virus as compared with the positive control, acyclovir.

2.2 Evaluation of cytotoxicity against KB cells

In this experiment, only compounds MP-1 [**40**], MP-2 [**123**], and MP-5 [**140**] were selected for cytotoxicity evaluation. MP-4 [**139**] and MP-7 [**141**] (Phommart et al., 2005) have been reported to be inactive against KB cells (Keawsa-ard et al., 2012), whereas the other compounds were not evaluated due to their insufficient amounts.

Table 25 Cytotoxic activity against KB cells of isolated compounds

Compounds	IC_{50} (μg/mL)
Aleuritolic acid 3-acetate (MP-1) [**40**]	Inactive
Bergenin (MP-2) [**123**]	Inactive
11-*O*-acetylbergenin (MP-5) [**140**]	Inactive
Doxorubicin	0.96
Ellipticine	1.00

Inactive = Less than 50 % inhibition at concentration of 50 μg/mL

From the results (Table 25), it can be seen that none of the tested compounds were active against KB cells. However, aleuritolic acid 3-acetate (MP-1) was reported to be cytotoxic against U251 neuroblastoma cells with an IC_{50} value of 8.4 μM (Reyes et al., 2010) and human lung carcinoma A549 cells with the IC_{50} value of 13.84 μM (Wada and Tanaka, 2006). Although scopoletin (MP-6) was not evaluated in this study, it was reported to have weakly cytotoxic activity against KB cells (IC_{50} 624 μM) (Thani et al., 2010).

2.3 Evaluation of scavenging activity against DPPH free radicals

Compound MP-2 [**123**], MP-5 [**140**], MP-7 [**141**] and MP-8 [**142**] were further evaluated for this activity, as judged from their sufficient amounts. All results are shown in Table 26.

Table 26 DPPH free radical scavenging activity of isolated compounds

Compounds	IC_{50} (µg/mL)
Bergenin (MP-2) [**123**]	Inactive
11-*O*-acetylbergenin (MP-5) [**140**])	Inactive
Blumenol A (MP-7) [**141**]	Inactive
Bergenin-8-*O*-**α**-L- rhamnoside (MP-8) [**142**]	Inactive
Vitamin C	5.2

Inactive = Less than 50 % inhibition at concentration of 100 µg/mL

In this study, none of the tested compounds were active against DPPH free radicals at a concentration of 100 µg/mL. However, bergenin [**123**] has been reported to have DPPH scavenging activity, but at a very high concentration (Rana et al., 2005). It is possible that the anti DPPH activity of the MeOH extract of *M. plicatus* as observed by TLC autography was due to the tannins present in the bark, which were not isolated in this study.

CHAPTER V

CONCLUSION

During the screening of medicinal plants for anti-herpetic activity, the EtOAc extract and MeOH extract from the stem bark of *Mallotus plicatus* showed antiviral potential. The chemical investigation of these extracts yielded nine pure compounds. Two compounds were determined to be new structures, including bergenin-8-*O*-**α**-L-rhamnoside [**142**] and *seco*-bergenin-8-*O*-**α**-L-rhamnoside [**143**]. Both compounds are derivatives of gallic acid *C*-glucoside, a very small group of secondary metabolites with limited distribution. The other seven isolates were identified as known compounds, which included aleuritolic acid 3-acetate [**40**], bergenin [**123**], daucosterol [**56**], protocatechuic acid [**139**], 11-*O*-acetylbergenin [**140**], scopoletin [**59**] and blumenol A [**141**]. All of the isolated compounds, except for bergenin [**123**], were not reported in the previous study of this plant (Van Minh et al., 2009). Among the known structures, 11-*O*-acetylbergenin and blumenol A were identified from the genus *Mallotus* for the first time in this study. It should be reiterated that compounds **123**, **140**, **142** and **143** represent a rare type of gallic acid *C*-glycoside. From the diversified structures of the compounds identified from *M. plicatus*, it can be said that several types of secondary metabolites are produced by this plant. The chemical data thus obtained in this investigation should be useful for the future chemotaxonomic study of the genus *Mallotus*.

The compounds isolated from *M. plicatus* were also investigated for anti-HSV activity by the plaque reduction assay. The results showed that two compounds, protocatechuic acid [**139**] and *seco*-bergenin-8-*O*-**α**-L-rhamnoside [**143**], possessed weak antiviral activity, while the others were totally devoid of activity. The two active compounds appeared to be, at least in part, responsible for the antiviral activities of the EtOAc and MeOH extracts. *seco*-Bergenin-8-*O*-**α**-L-rhamnoside was more potent than protocatechuic acid. This fact could explain the higher antiviral activity of the MeOH extract as compared to that of the EtOAc extract. It should be noted that

both compounds [**139** and**143**] have a free carboxyl group in their structures, suggesting that this moiety might be important for the antiviral activity. It could be further postulated that these compounds inhibited the viral infection by reducing the ability of HSV to infect host cells, leading to decrease in the number of host cell death. Finally, some of the compounds isolated from *M. plicatus* were also evaluated for cytotoxicity and DPPH free radical scavenging activity, but none of them showed the activities.

REFERENCES

Akhtar, P., Ali, M., Sharma, M. P., Farooqi, H. and Khan, H. N. 2010. Phytochemical investigation of fruits of *Corylus colurna* Linn. Journal of Phytology 2: 89-100.

Alvarez, A. L., et al. 2012. Apple pomace, a by-product from the asturian cider industry, inhibits herpes simplex virus types 1 and 2 in vitro replication: study of its mechanisms of action. J Med Food 15(6): 581-587.

An, T. Y., Hu, L. H., Cheng, X. F. and Chen, Z. L. 2001. Benzopyran derivatives from *Mallotus apelta*. Phytochemistry 57(2): 273-278.

Arfan, M., et al. 2007. Antioxidant activity of extracts of *Mallotus philippinensis* fruit and bark. Journal of Food Lipids 14(3): 280-297.

Bai, Y., Yang, Y. p. and Ye, Y. 2006. Hookerianolides A-C: three novel casbane-type diterpenoid lactones from *Mallotus hookerianus*. Tetrahedron Lett 47(37): 4-4.

Bandopadhyay, M., Dhingra, V. K., Mukerjee, S. K., Pardeshi, N. P. and Seshadri, T. R. 1972. Triterpenoid and other components of *Mallotus Philippinensis*. Phytochemistry 11(4): 1511.

Bao, L. M., et al. 2012. Hydrolysable tannins isolated from *Syzygium aromaticum*: structure of a new C-glucosidic ellagitannin and spectral features of tannins with a tergalloyl group. Heterocycles 85(2): 365-381.

Bollendorff, S. M., Welzen, P. C. and Silk, J. W. F. 2000. A taxonomic revision of *Mallotus* section *Polyadenii* (Euphorbiaceae). Blumea 45(2): 319-340.

Chattopadhyay, D., Arunachalam, G., Mandal, A. B. and Bhattacharya, S. K. 2006. Dose-dependent therapeutic antiinfectives from ethnomedicines of bay islands. Chemotherapy 52(3): 151-157.

Chattopadhyay, D., et al. 2002. Antimicrobial and anti-inflammatory activity of folklore: *Mallotus peltatus* leaf extract. Journal of Ethnopharmacology 82(2–3): 229-237.

Chattopadhyay, D., Arunachalam, G., Mandal, S. C., Bhadra, R. and Mandal, A. B. 2003. CNS activity of the methanol extract of *Mallotus peltatus* (Geist) Muell Arg. leaf: an ethnomedicine of Onge. Journal of Ethnopharmacology 85(1): 99-105.

Chaudhuri, S. K., et al. 1995. Isolation and structural elucidation of pentacyclic triterpenoids from *Maprounea africana*. Journal of Natural Products 58(1): 1-9.

Cheng, X. F. and Chen, Z. L. 1999. Three new diterpenoids from *Mallotus apelta* Muell.Arg. Journal of Asian Natural Products Research 1(4): 319-325.

Cheng, X. F. and Chen, Z. L. 2000. Coumarinolignoids of *Mallotus apelta*. Fitoterapia 71(3): 341-342.

Cheng, X. F., Chen, Z. L. and Zeng-Mu, M. 1999. Three new diterpenoids from *Mallotus apelta* Muell. Arg. Journal of Asian Natural Products Research 1(163-168).

Cheng, X. F., Meng, Z. M. and Chen, Z. L. 1998. A pyridine-type alkaloid from *Mallotus apelta*. Phytochemistry 49(7): 2193-2194.

Daikonya, A., Katsuki, S. and Kitanaka, S. 2004. Antiallergic Agents from Natural Sources 9. Inhibition of Nitric Oxide Production by Novel Chalcone Derivatives from *Mallotus philippinensis* (Euphorbiaceae). Chemical and Pharmaceutical Bulletin 52(11): 1326-1329.

Deng, J., Xiao, X., Tong, X. and Li, G. 2010. Preparation of bergenin from *Ardisia crenata* sims and *Rodgersia sambucifolia* hemsl based on microwave-assisted extraction/high-speed counter-current chromatography. Separation and Purification Technology 74(2): 155-159.

Department of National Park, W. a. P. C., the Forest Herbarium (2007). Flora of Thailand. Bangkok, Ministry of Natural Resource and Environment.

Giang, P., Trang, V. and Son, P. 2013. Phytochemical studies on *Mallotus barbatus*. Chemistry of Natural Compounds 49(1): 129-130.

Hikino, H., Tamada, M. and Yen, K. Y. 1978. Mallorepine, cyano–γ–pyridone from *Mallotus repandus*. Planta Med 33(04): 385-388.

Huang, P. L., Wang, L. W. and Lin, C. N. 1999. New triterpenoids of *Mallotus repandus*. Journal of Natural Products 62(6): 891-892.

Hui, W. H., Chan, C. K., Chow, L. C., Ng, H. Y. and Siu, Y. K. 1969. Triterpenoids and sterols of *Aporosa chinensis* and *Mallotus paniculatus*. Phytochemistry 8(2): 519.

Intahphuak, S., et al. 2004. Anti-inflammatory and analgesic activities of *Mallotus spodocarpus* Airy Shaw. Journal of Ethnopharmacology 90(1): 69-72.

Kato-Noguchi, H., Tamura, K., Sasaki, H. and Suenaga, K. 2012. Identification of two phytotoxins, blumenol A and grasshopper ketone, in the allelopathic Japanese rice variety *Awaakamai*. Journal of Plant Physiology 169(7): 682-685.

Keawsa-ard, S., et al. 2012. Anticancer and antibacterial activities of the isolated compounds from *Solanum spirale* Roxb. leaves. Chiang Mai Journal of Science 39(3): 445-454.

Kiem, P., et al. 2005. New cytotoxic benzopyrans from the leaves of *Mallotus apelta*. Archives of Pharmacal Research 28(10): 1131-1134.

Kiem, P., et al. 2004. Pentacyclic triterpenoids from *Mallotus apelta*. Archives of Pharmacal Research 27(11): 1109-1113.

Kim, E. K., et al. 2005. Scopoletin induces apoptosis in human promyeloleukemic cells, accompanied by activations of nuclear factor **κ**B and caspase-3. Life Sciences 77(7): 824-836.

Kumar, V. P., Chauhan, N. S., Padh, H. and Rajani, M. 2006. Search for antibacterial and antifungal agents from selected Indian medicinal plants. Journal of Ethnopharmacology 107(2): 182-188.

Lee, J. H., et al. 2007. Immunoregulatory activity by daucosterol, a β-sitosterol glycoside, induces protective Th1 immune response against disseminated Candidiasis in mice. Vaccine 25(19): 3834-3840.

Likhitwitayawuid, K., et al. 2005. Phenolics with Anti-HSV and Anti-HIV Activities from *Artocarpus gomezianus*, *Mallotus pallidus*, and *Triphasia trifolia*. Pharmaceutical Biology 43(8): 651-657.

Lin, H. H., Chen, J. H., Chou, F. P. and Wang, C. J. 2011. Protocatechuic acid inhibits cancer cell metastasis involving the down-regulation of Ras/Akt/NF-**K**B pathway and MMP-2 production by targeting RhoB activation. British Journal of Pharmacology 162(1): 237-254.

Lin, J. M., Lin, C. C., Chen, M. F., Ujiie, T. and Takada, A. 1995. Scavenging effects of *Mallotus repandus* on active oxygen species. Journal of Ethnopharmacology 46(3): 175-181.

Liu, C. L., Wang, J. M., Chu, C. Y., Cheng, M. T. and Tseng, T. H. 2002. In vivo protective effect of protocatechuic acid on tert-butyl hydroperoxide-induced rat hepatotoxicity. Food and Chemical Toxicology 40(5): 635-641.

Liu, X., Tian, F., Zhang, H. B., Pilarinou, E. and McLaughlin, J. L. 1999. Biologically active blumenol A from the leaves of *Annona Glabra*. Natural Product Letters 14(1): 77-81.

Lounasmaa, M., Widén, C. J., Tuuf, C. M. and Huhtikangas, A. 1975. On the phloroglucinol derivatives of *Mallotus philippinensis*. Planta Med 28(05): 16-31.

Ma, J., Jones, S. H. and Hecht, S. M. 2004. A Coumarin from *Mallotus resinosus* that mediates DNA cleavage. Journal of Natural Products 67(9): 1614-1616.

Moorty, K., Srinivasan, K., Subramanian, C., Mohanasundari, C. and Palaniswamy, M. 2007. Phytochemical screening and antibacterial evaluation of stem bark of *Mallotus philippinensis* var. Tomentosus. African Journal of Biotechnology 6(13): 1521-1523.

Nair, S. P. and Madhusudana Rao, J. 1993. Kamaladiol-3-acetate from the stem bark of *Mallotus philippinensis*. Phytochemistry 32(2): 407-409.

Nasser, J. A., Yaacob, W. A., Din, L. B., Yamin, B. M. and Latip, J. 2009. Isolation of atranorin, bergenin and goniothalamin from *Hopea sangal*. ARPN Journal of Engineering and Applied Science 4(1): 92-95.

O'Brien, J., Wilson, I., Orton, T. and Pognan, F. 2000. Investigation of the Alamar Blue (resazurin) fluorescent dye for the assessment of mammalian cell cytotoxicity. Eur J Biochem 267(17): 5421-5426.

Ono, K., et al. 1989. Differential inhibitory effects of various herb extracts on the activities of reverse transcriptase and various deoxyribonucleic acid (DNA) polymerases. CHEMICAL & PHARMACEUTICAL BULLETIN 37(7): 1810-1812.

Patel, D. K., Patel, K., Kumar, R., Gadewar, M. and Tahilyani, V. 2012. Pharmacological and analytical aspects of bergenin: a concise report. Asian Pacific Journal of Tropical Disease 2(2): 163-167.

Phommart, S., Sutthivaiyakit, P., Chimnoi, N., Ruchirawat, S. and Sutthivaiyakit, S. 2005. Constituents of the leaves of *Macaranga tanarius*. Journal of Natural Products 68(6): 927-930.

Prachayasittikul, S., et al. 2009. Bioactive metabolites from *Spilanthes acmella* Murr. Molecules 14(2): 850-867.

Rahman, A. and Ahmad, V. U. (1994). Handbook of natural products data. Amsterdam, Elsvier Science.

Rana, V. S., Rawat, M. S. M., Pant, G. and Nagatsu, A. 2005. Chemical constituents and antioxidant activity of *Mallotus roxburghianus* leaves. Chemistry & Biodiversity 2(6): 792-798.

Reyes, B. M., Ramírez-Apan, M. a. T., Toscano, R. n. A. and Delgado, G. 2010. Triterpenes from *Garcia parviflora*. Cytotoxic evaluation of natural and semisynthetic friedelanes. Journal of Natural Products 73(11): 1839-1845.

Rivière, C., et al. 2009. Polyphenols isolated from antiradical extracts of *Mallotus metcalfianus*. Phytochemistry 70(1): 86-94.

Rivière, C., et al. 2010. Mallotus species from Vietnamese mountainous areas: phytochemistry and pharmacological activities. Phytochemistry Reviews 9(2): 217-253.

Saijo, R., Nonaka, G. I. and Nishioka, I. 1989. Tannins and related compounds. LXXXVII. : isolation and characterization of four new hydrolysable tannins from the leaves of *Mallotus repandus*. CHEMICAL & PHARMACEUTICAL BULLETIN 37(10): 2624-2630.

Silva, S. L. d., Oliveira, V. G. d., Yano, T. and Nunomura, R. d. C. S. 2009. Antimicrobial activity of bergenin from *Endopleura uchi* (Huber) Cuatrec. Acta Amazonica 39: 187-191.

Sritularak, B., Tantrakarnsakul, K., Lipipun, V. and Likhitwitayawuid, K. 2013. Flavonoids with anti-HSV activity from the root bark of *Artocarpus lakoocha*. Nat Prod Commun 8(8): 1079-1080.

Supudompol, B., Likhitwitayawuid, K. and Houghton, P. J. 2004. Phloroglucinol derivatives from *Mallotus pallidus*. Phytochemistry 65(18): 2589-2594.

Sutthivaiyakit, S., Thongtan, J., Pisutjaroenpong, S., Jiaranantanont, K. and Kongsaeree, P. 2001. D:A Friedo-oleanane lactones from the stems of *Mallotus repandus*. Journal of Natural Products 64(5): 569-571.

Tanaka, T., Ito, T., Iinuma, M., Takahashi, Y. and Naganawa, H. 1998. Dimeric chalcone derivatives from *Mallotus philippensis*. Phytochemistry 48(8): 1423-1427.

Taneyama, M. and Yoshida, S. 1978. Studies on C-glycosides in higher plants. The botanical magazine = Shokubutsu-gaku-zasshi 91(2): 109-112.

Taneyama, M., Yoshida, S., Kobayashi, M. and Hasegawa, M. 1983. Isolation of norbergenin from *Saxifraga stolonifera*. Phytochemistry 22(4): 1053-1054.

Thakur, S. C., Thakur, S. S., Chaube, S. K. and Singh, S. P. 2005. An etheral extract of Kamala (*Mallotus philippinensis* (Moll.Arg) Lam.) seed induce adverse effects on reproductive parameters of female rats. Reproductive Toxicology 20(1): 149-156.

Thani, W., Vallisuta, O., Siripong, P. and Ruangwises, N. 2010. Anti-proliferative and antioxidative activities of Thai noni/Yor (*Morinda citrifolia* Linn.) leaf extract. Southeast Asian J Trop Med Public Health 41(2): 482-489.

Tomizawa, S., Asuke, K. and Suguro, N. 1976. Bergenin: isocoumarin from the stems of *Mallotus repandus*. Phytochemistry 15(2): 328.

Van Minh, C., et al. 2009. Two new megastigmane sulphonoglucosides from *Mallotus anisopodus*. (1934-578X (Print)).

Vasconcelos, J. M. J., Silva, A. M. S. and Cavaleiro, J. A. S. 1998. Chromones and flavanones from *Artemisia campestris* subsp. maritima. Phytochemistry 49(5): 1421-1424.

Wada, S. I. and Tanaka, R. 2006. Isolation, DNA topoisomerase-II inhibition, and cytotoxicity of three new terpenoids from the bark of *Macaranga tanarius*. Chemistry & Biodiversity 3(4): 473-479.

Wai-Haan, H. and Man-Moon, L. 1976. Triterpenoids from two *Mallotus* species: a nor-triterpene and two new acids. Phytochemistry 15(6): 985-986.

Wai-Haan, H. and Man-Moon, L. 1977. Triterpenoids from *Mallotus repandus*: Three new δ-lactones. Phytochemistry 16(1): 113-115.

Wang, G. C., Liang, J. P., Wang, Y., Li, Q. and Ye, W. C. 2008. Chemical constituents from *Flueggea virosa*. Chinese Journal of Natural Medicines 6(4): 251-253.

Welzen, P. C., V. . 2013. *Mallotus actinoneurus* and *Mallotus tokiae* (Euphorbiaceae), a new record and a new species in Thailand. . Thai Forest Bulletin (Botany) 41: 85-89.

Xu, J. F., Feng, Z. M., Liu, J. and Zhang, P. C. 2008. New hepatoprotective coumarinolignoids from *Mallotus apelta*. Chemistry & Biodiversity 5(4): 591-597.

Yang, L. L., Yen, K. Y., Kiso, Y. and Hikino, H. 1987. Antihepatotoxic actions of formosan plant drugs. Journal of Ethnopharmacology 19(1): 103-110.

Yen, G. C. and Hsieh, C. L. 2000. Reactive oxygen species scavenging activity of Du-zhong (*Eucommia ulmoides* Oliv.) and its active compounds. Journal of Agricultural and Food Chemistry 48(8): 3431-3436.

Zaidi, S. F. H., et al. 2009. Potent bactericidal constituents from *Mallotus philippinensis* against clarithromycin and metronidazole resistant strains of Japanese and Pakistani *Helicobacter pylori*. Biological and Pharmaceutical Bulletin 32(4): 631-636.

APPENDIX

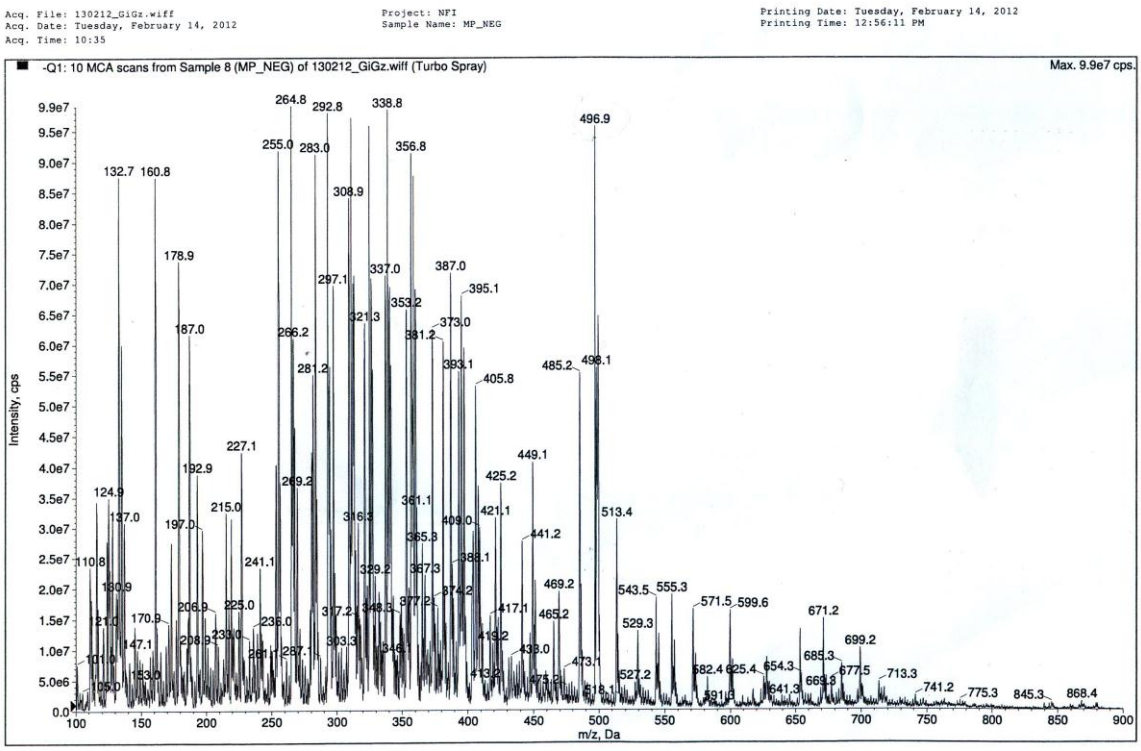

Figure 15 ESI Mass spectrum of compound MP-1[**40**]

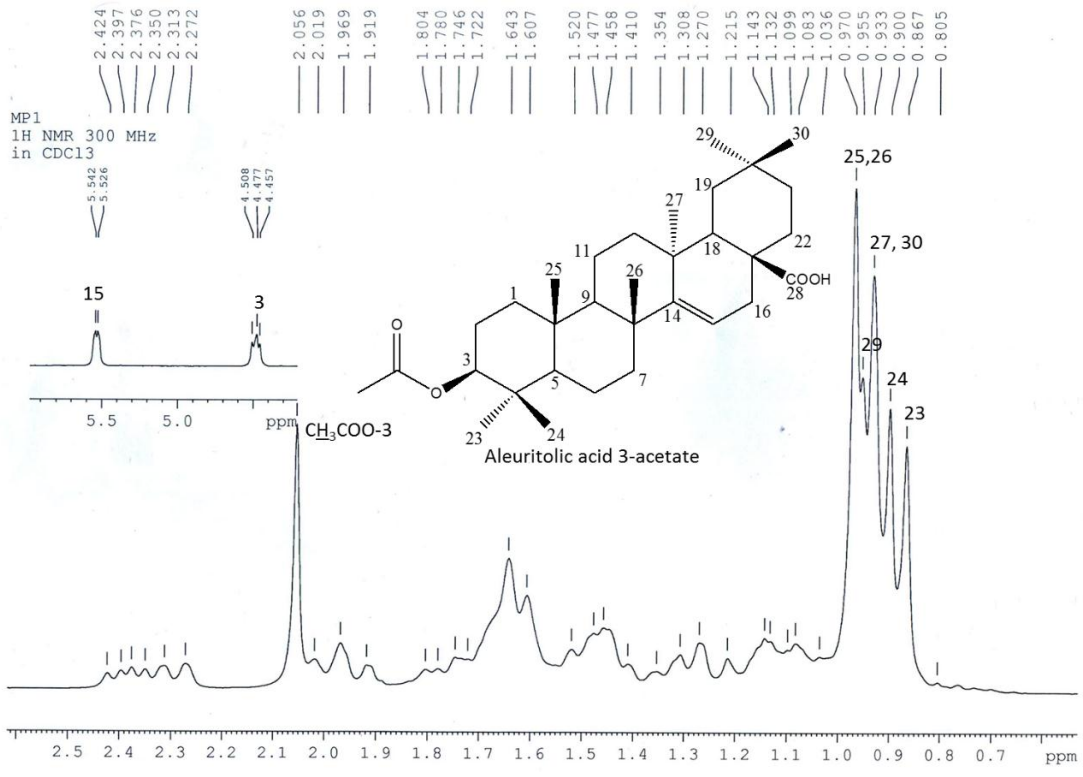

Figure 16 ^{1}H-NMR (300 MHz) Spectrum of compound MP-1 [**40**] ($CDCl_3$)

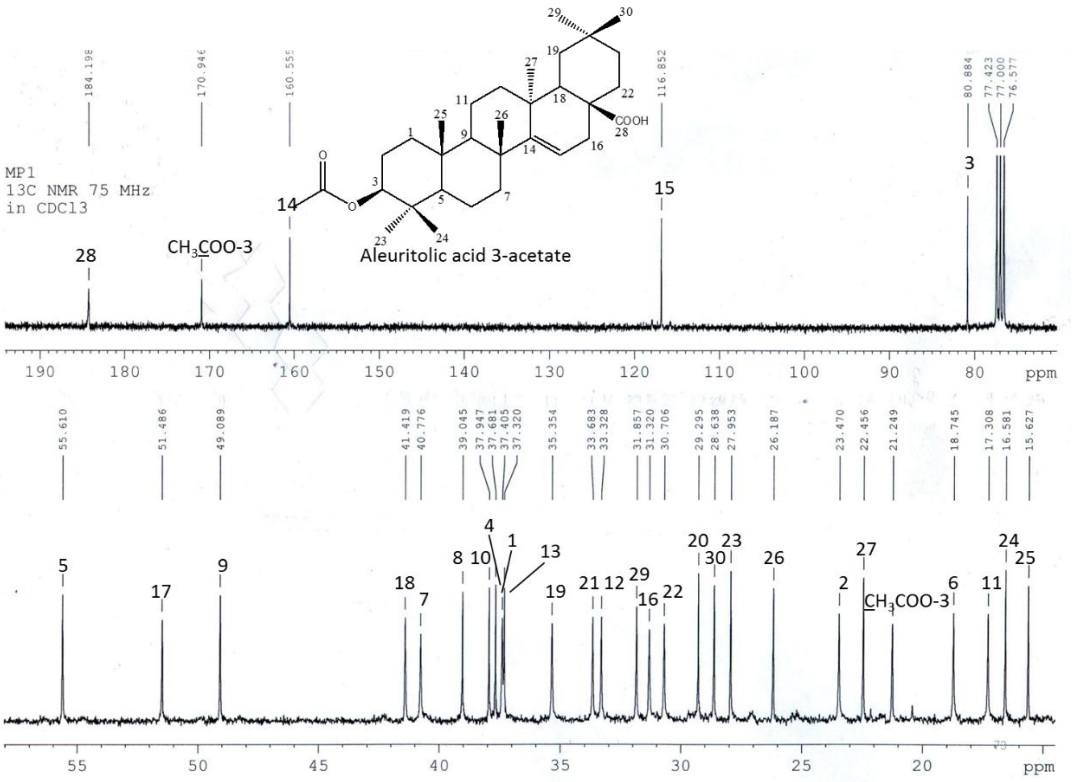

Figure 17 ^{13}C-NMR (75 MHz) Spectrum of compound MP-1 [**40**] ($CDCl_3$)

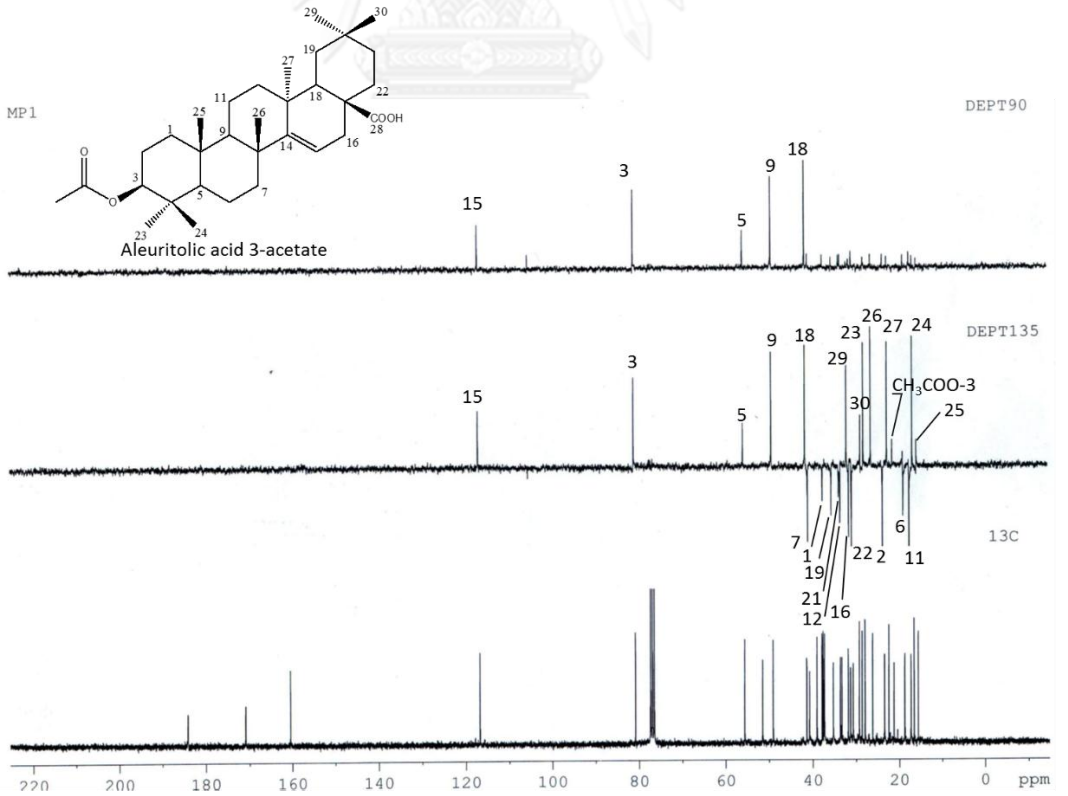

Figure 18 ^{13}C-NMR, DEPT-90 and DEPT-135 (75 MHz) Spectra of compound MP-1 [**40**] ($CDCl_3$)

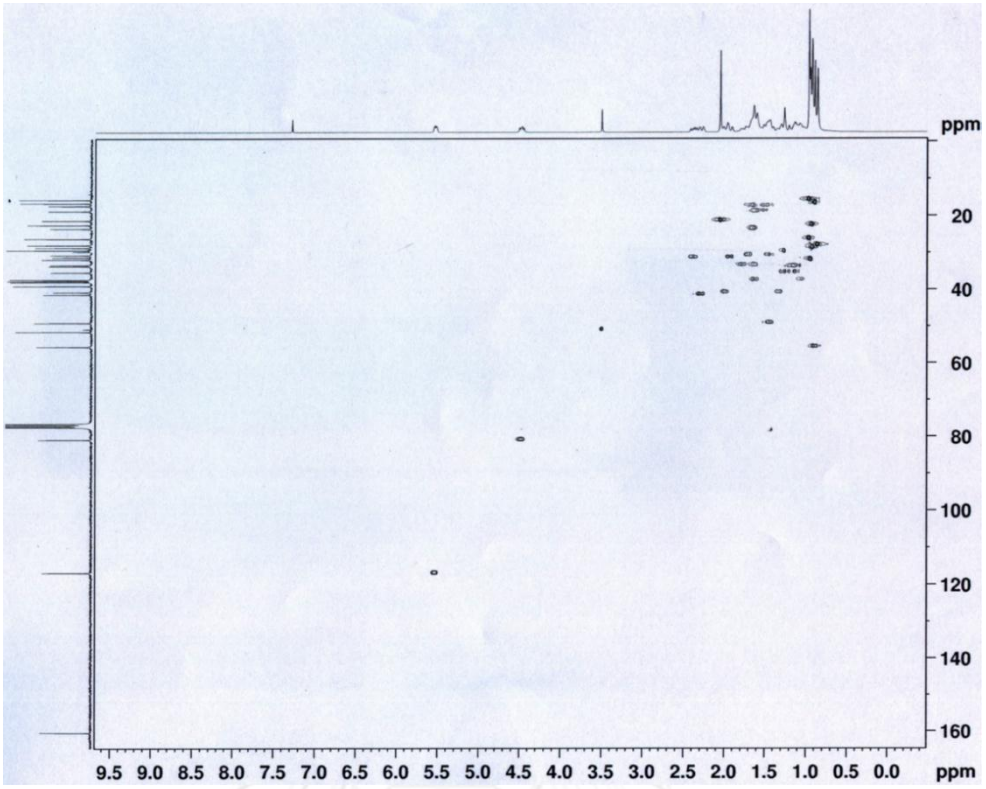

Figure 19 HSQC Spectrum of compound MP-1 [**40**] ($CDCl_3$)

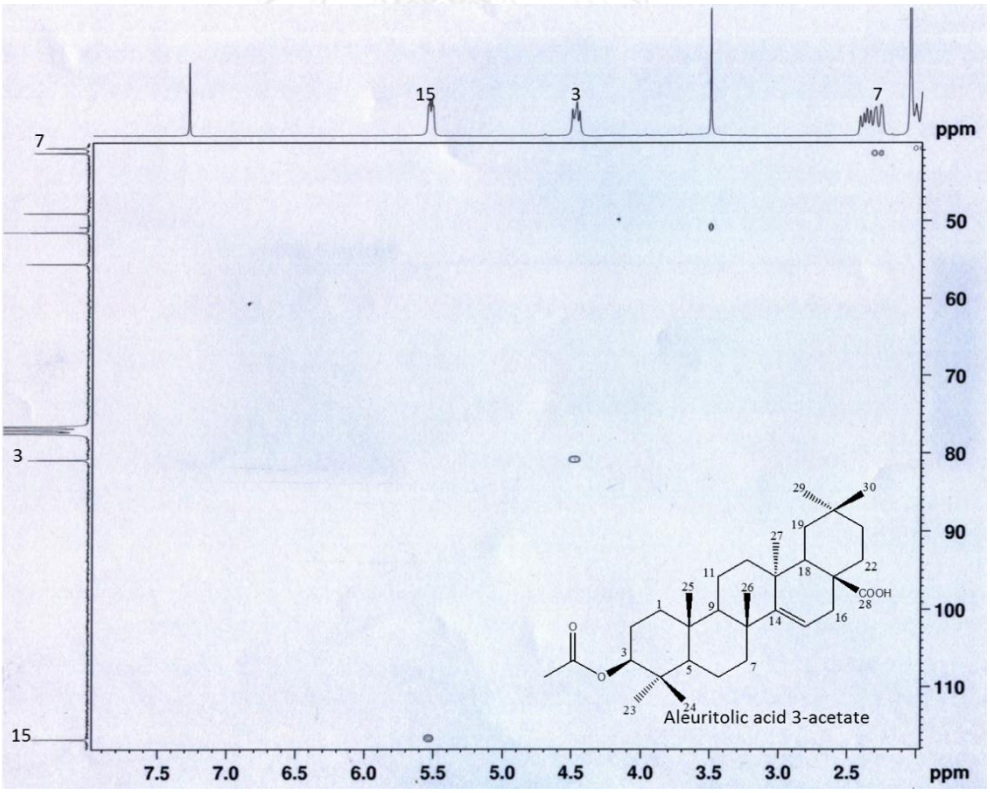

Figure 20 HSQC Spectrum of compound MP-1 [**40**] ($CDCl_3$)

(δ_H 2.0-8.0, δ_C 40-118 ppm)

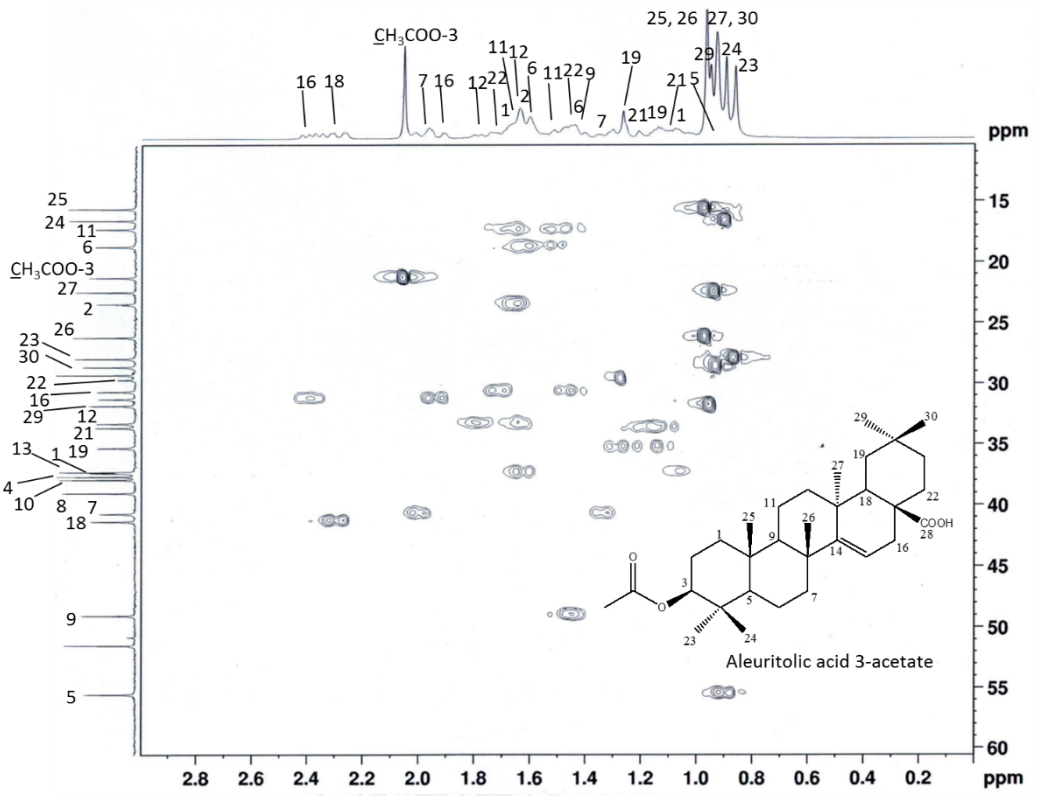

Figure 21 HSQC Spectrum of compound MP-1 [**40**] ($CDCl_3$)

(δ_H 0.0-3.0, δ_C 10-60 ppm)

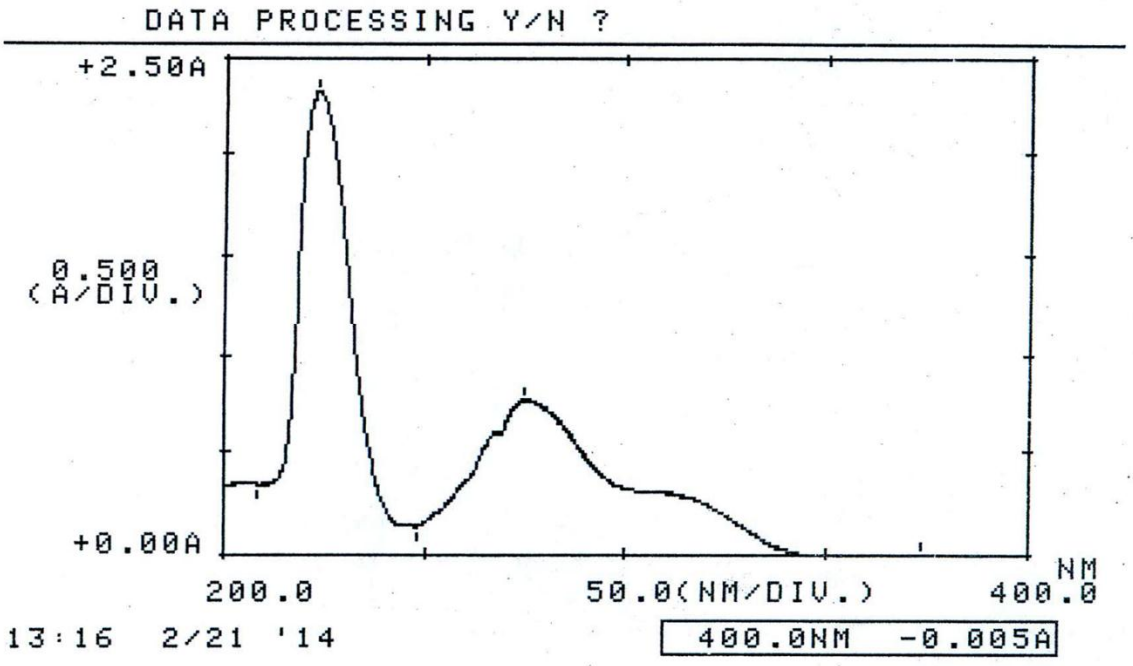

Figure 22 UV Spectrum of compound MP-2 [**123**]

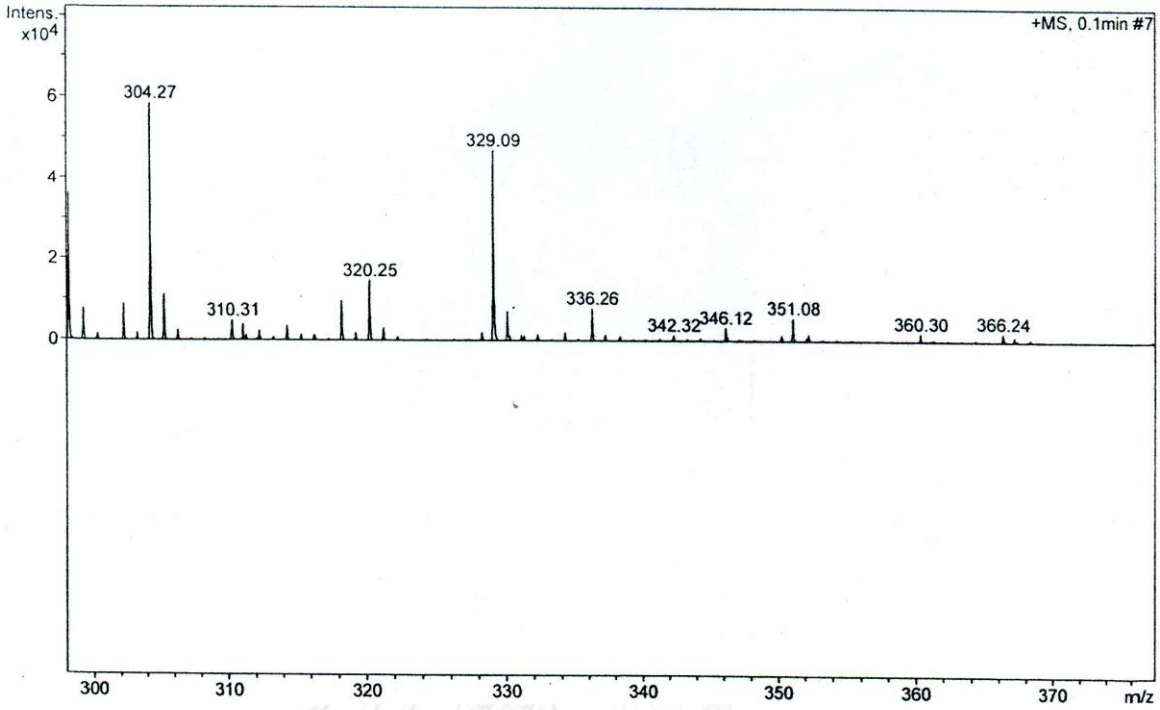

Figure 23 ESI Mass spectrum of compound MP-2 [**123**]

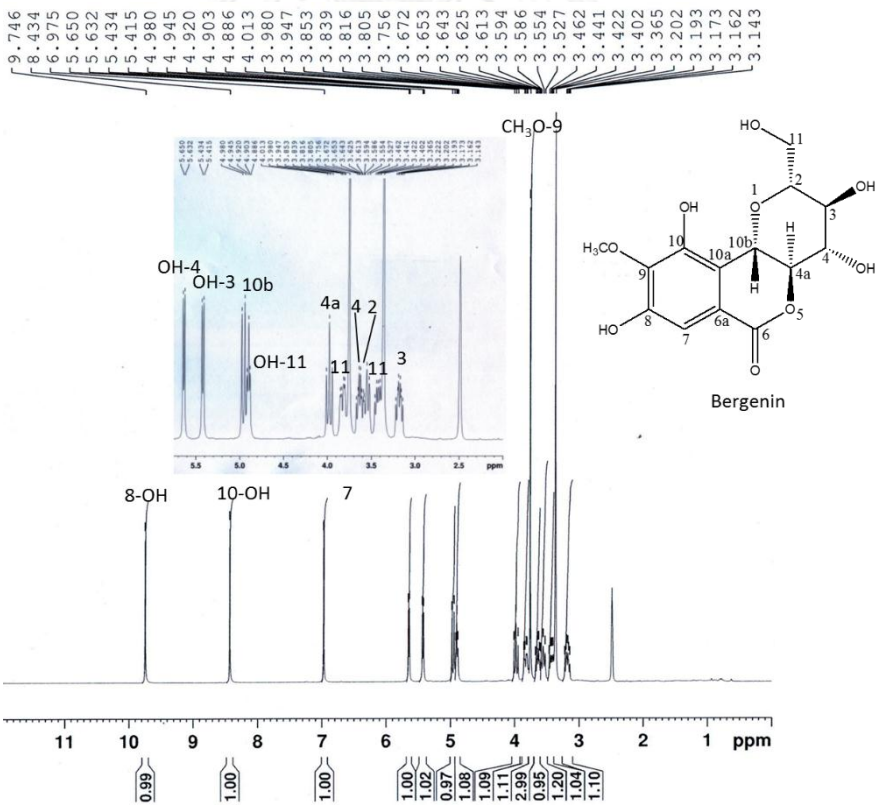

Figure 24 ^{1}H-NMR (300 MHz) Spectrum of compound MP-2 [**123**] (DMSO-d_6)

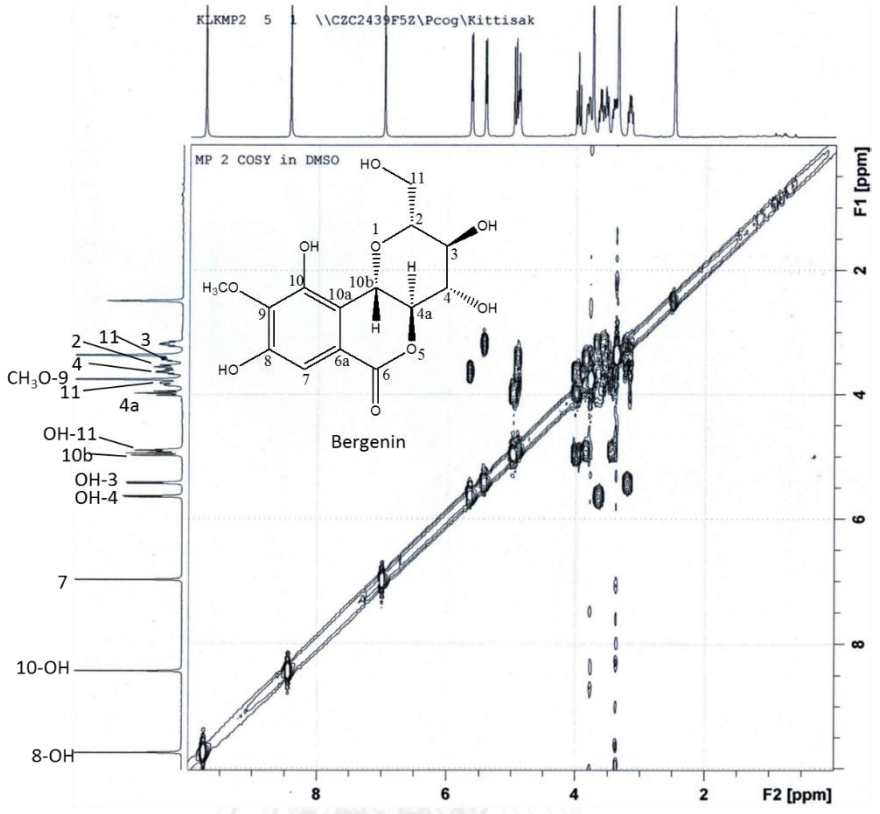

Figure 25 ^{1}H-^{1}H COSY Spectrum (300 MHz) of compound MP-2 [**123**] (DMSO-d_6)

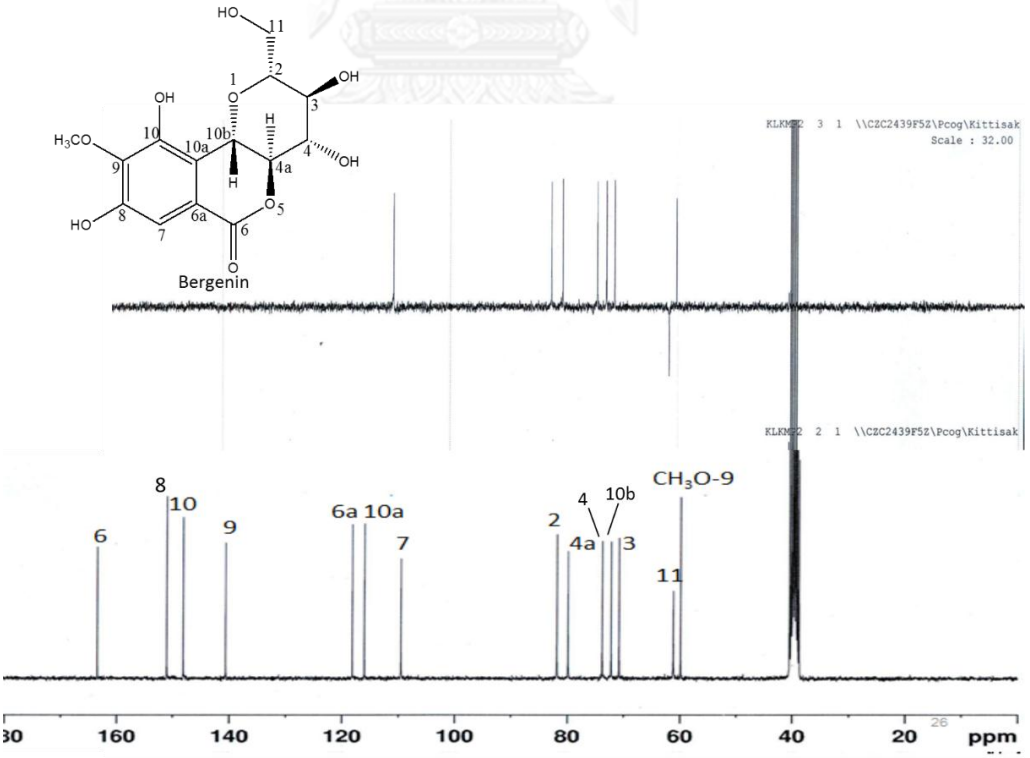

Figure 26 ^{13}C-NMR and DEPT-135 Spectra (75 MHz) of compound MP-2 [**123**] (DMSO-d_6)

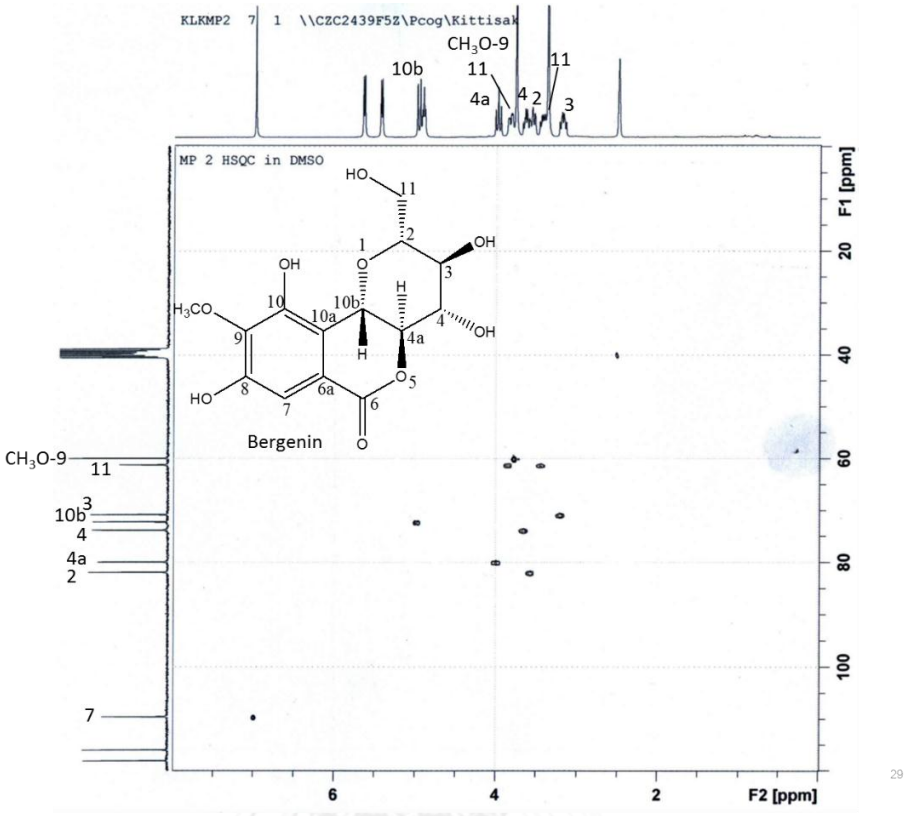

Figure 27 HSQC Spectrum of compound MP-2 [**123**] (DMSO-d_6)

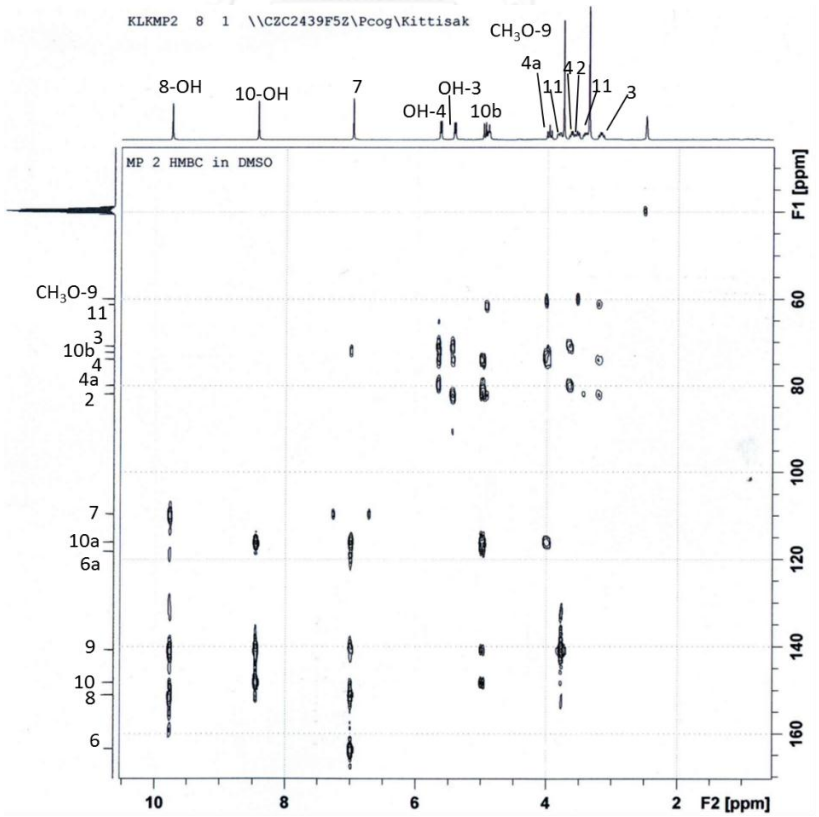

Figure 28 HMBC Spectrum of compound MP-2 [**123**] (DMSO-d_6)

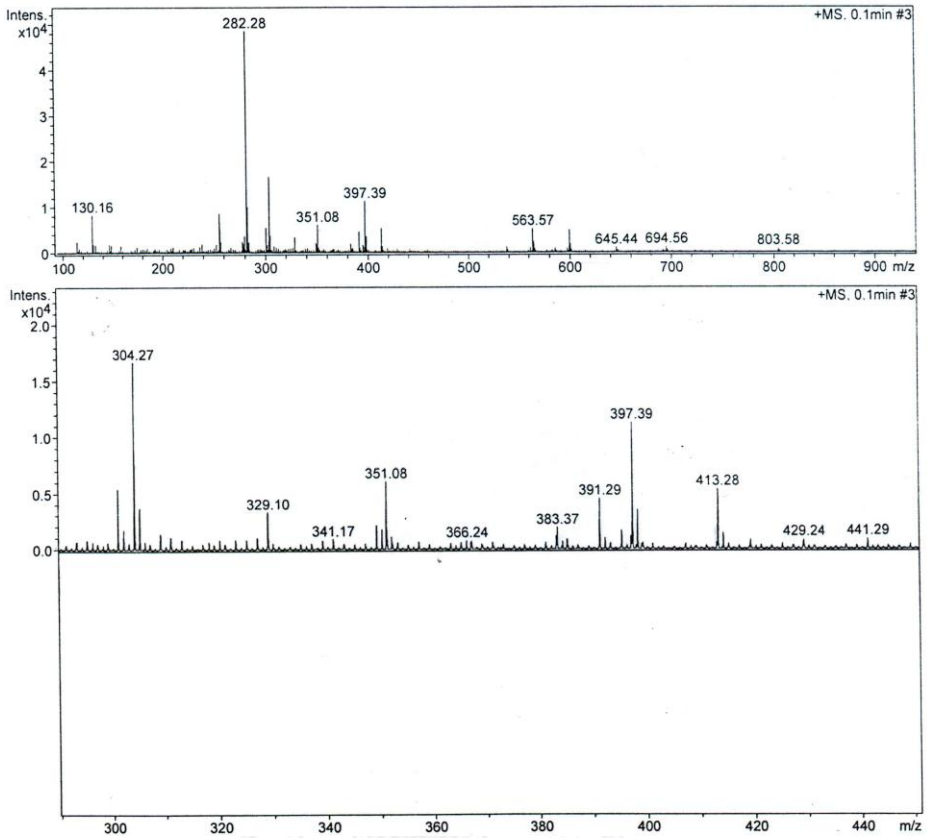

Figure 29 ESI Mass spectrum of compound MP-3 [**56**]

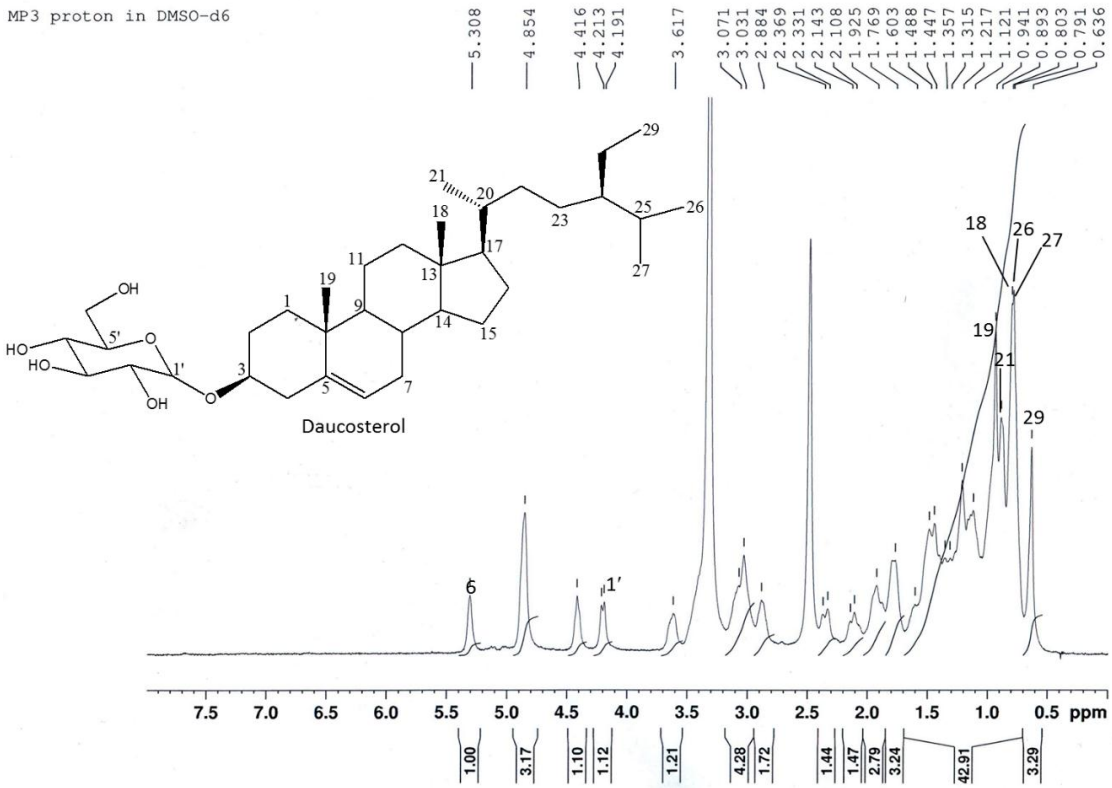

Figure 30 ^{1}H-NMR (300 MHz) Spectrum of compound MP-3 [**56**] (DMSO-d_6)

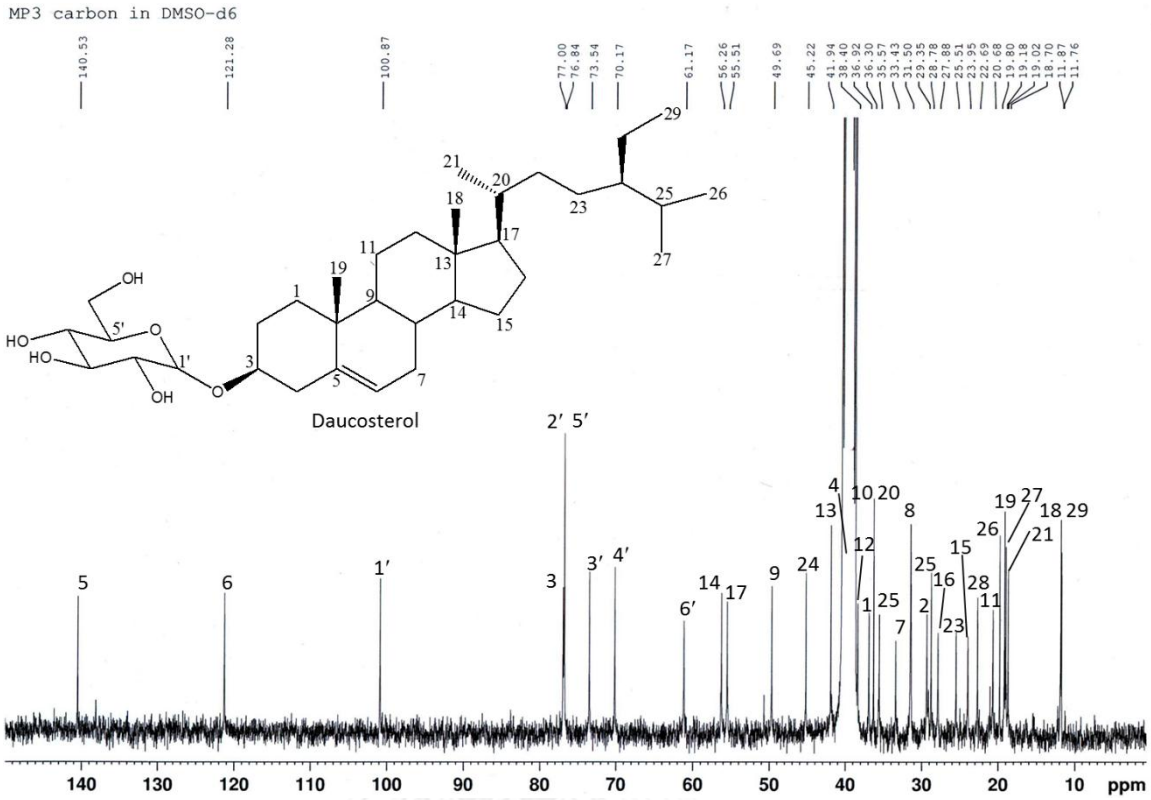

Figure 31 ^{13}C-NMR (75 MHz) Spectrum of compound MP-3 [**56**] (DMSO-d_6)

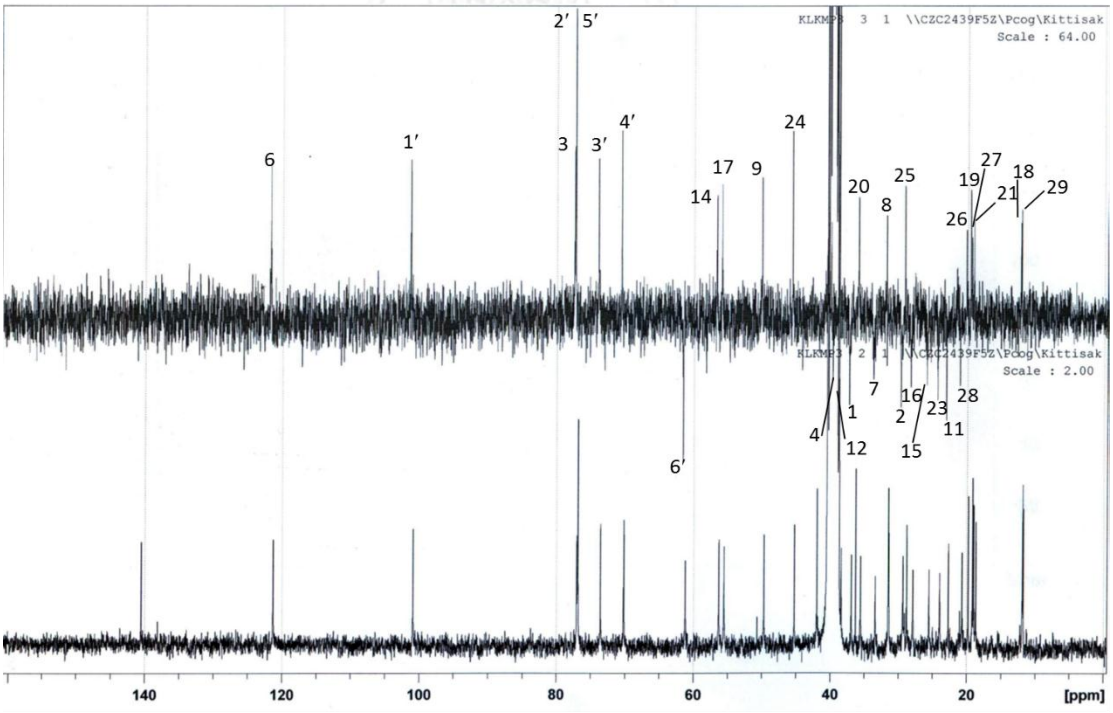

Figure 32 ^{13}C-NMR and DEPT-135 (75 MHz) Spectra of compound MP-3 [**56**]

(DMSO-d_6)

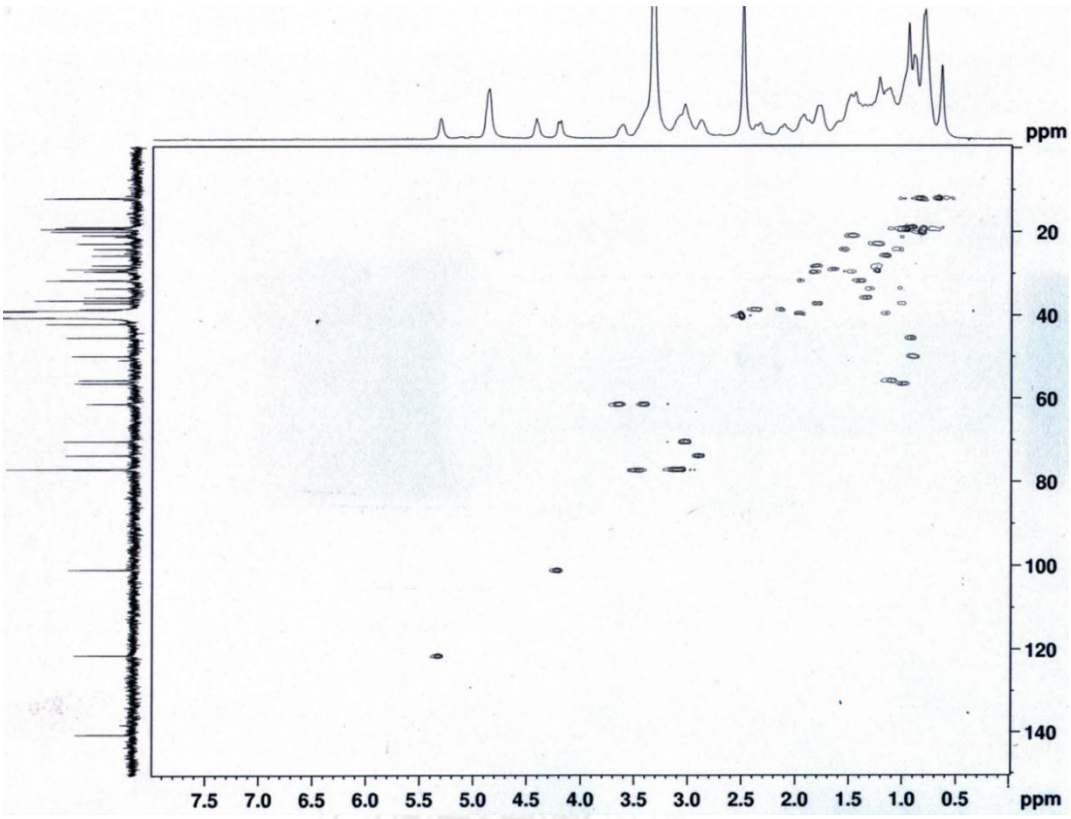

Figure 33 HSQC Spectrum of compound MP-3 [**56**] (DMSO-d_6)

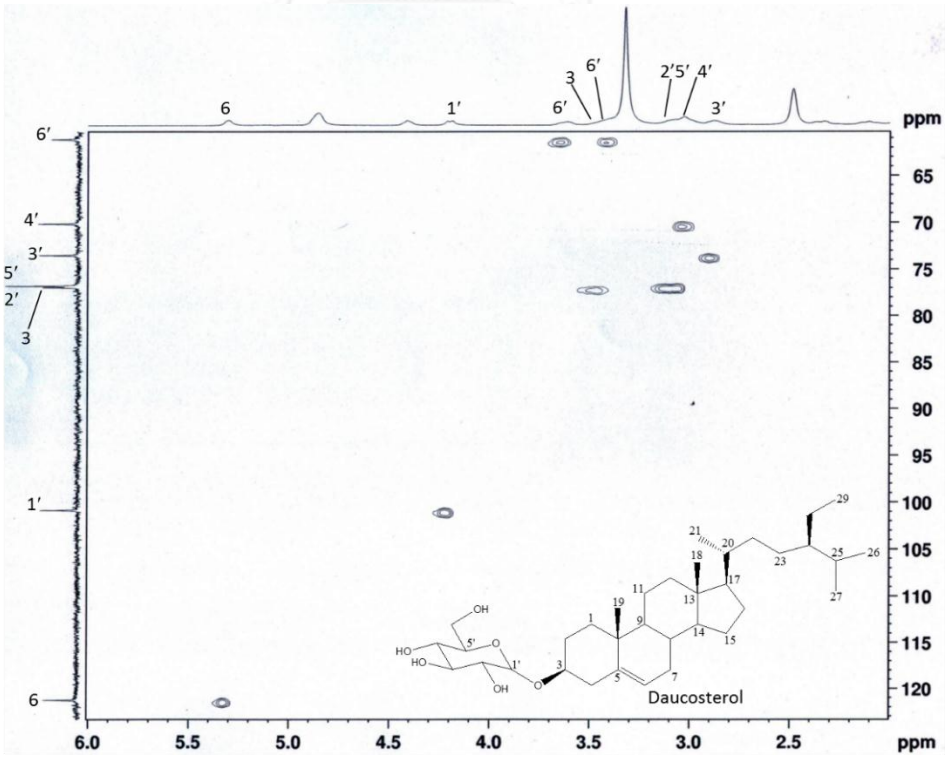

Figure 34 HSQC Spectrum of compound MP-3 [**56**] (DMSO-d_6)

(δ_H 2.0-6.0, δ_C 61-123 ppm)

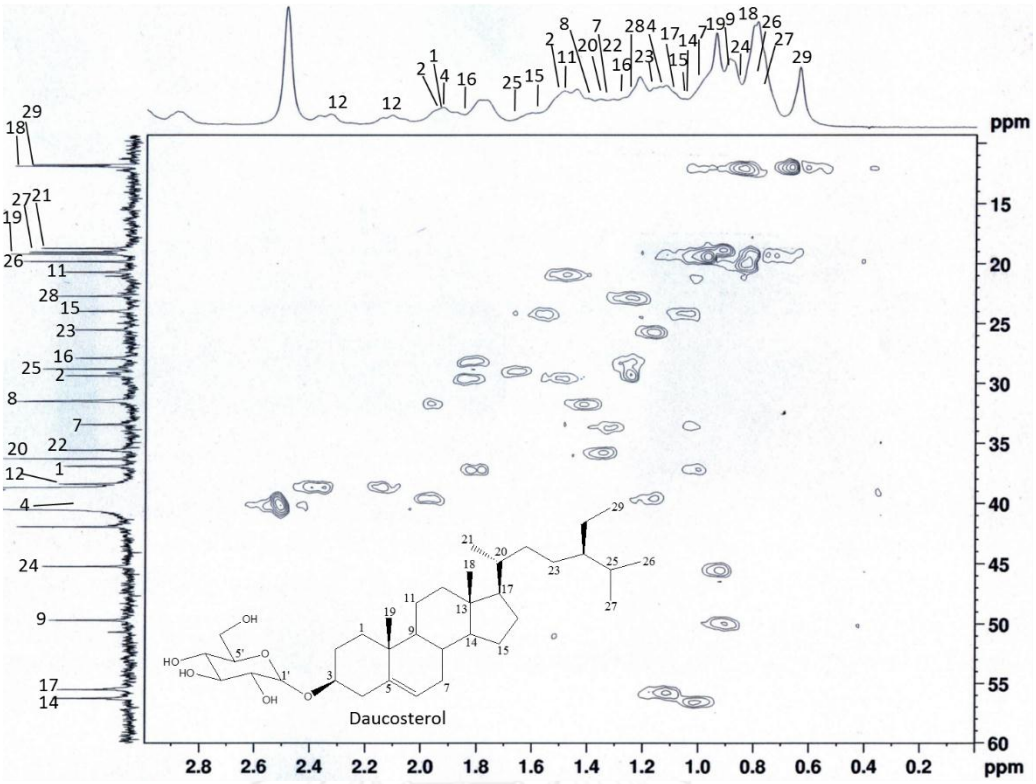

Figure 35 HSQC Spectrum of compound MP-3 [**56**] (DMSO-d_6)

(δ_H 0.0-3.0, δ_C 10-60 ppm)

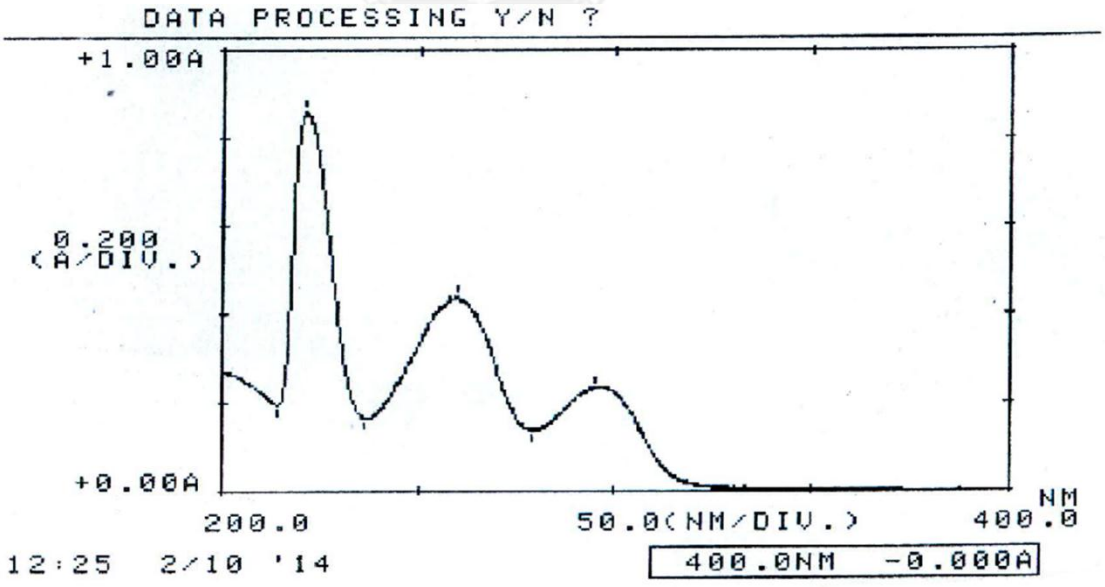

Figure 36 UV Spectrum of compound MP-4 [**139**]

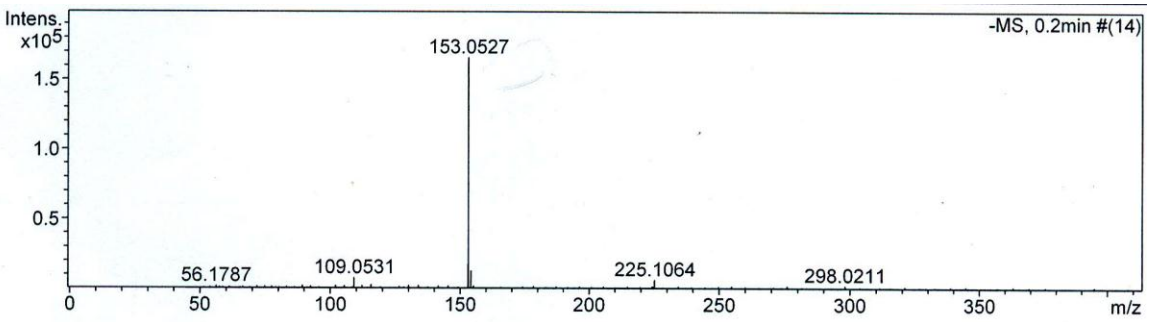

#	m/z	I	I %	S/N	FWHM	Res.
1	56.1787	2228	1.3	7.4	0.0101	5580
2	89.2138	1906	1.2	6.3	0.0078	11489
3	89.2721	2391	1.4	8.0	0.0125	7124
4	92.4138	1878	1.1	6.2	0.0079	11707
5	101.9382	2279	1.4	7.6	0.0072	14095
6	105.3600	2369	1.4	7.9	0.0083	12735
7	109.0531	7963	4.8	27.5	0.0305	3577
8	112.1485	2298	1.4	7.7	0.0094	11976
9	115.5817	3082	1.9	10.4	0.0089	13016
10	141.4298	2114	1.3	7.0	0.0085	16624
11	145.2414	2148	1.3	7.2	0.0172	8426
12	145.2832	2056	1.2	6.8	0.0172	8456
13	152.9195	3436	2.1	11.8	0.0725	2109
14	153.0527	165735	100.0	586.8	0.0367	4165
15	154.0561	12957	7.8	45.6	0.0366	4207
16	155.0576	2178	1.3	7.4	0.0322	4808
17	178.3305	1994	1.2	6.9	0.0168	10603
18	178.3807	1956	1.2	6.8	0.0214	8348
19	224.5329	1882	1.1	6.9	0.0123	18214
20	225.1064	6452	3.9	24.5	0.0519	4340
21	254.7466	1959	1.2	7.5	0.0135	18920
22	298.0211	2432	1.5	9.9	0.0181	16503
23	766.2549	1916	1.2	7.9	0.0290	26391
24	1451.6118	2769	1.7	13.0	0.0328	44236
25	1451.8163	2406	1.5	11.2	0.0928	15637
26	1876.0475	2551	1.5	11.5	0.0659	28460
27	2354.2874	2538	1.5	11.4	0.0397	59290
28	2354.4376	2490	1.5	11.2	0.0525	44862
29	2852.3051	2151	1.3	9.3	0.0726	39305
30	2887.2333	2233	1.3	9.7	0.0715	40403

Figure 37 HR-ESI Mass spectrum of compound MP-4 [**139**]

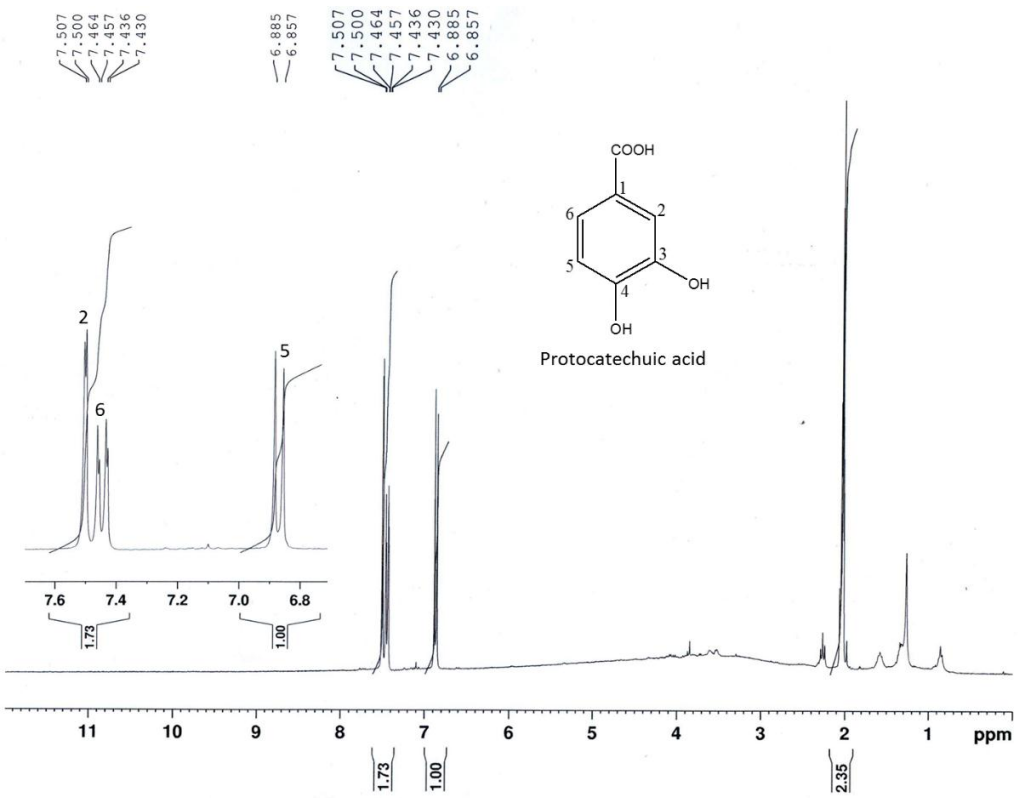

Figure 38 ^{1}H-NMR (300 MHz) Spectrum of compound MP-4 [**139**] (acetone-d_6)

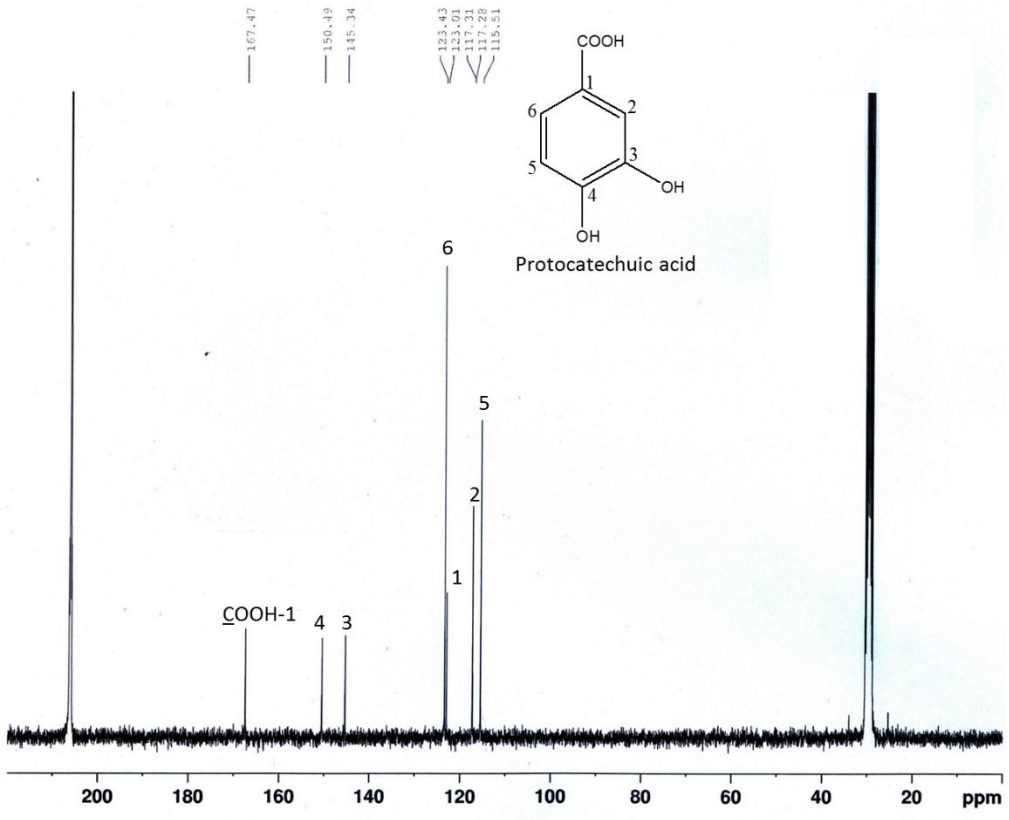

Figure 39 ^{13}C-NMR (75 MHz) Spectrum of compound MP-4 [**139**] (acetone-d_6)

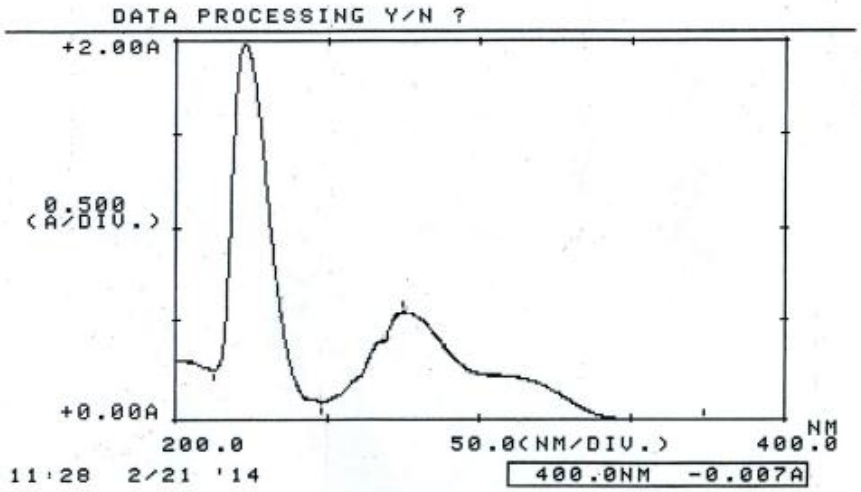

Figure 40 UV Spectrum of compound MP-5 [**140**]

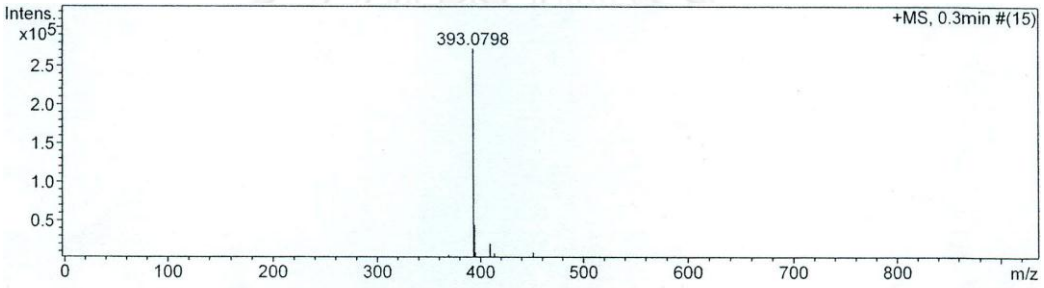

#	m/z	I	I %	S/N	FWHM	Res.
1	150.9493	1443	0.5	152.9	0.0264	5711
2	301.1358	1958	0.7	80.6	0.0509	5917
3	339.1770	993	0.4	35.1	0.0661	5135
4	353.1914	924	0.3	33.2	0.0690	5119
5	369.0271	6117	2.3	230.2	0.0594	6214
6	370.0288	2081	0.8	78.0	0.0544	6797
7	371.0318	1557	0.6	58.3	0.0632	5875
8	393.0798	271707	100.0	10777.5	0.0635	6188
9	394.0826	44834	16.5	1781.5	0.0608	6480
10	395.0839	9129	3.4	362.9	0.0602	6563
11	396.0873	1112	0.4	43.7	0.0671	5902
12	401.0212	880	0.3	34.7	0.1108	3618
13	409.0534	20354	7.5	834.9	0.0627	6528
14	410.0565	3494	1.3	143.0	0.0631	6502
15	411.0604	2260	0.8	92.4	0.0794	5176
16	413.2668	7782	2.9	321.7	0.0664	6224
17	414.2723	1846	0.7	75.9	0.0675	6142
18	415.0627	3861	1.4	159.8	0.0632	6566
19	421.2367	3032	1.1	127.1	0.0738	5708
20	425.1073	2973	1.1	125.7	0.0670	6341
21	441.2953	1626	0.6	71.0	0.0690	6393
22	451.0393	9008	3.3	406.4	0.0667	6765
23	452.0428	1557	0.6	69.7	0.0653	6926
24	453.0349	3069	1.1	138.5	0.0690	6562
25	453.2487	1539	0.6	69.1	0.0722	6280
26	467.0171	1043	0.4	48.1	0.0708	6594
27	497.1297	848	0.3	42.2	0.0740	6722
28	508.9999	1159	0.4	59.9	0.0800	6365
29	763.2586	2995	1.1	370.8	0.1573	4853
30	764.2666	971	0.4	120.0	0.1575	4852

Figure 41 HR-ESI Mass spectrum of compound MP-5 [**140**]

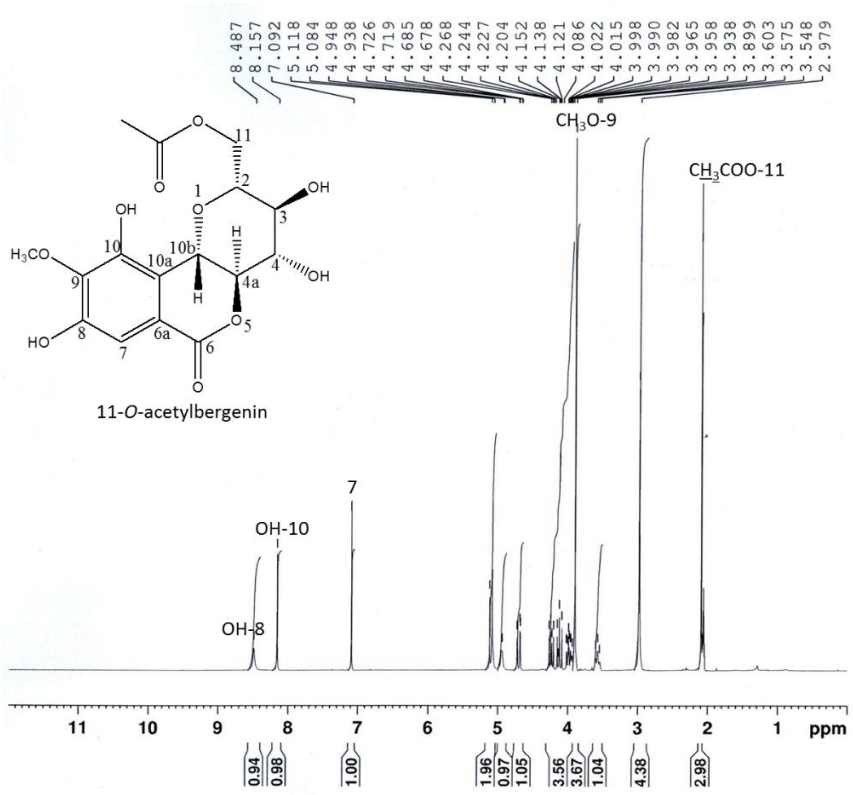

Figure 42 ^{1}H-NMR (300 MHz) Spectrum of compound MP-5 [**140**] (acetone-d_6)

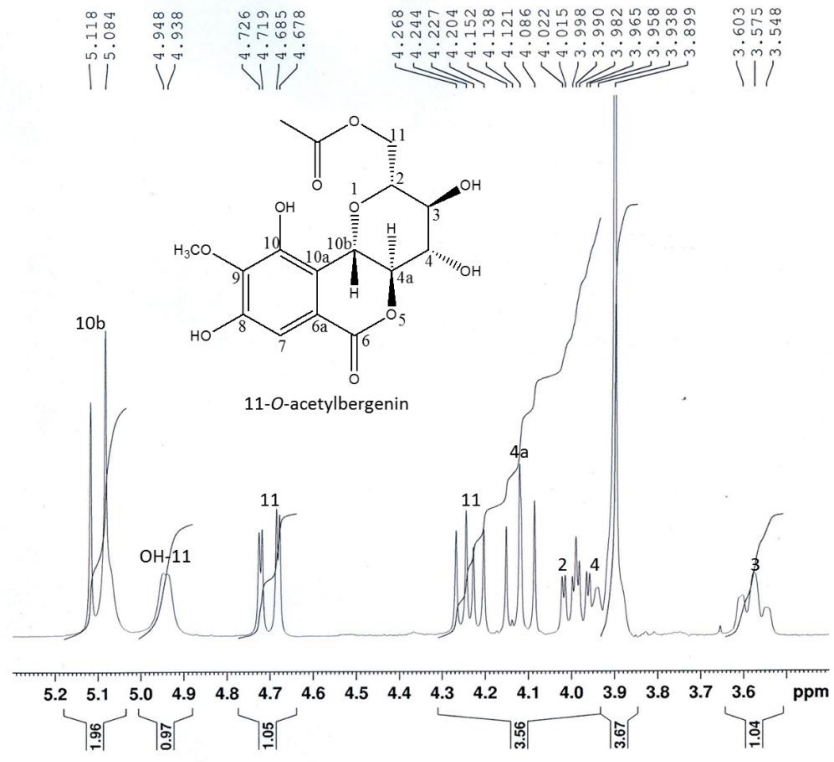

Figure 43 ^{1}H-NMR (300 MHz) Spectrum of compound MP-5 [**140**] (acetone-d_6) (δ_H 3.4-5.3 ppm)

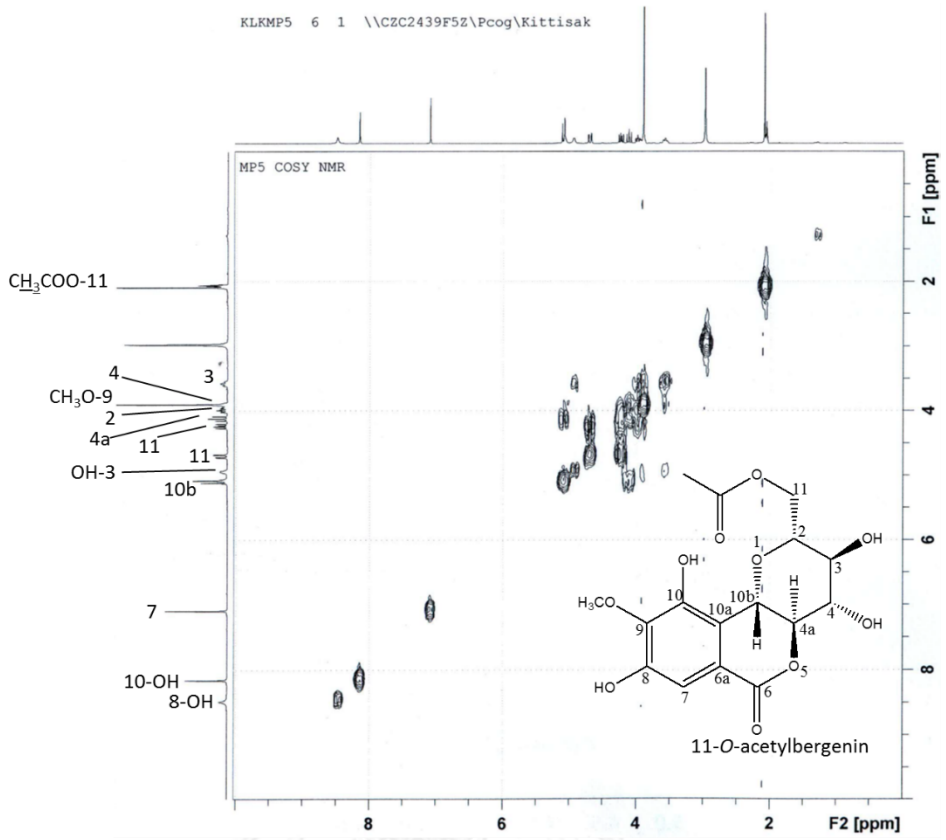

Figure 44 ^{1}H-^{1}H COSY Spectrum (300 MHz) of compound MP-5 [**140**] (acetone-d_6)

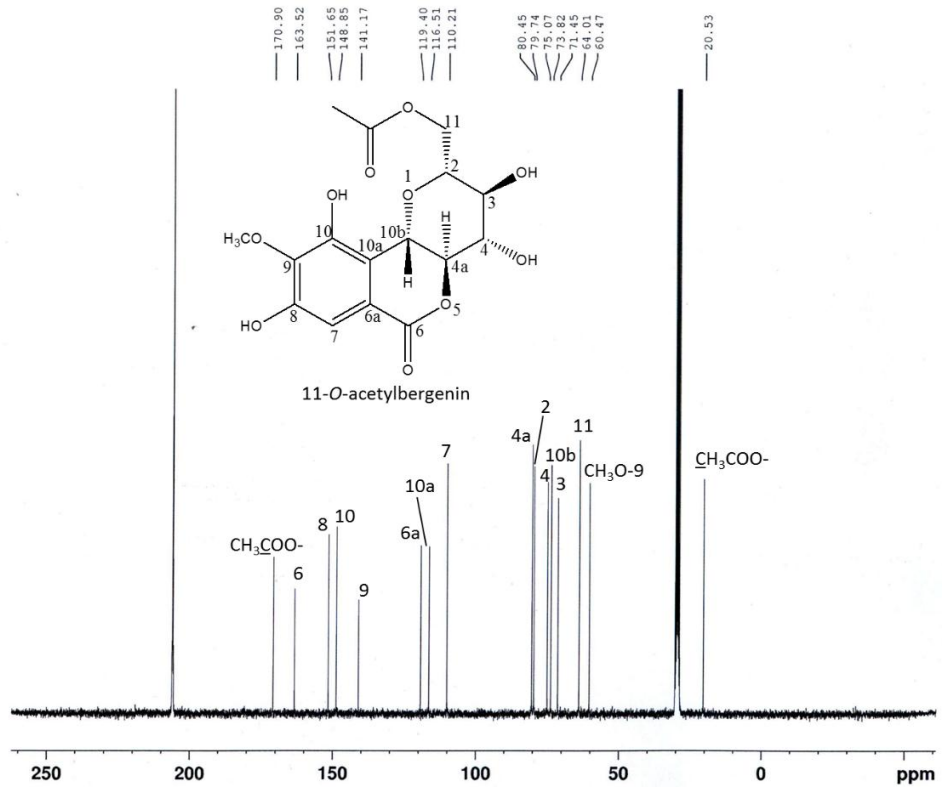

Figure 45 ^{13}C-NMR (75 MHz) Spectrum of compound MP-5 [**140**] (acetone-d_6)

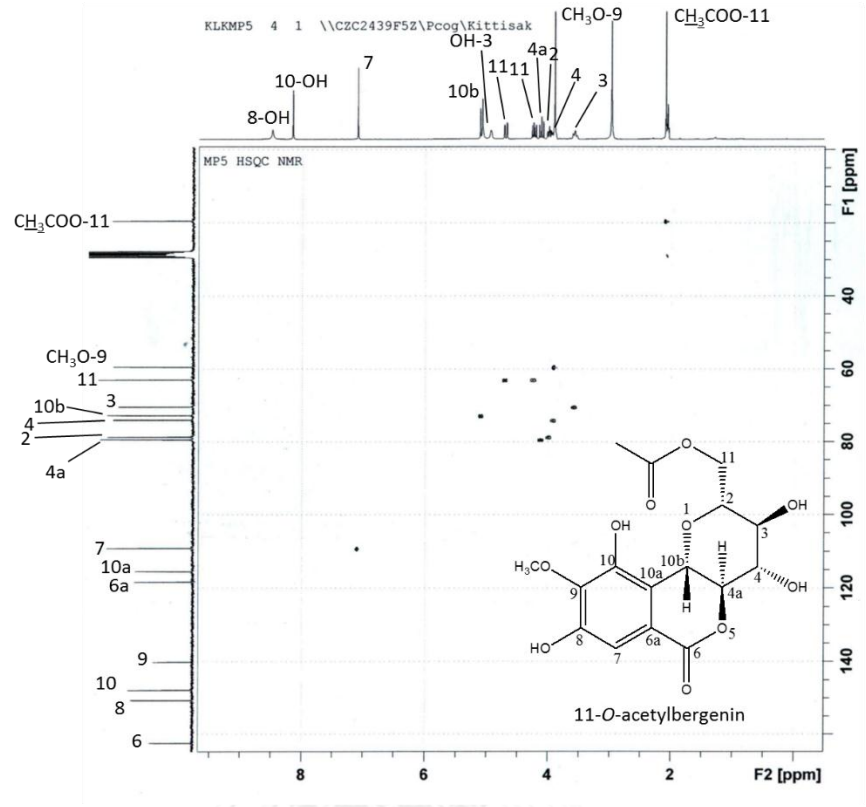

Figure 46 HSQC Spectrum of compound MP-5 [**140**] (acetone-d_6)

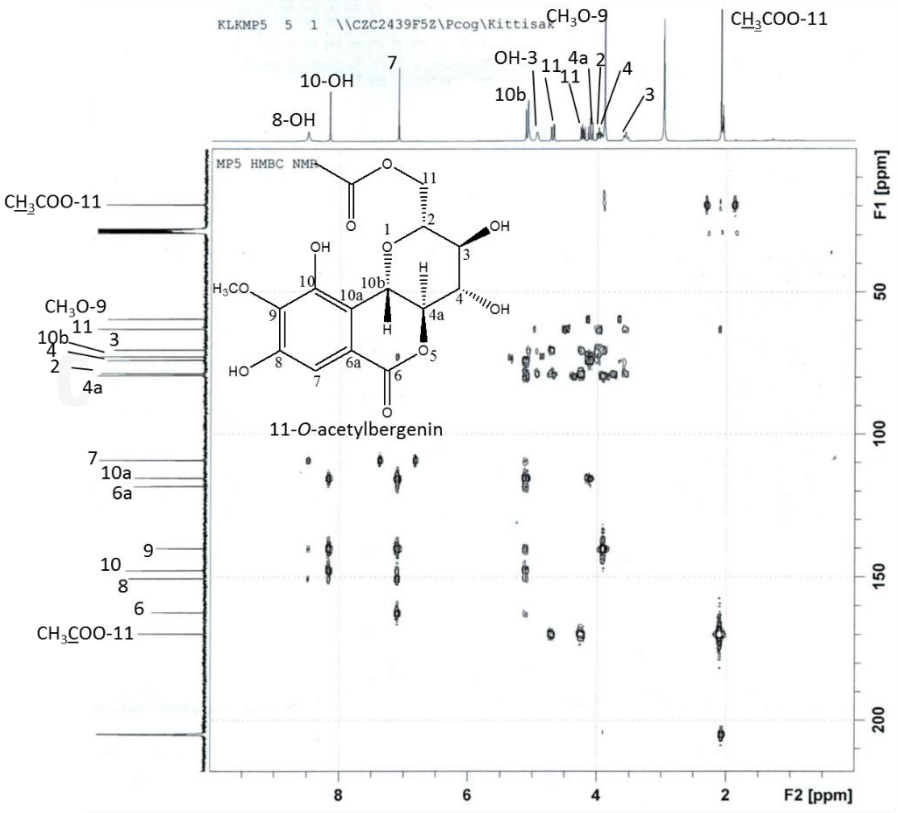

Figure 47 HMBC Spectrum of compound MP-5 [**140**] (acetone-d_6)

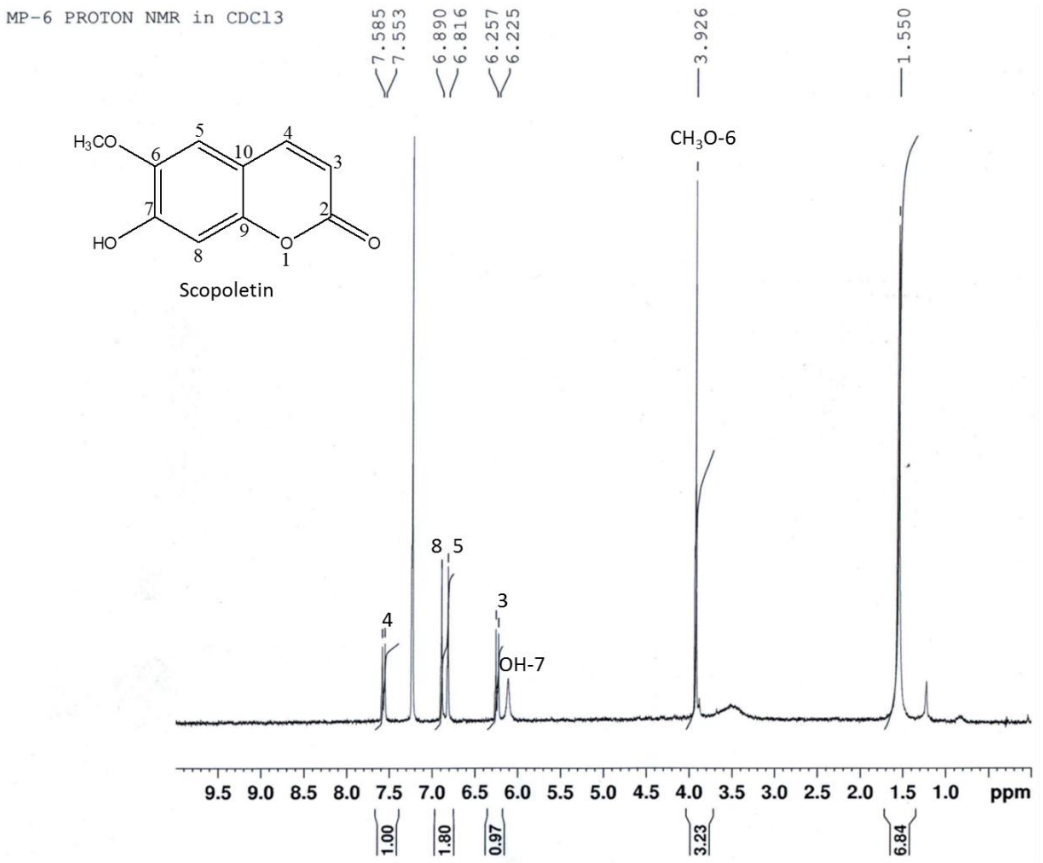

Figure 48 ^{1}H-NMR (300 MHz) Spectrum of compound MP-6 [**60**] ($CDCl_3$)

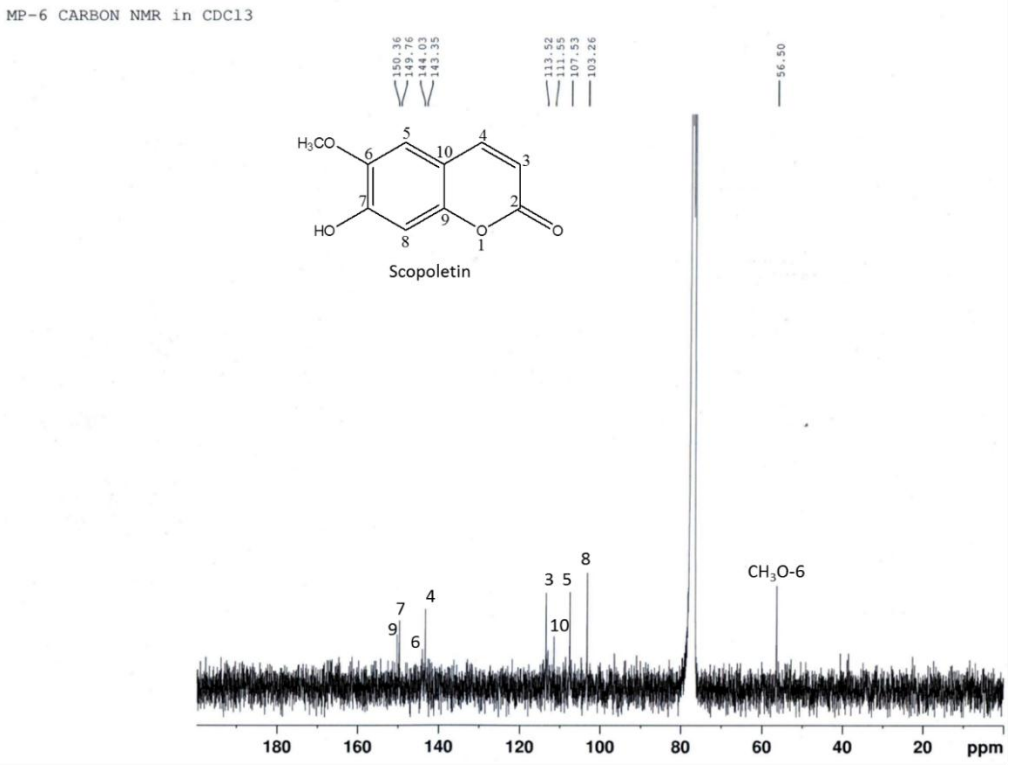

Figure 49 ^{13}C-NMR (75 MHz) Spectrum of compound MP-6 [**60**] ($CDCl_3$)

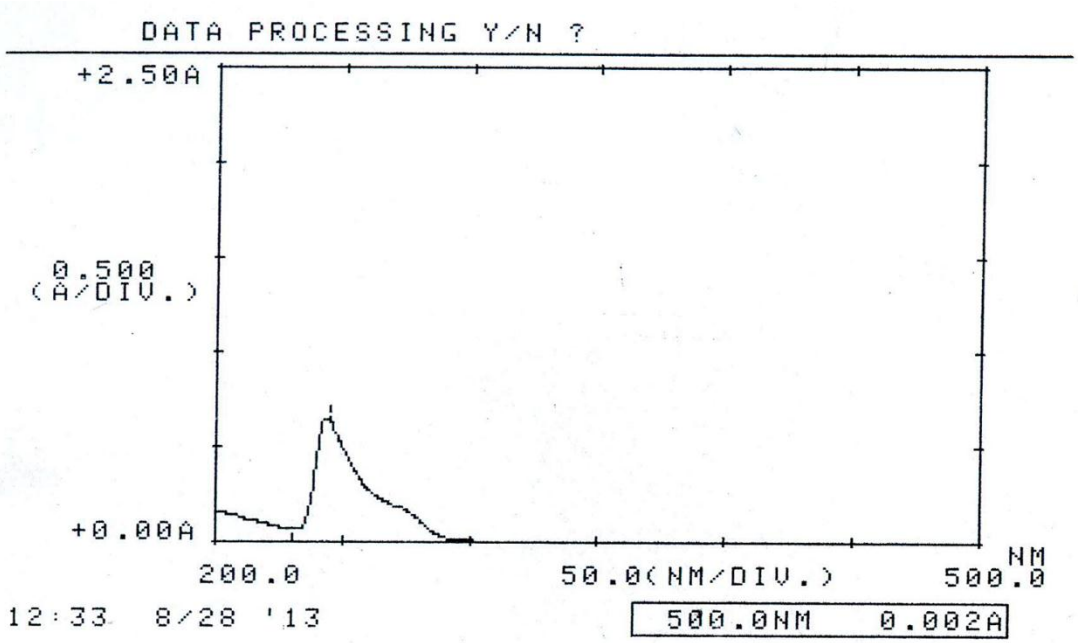

Figure 50 UV Spectrum of compound MP-7 [**141**]

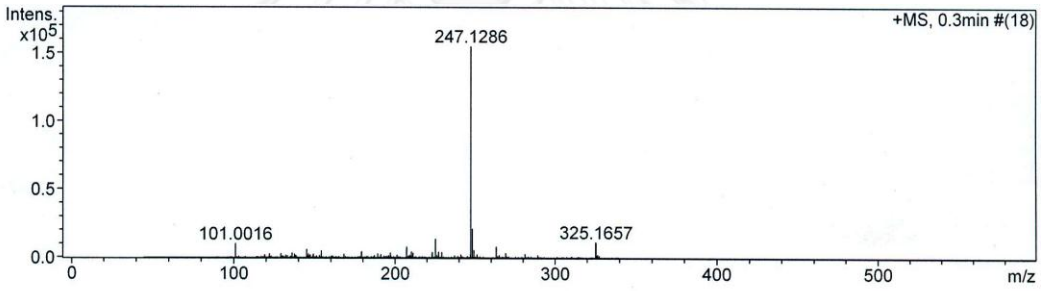

#	m/z	I	I %	S/N	FWHM	Res.
1	101.0016	10250	6.6	683.0	0.0210	4807
2	122.0314	2710	1.8	180.5	0.0239	5106
3	129.0486	2975	1.9	198.1	0.0245	5271
4	136.0723	3237	2.1	215.6	0.0248	5478
5	137.5131	2480	1.6	165.1	0.0250	5503
6	145.0277	6055	3.9	403.4	0.0293	4953
7	146.0298	2760	1.8	183.8	0.0307	4750
8	149.0945	2587	1.7	172.3	0.0265	5623
9	154.0472	5122	3.3	341.3	0.0288	5343
10	168.0625	2527	1.6	168.3	0.0283	5944
11	179.0142	4376	2.8	291.6	0.0329	5438
12	189.1249	2861	1.9	190.6	0.0336	5621
13	191.0208	2396	1.5	159.6	0.0337	5663
14	197.0757	3515	2.3	234.2	0.0363	5431
15	207.1350	7923	5.1	528.2	0.0368	5635
16	210.1005	4420	2.9	294.6	0.0380	5534
17	211.0925	3422	2.2	228.0	0.0463	4556
18	223.0908	3991	2.6	266.0	0.0409	5455
19	225.1093	13715	8.9	914.7	0.0392	5743
20	227.1220	4330	2.8	288.6	0.0404	5621
21	229.1172	4020	2.6	268.0	0.0390	5877
22	241.0853	2260	1.5	150.6	0.0494	4878
23	247.1286	154636	100.0	10316.8	0.0411	6007
24	248.1315	21180	13.7	1412.9	0.0394	6295
25	249.1381	5596	3.6	373.2	0.0442	5632
26	251.1144	2167	1.4	144.4	0.0716	3505
27	263.1032	8128	5.3	542.2	0.0430	6119
28	269.0372	3327	2.2	221.8	0.0432	6223
29	281.1020	2718	1.8	181.2	0.0473	5942
30	325.1657	11379	7.4	759.5	0.0731	4451

Figure 51 HR-ESI Mass spectrum of compound MP-7 [**141**]

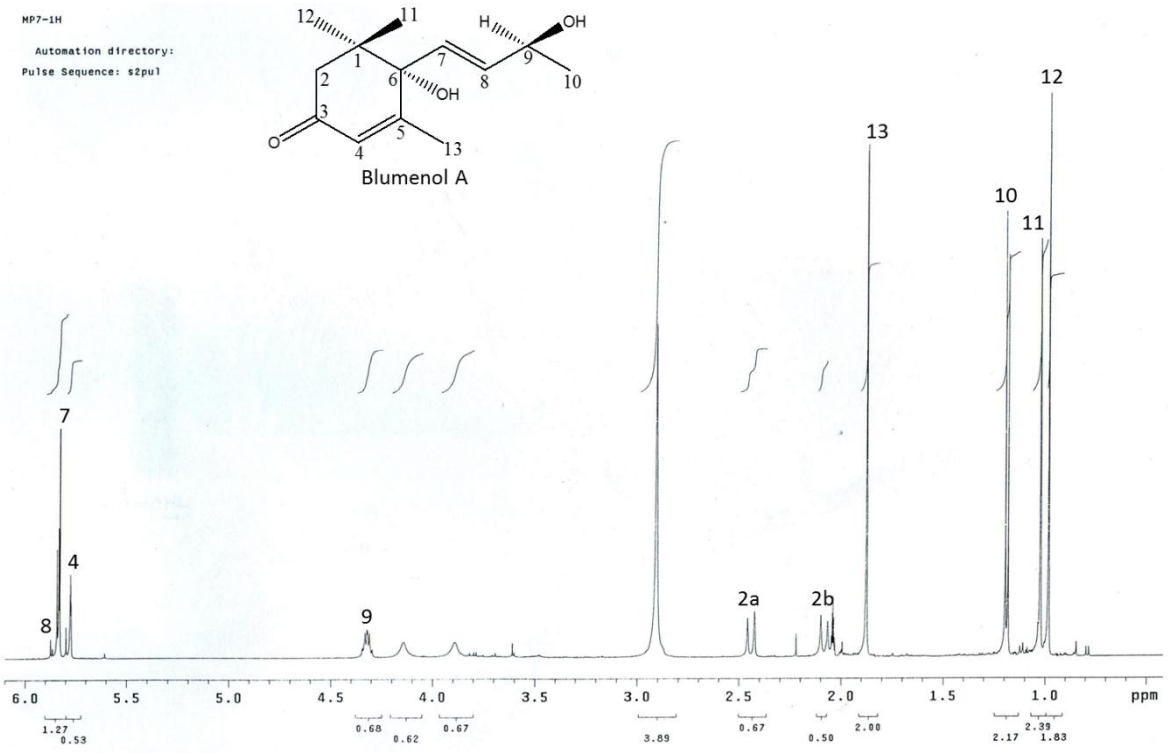

Figure 52 ^{1}H-NMR (500 MHz) Spectrum of compound MP-7 [**141**] (acetone-d_6)

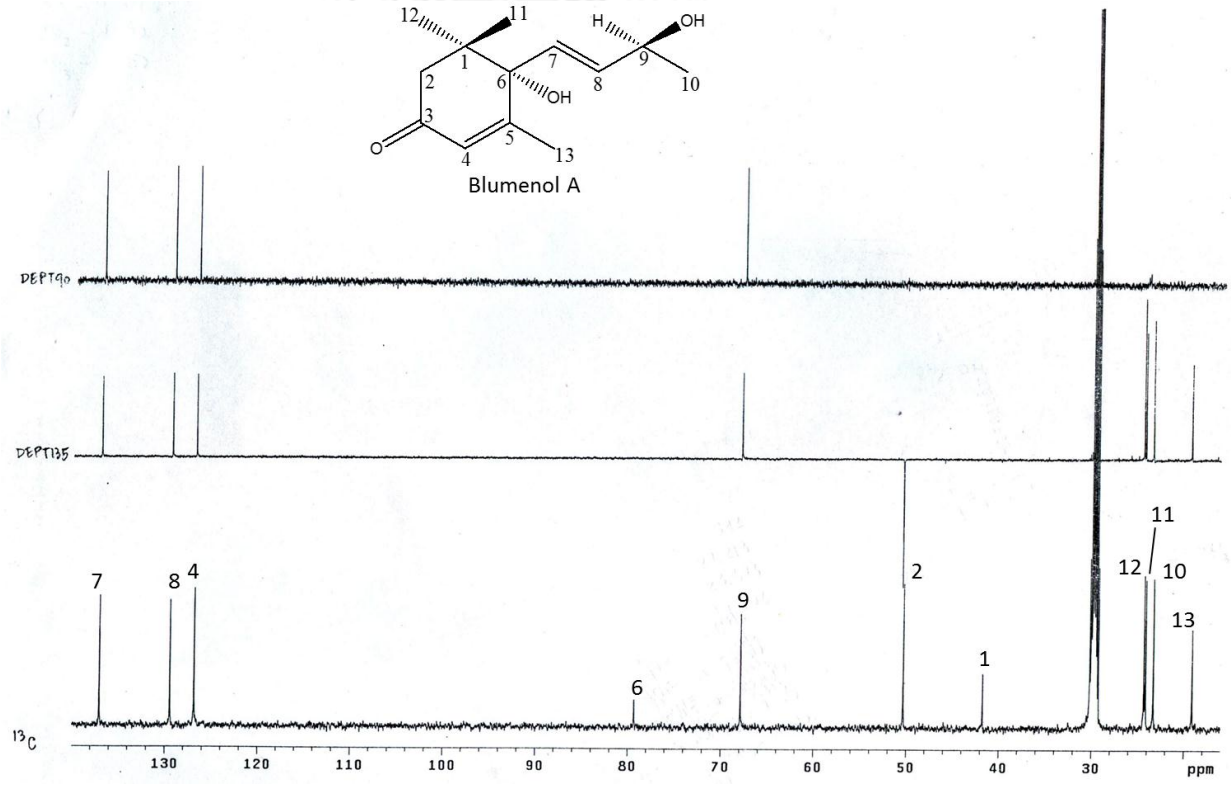

Figure 53 ^{13}C-NMR, DEPT-90 and DEPT-135 (125 MHz) Spectra of compound MP-7 [**141**] (acetone-d_6)

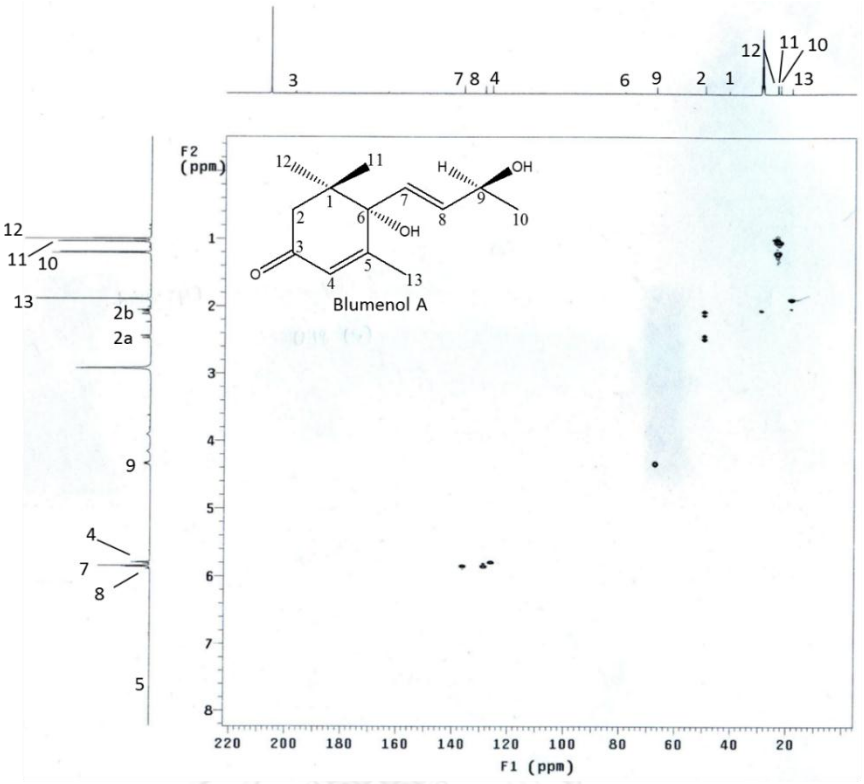

Figure 54 HSQC Spectrum of compound MP-7 [**141**] (acetone-d_6)

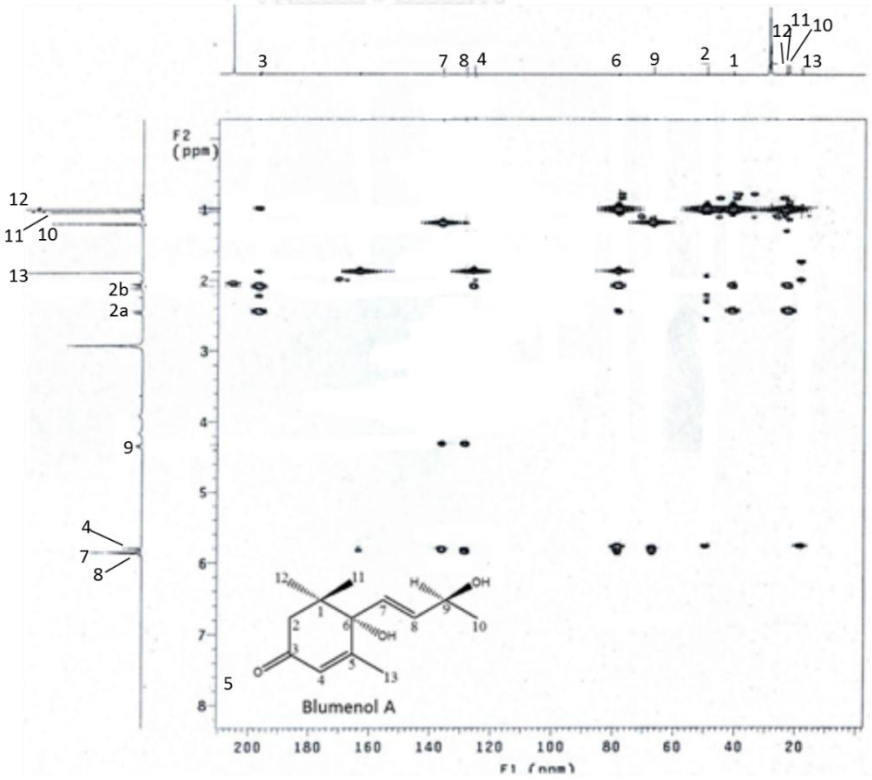

Figure 55 HMBC Spectrum of compound MP-7 [**141**] (acetone-d_6)

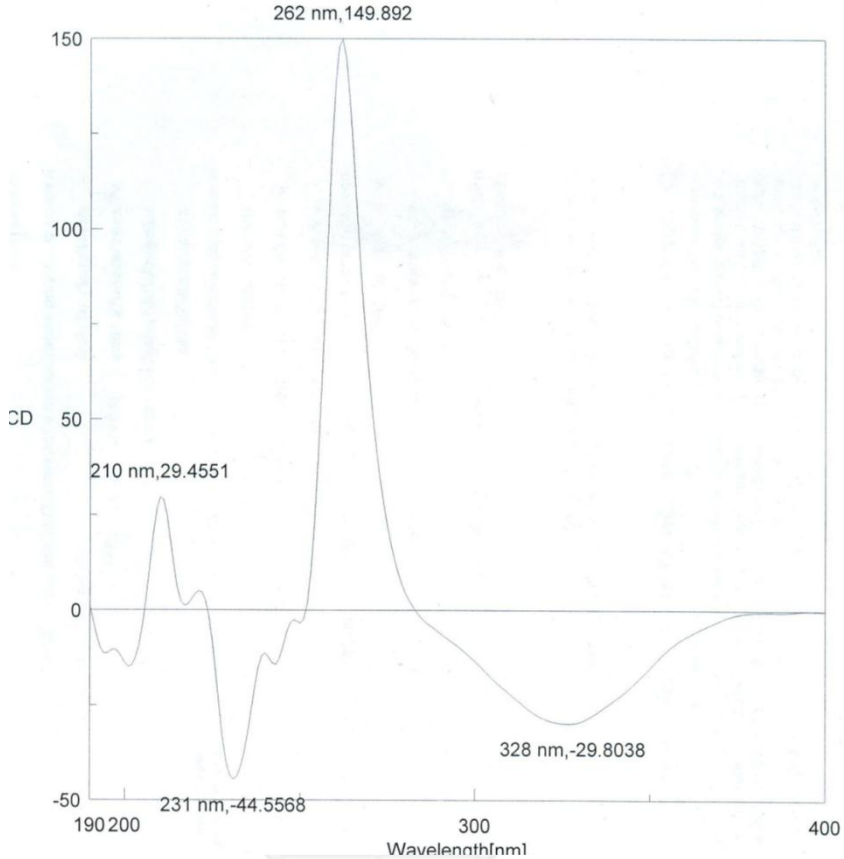

Figure 56 CD Spectrum of compound MP-7 [**141**] (MeOH)

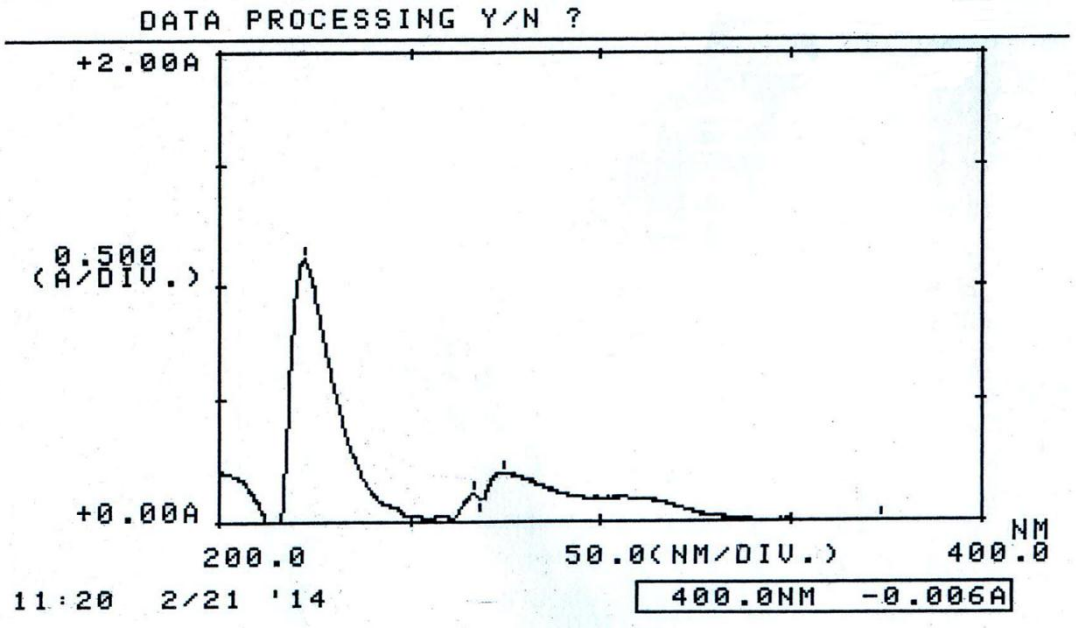

Figure 57 UV Spectrum of compound MP-8 [**142**]

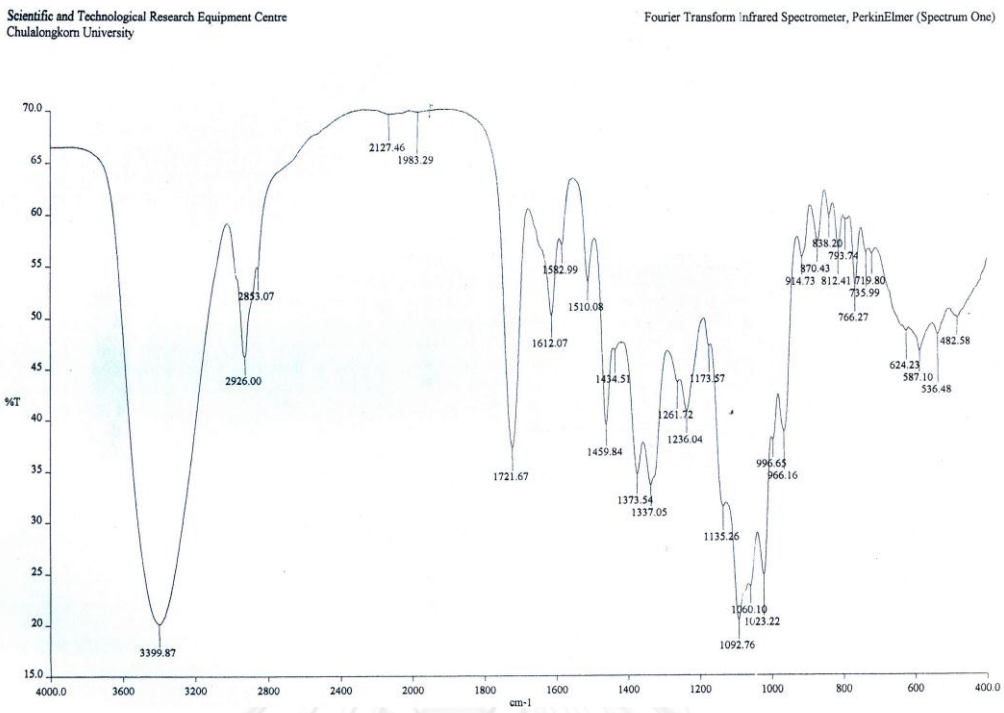

Figure 58 FT-IR Spectrum of compound MP-8 [**142**]

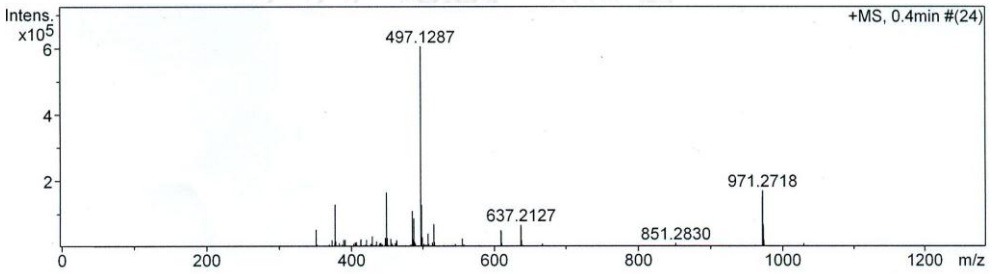

#	m/z	I	I %	S/N	FWHM	Res.
1	351.0678	53653	8.9	737.7	0.0454	7726
2	373.1824	22388	3.7	257.1	0.0478	7808
3	377.1418	129274	21.4	1446.4	0.0501	7526
4	378.1440	20243	3.3	224.2	0.0494	7648
5	389.1767	23119	3.8	237.4	0.0506	7694
6	391.1690	22891	3.8	232.0	0.0696	5622
7	413.1425	23272	3.8	206.3	0.0514	8035
8	413.2653	24177	4.0	214.2	0.0533	7760
9	421.1695	23287	3.9	197.4	0.0535	7873
10	429.2016	33303	5.5	270.7	0.0552	7776
11	447.1511	28744	4.8	213.5	0.0585	7638
12	449.1288	165120	27.3	1219.0	0.0576	7801
13	450.1322	29105	4.8	213.1	0.0575	7822
14	455.1534	25668	4.2	183.5	0.0570	7986
15	463.2144	22184	3.7	152.8	0.0588	7872
16	485.1643	109638	18.1	691.3	0.0616	7875
17	486.1677	24262	4.0	151.7	0.0602	8075
18	487.1715	84961	14.0	531.2	0.1168	4172
19	497.1287	604715	100.0	3640.8	0.0643	7728
20	498.1317	127508	21.1	764.1	0.0620	8034
21	499.1415	30146	5.0	179.3	0.0755	6615
22	507.1846	42069	7.0	243.1	0.0631	8044
23	515.1744	70362	11.6	395.4	0.0645	7987
24	555.0999	26535	4.4	146.7	0.0925	6003
25	609.2175	52134	8.6	371.1	0.0757	8049
26	637.2127	68317	11.3	570.2	0.0793	8040
27	638.2153	20640	3.4	172.5	0.0794	8043
28	971.2718	170759	28.2	2366.1	0.1205	8060
29	972.2741	71063	11.8	987.0	0.1192	8159
30	973.2779	23534	3.9	326.6	0.1190	8176

Figure 59 HR-ESI Mass spectrum of compound MP-8 [**142**]

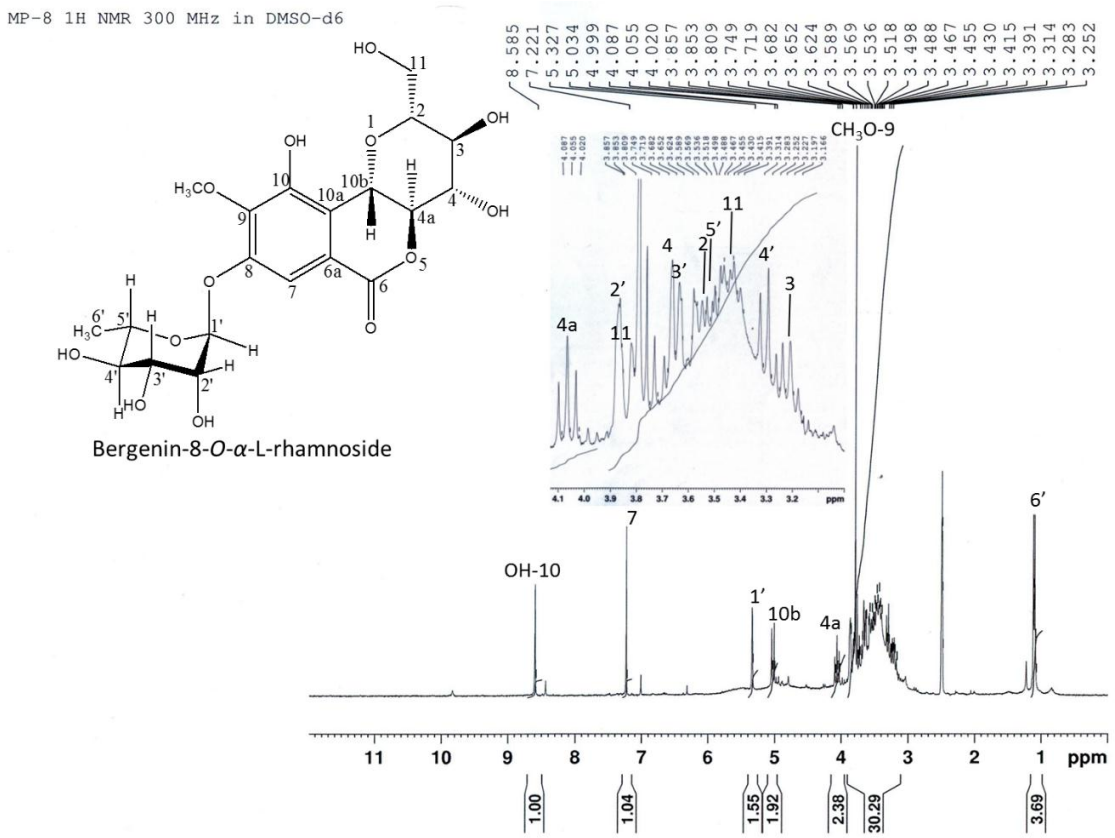

Figure 60 ^{1}H-NMR (300 MHz) Spectrum of compound MP-8 [**142**] (DMSO-d_6)

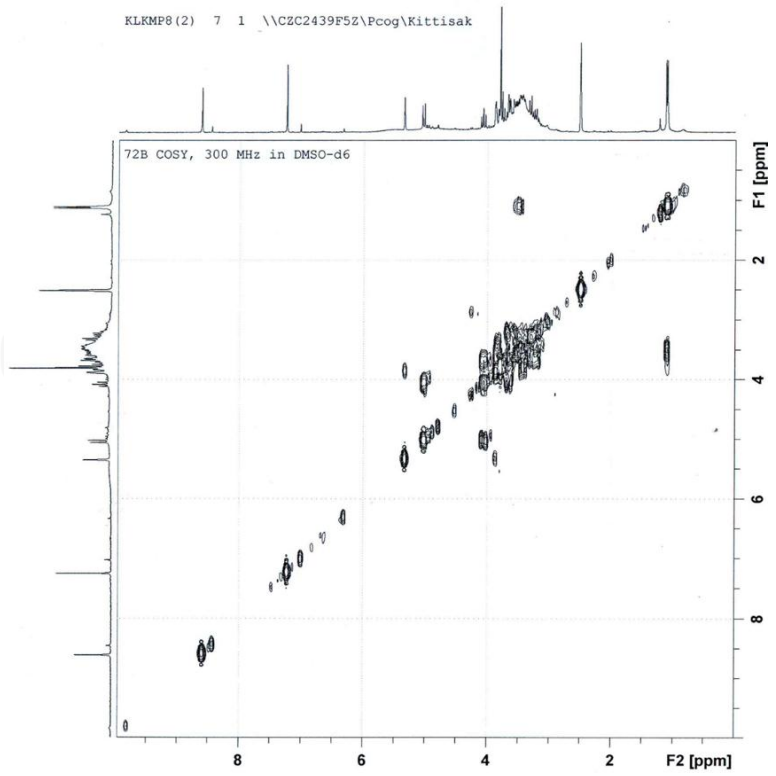

Figure 61 ^{1}H-^{1}H COSY Spectrum (300 MHz) of compound MP-8 [**142**] (DMSO-d_6)

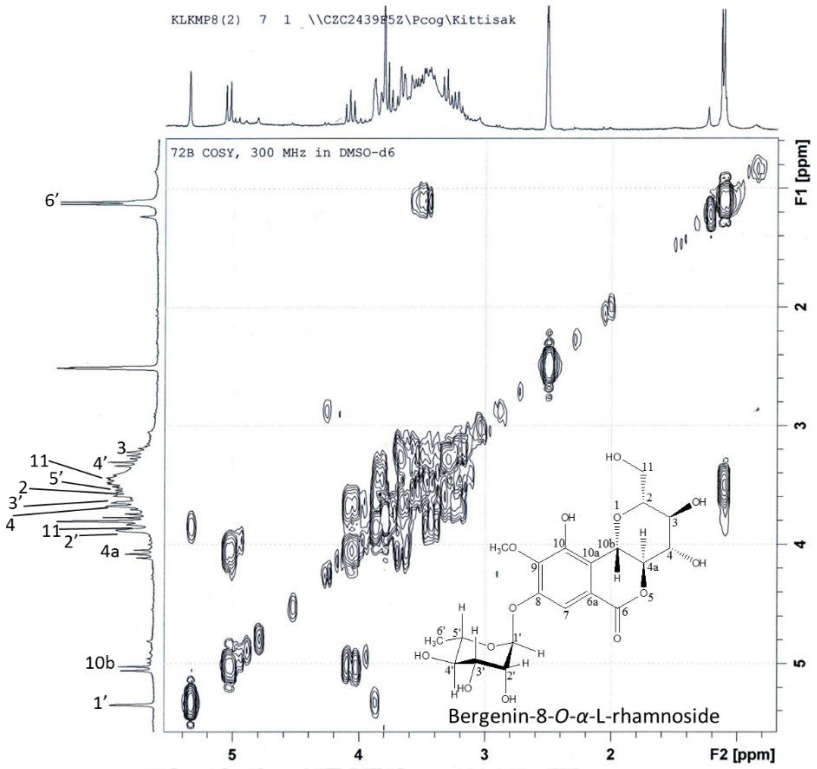

Figure 62 ^{1}H-^{1}H COSY Spectrum (300 MHz) of compound MP-8 [**142**] (DMSO-d_6)

(δ_H 1.6-5.6, δ_H 1.6-5.6 ppm)

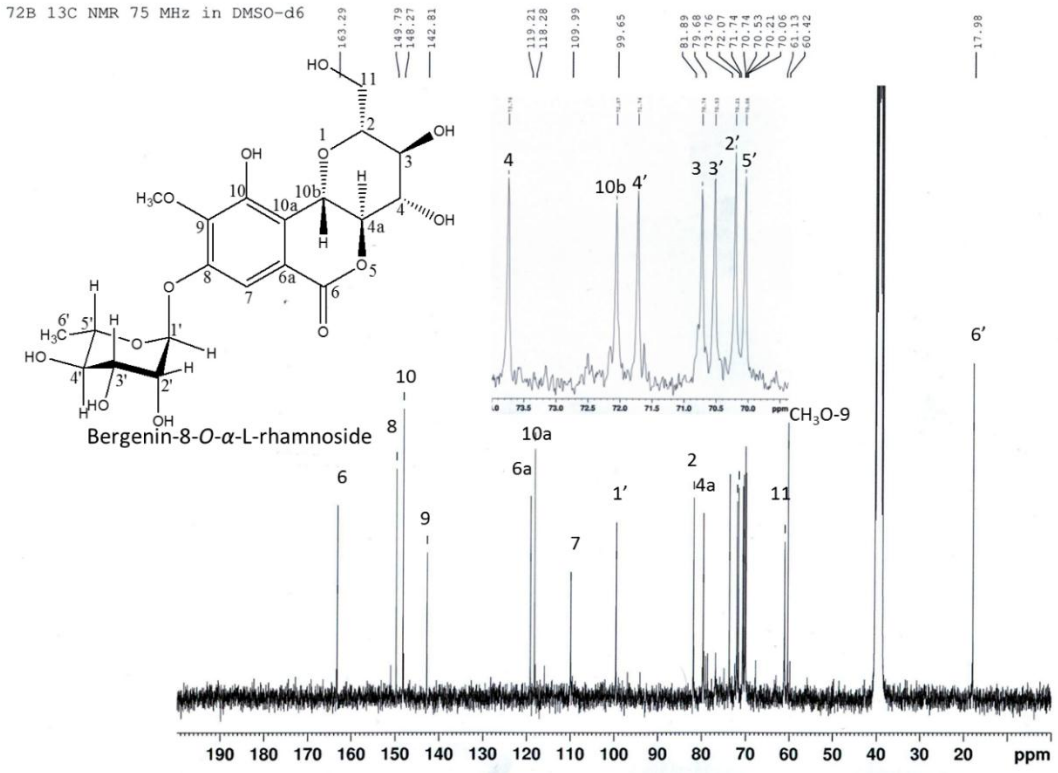

Figure 63 ^{13}C-NMR (75 MHz) Spectrum of compound MP-8 [**142**] (DMSO-d_6)

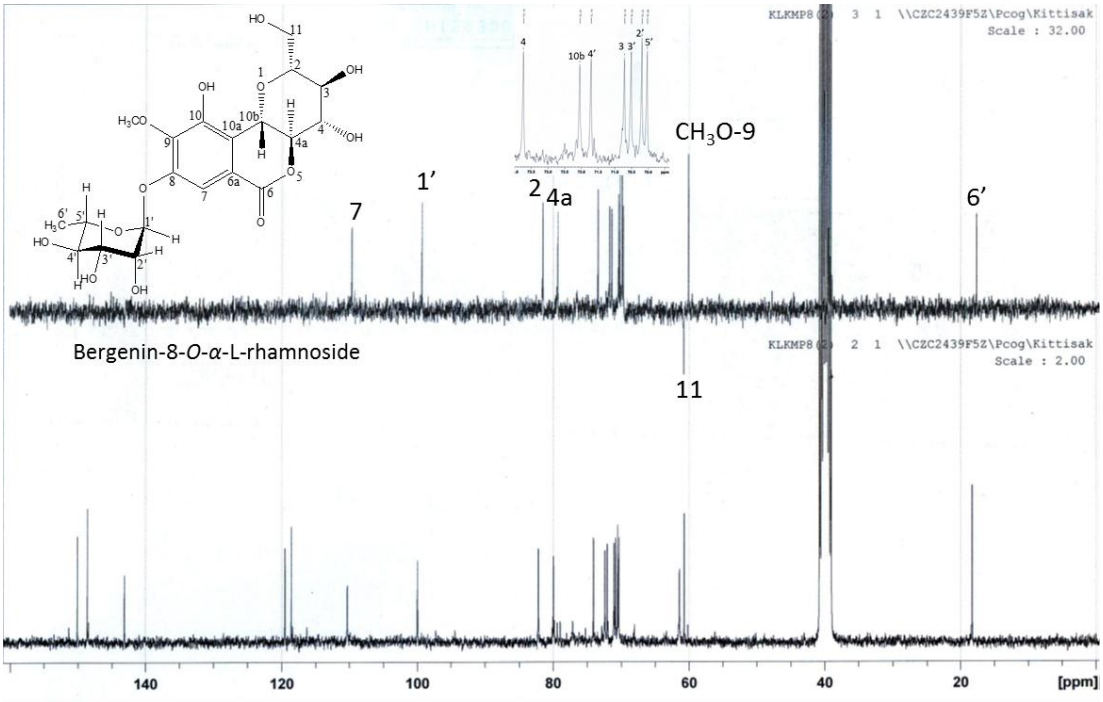

Figure 64 ^{13}C-NMR and DEPT-135 (75 MHz) Spectra of compound MP-8 [**142**] (DMSO-d_6)

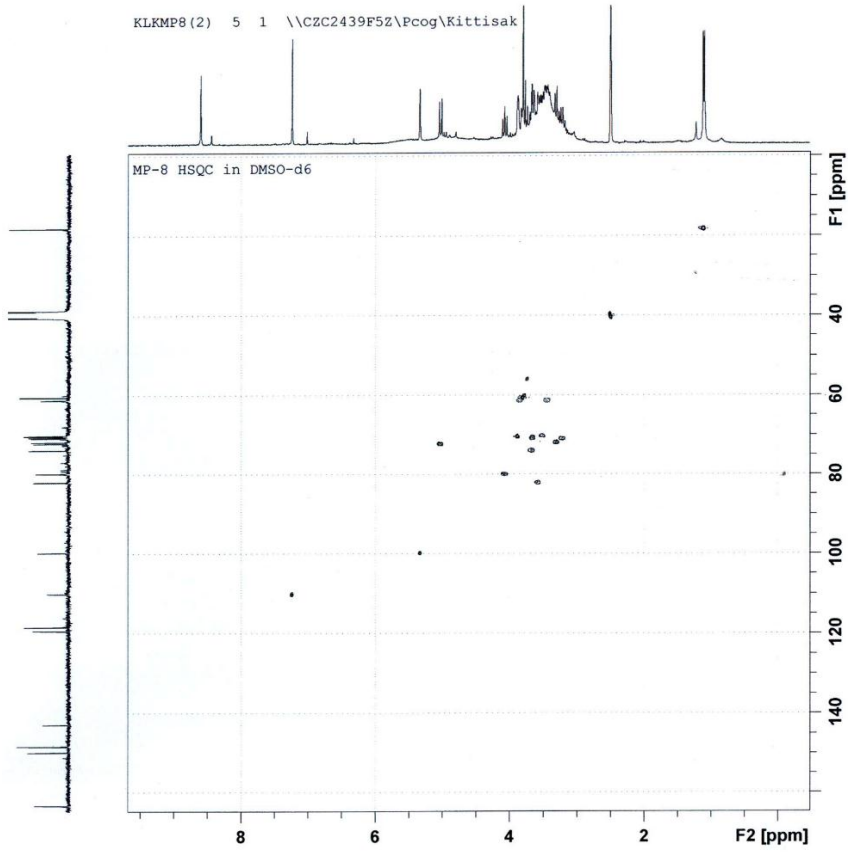

Figure 65 HSQC Spectrum of compound MP-8 [**142**] (DMSO-d_6)

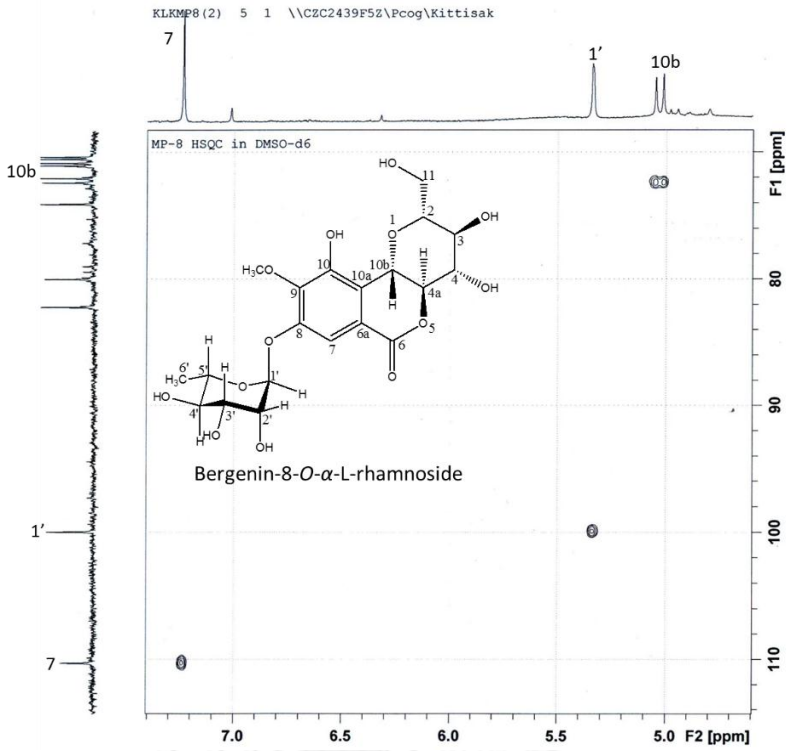

Figure 66 HSQC Spectrum of compound MP-8 [**142**] (DMSO-d_6)

(δ_H 4.2-7.8, δ_C 68-114 ppm)

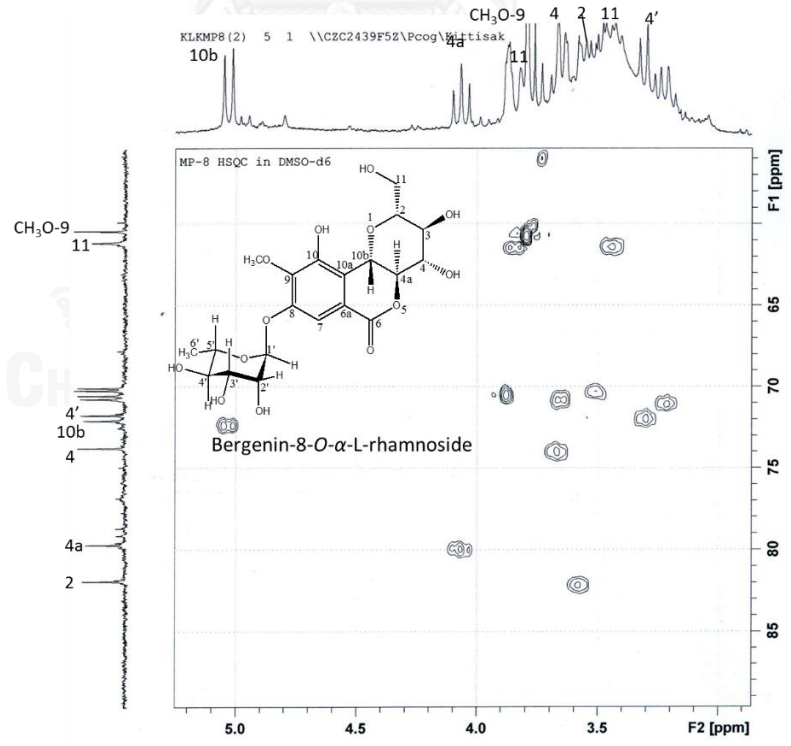

Figure 67 HSQC Spectrum of compound MP-8 [**142**] (DMSO-d_6)

(δ_H 2.9-5.2, δ_C 71-90 ppm)

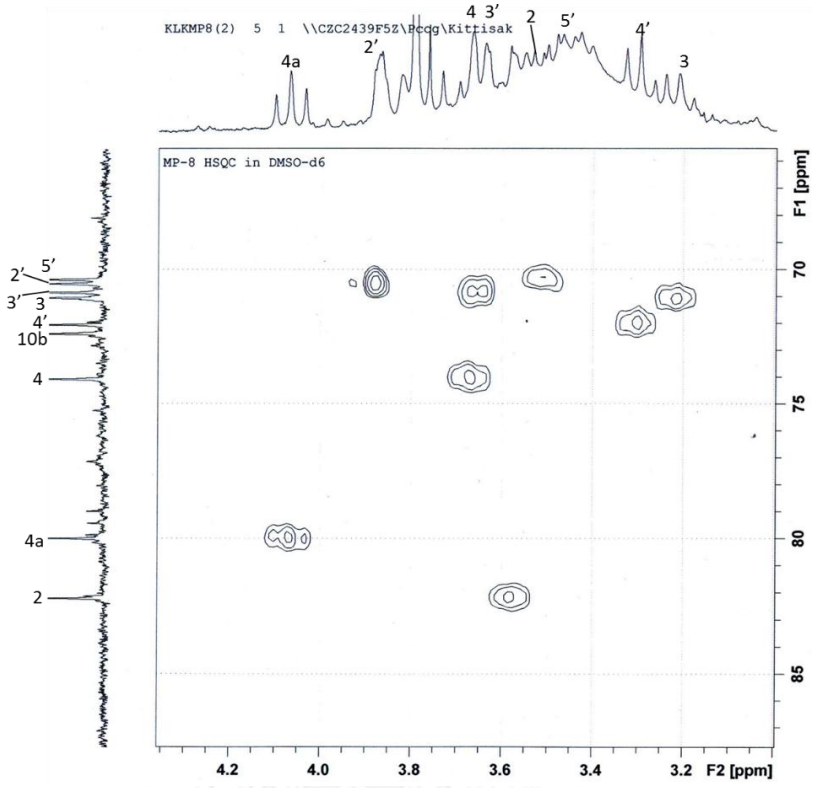

Figure 68 HSQC Spectrum of compound MP-8 [**142**] (DMSO-d_6)

(δ_H 3.00-4.35, δ_C 66-87 ppm)

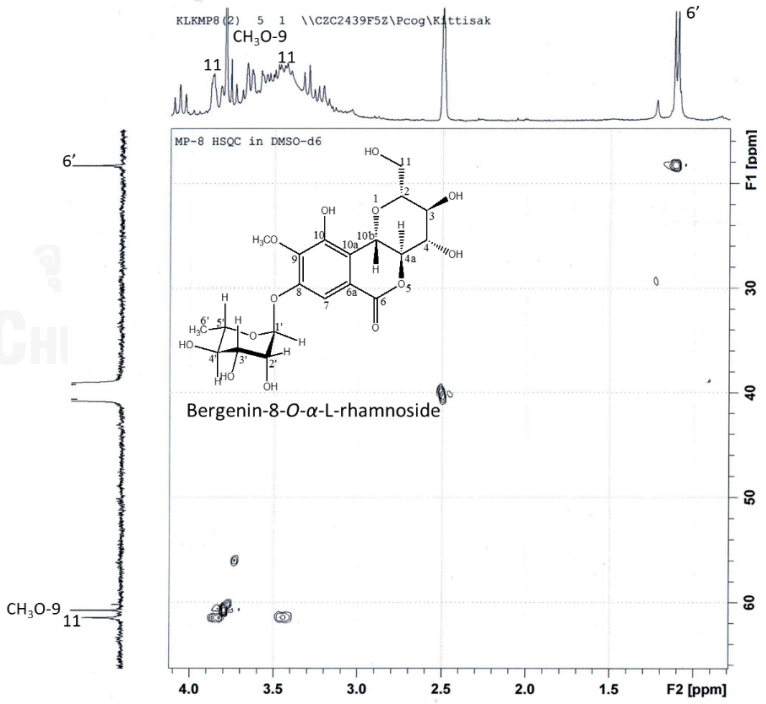

Figure 69 HSQC Spectrum of compound MP-8 [**142**] (DMSO-d_6)

(δ_H 0.8-4.1, δ_C 28-66 ppm)

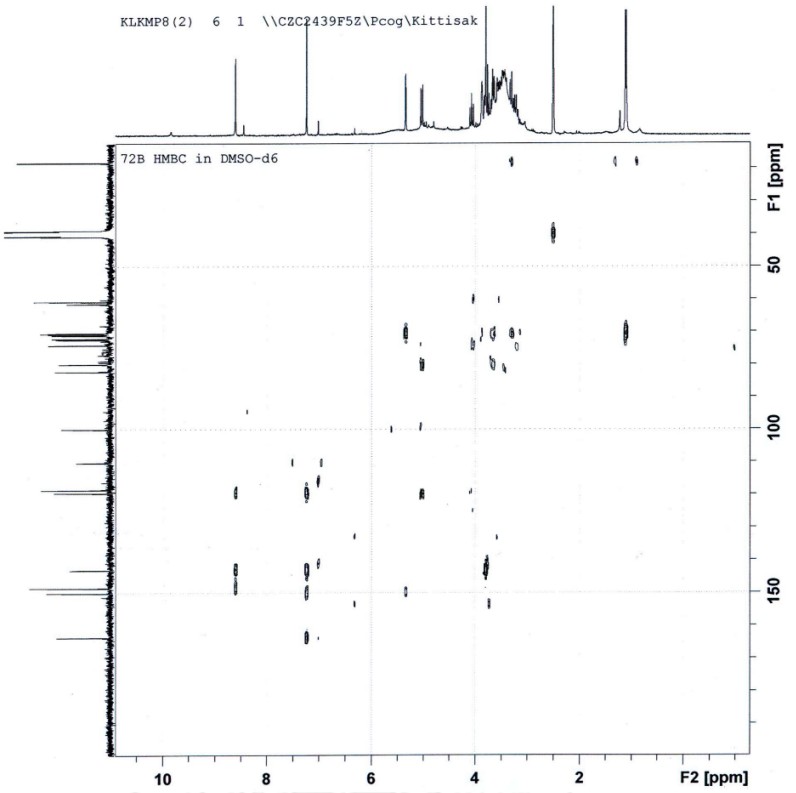

Figure 70 HMBC Spectrum of compound MP-8 [**142**] (DMSO-d_6)

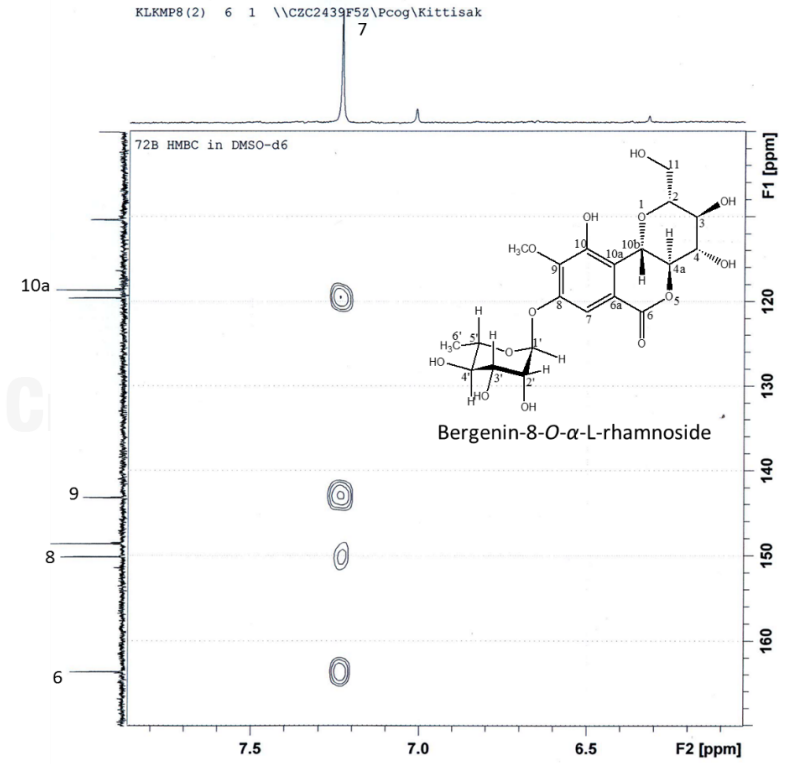

Figure 71 HMBC Spectrum of compound MP-8 [**142**] (DMSO-d_6)

(δ_H 6.1-7.9, δ_C 100-170 ppm)

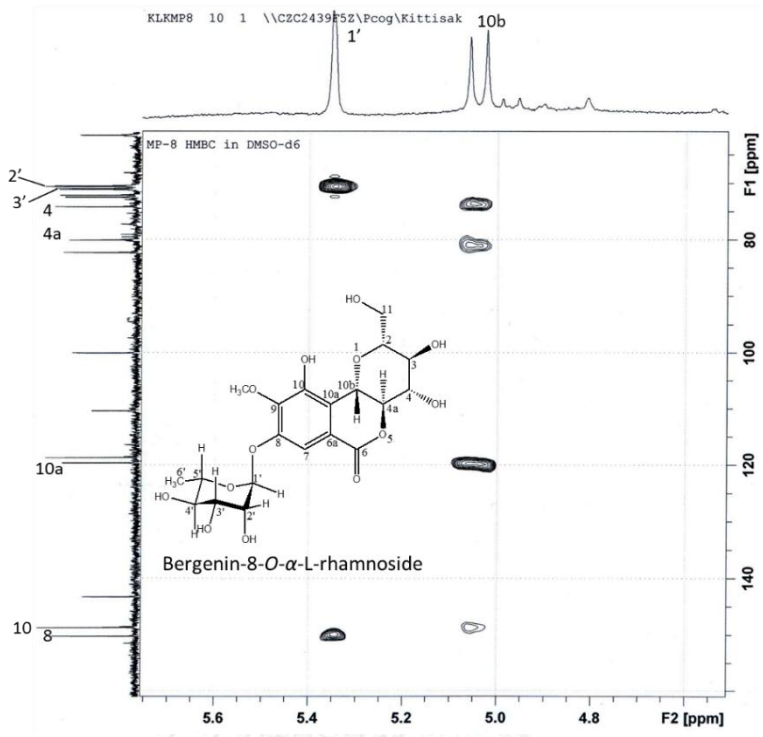

Figure 72 HMBC Spectrum of compound MP-8 [**142**] (DMSO-d_6)

(δ_H 4.50-5.75, δ_C 60-160 ppm)

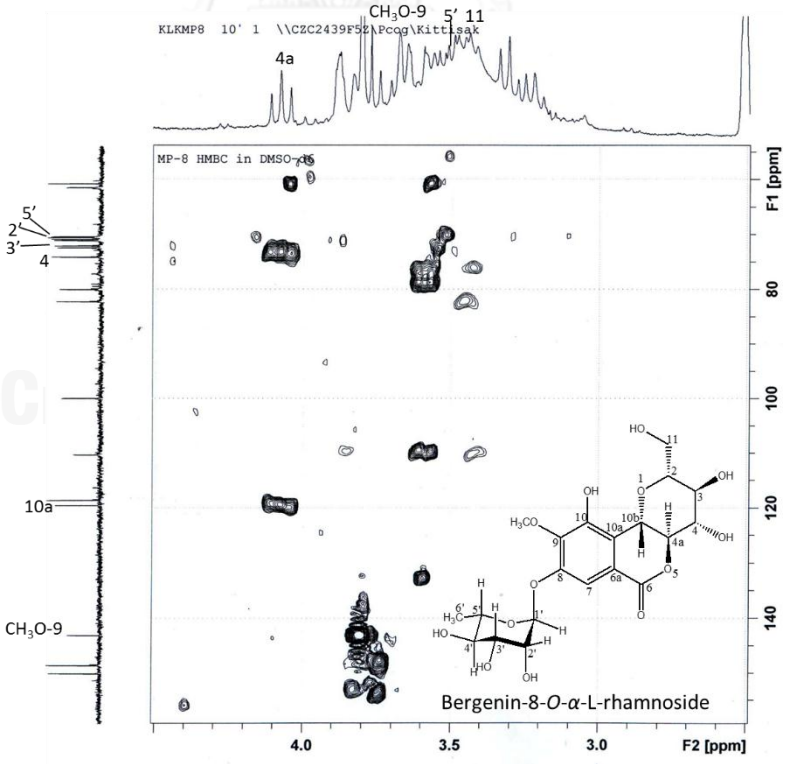

Figure 73 HMBC Spectrum of compound MP-8 [**142**] (DMSO-d_6)

(δ_H 2.5-4.5, δ_C 55-160 ppm)

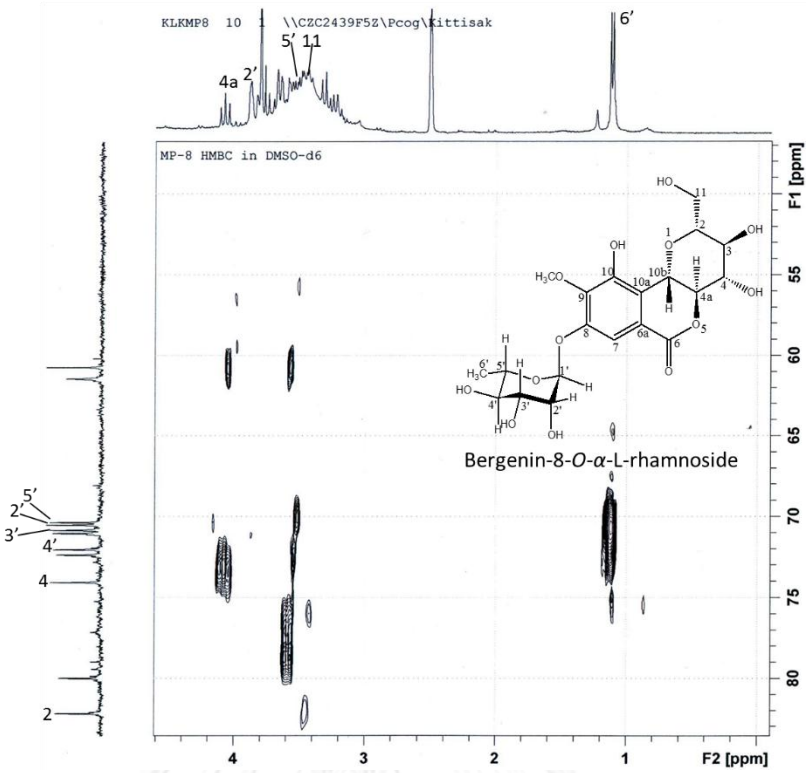

Figure 74 HMBC Spectrum of compound MP-8 [**142**] (DMSO-d_6)

(δ_H 0.0-4.6, δ_C 47-83 ppm)

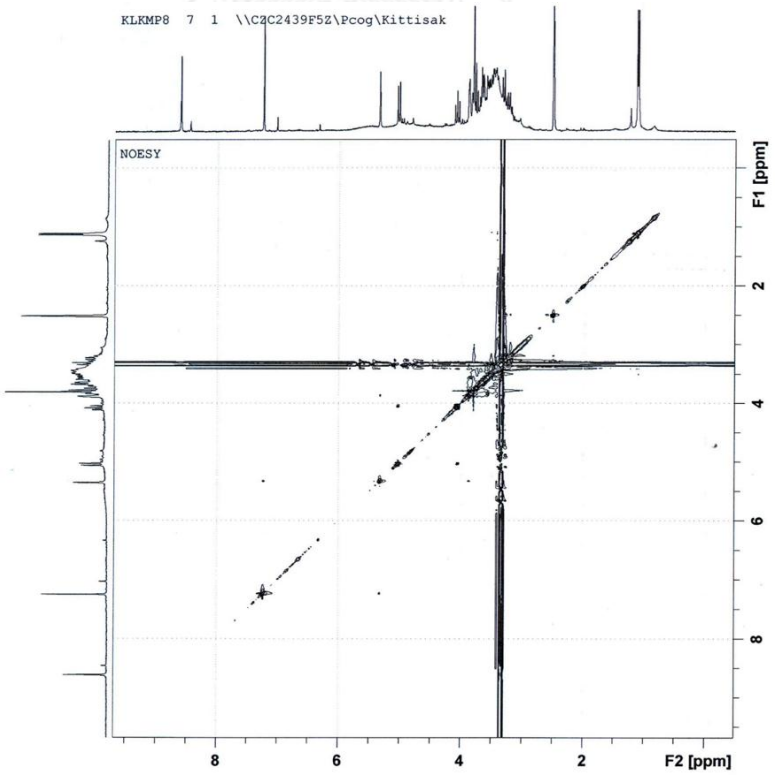

Figure 75 NOESY Spectrum (300 MHz) of compound MP-8 [**142**] (DMSO-d_6)

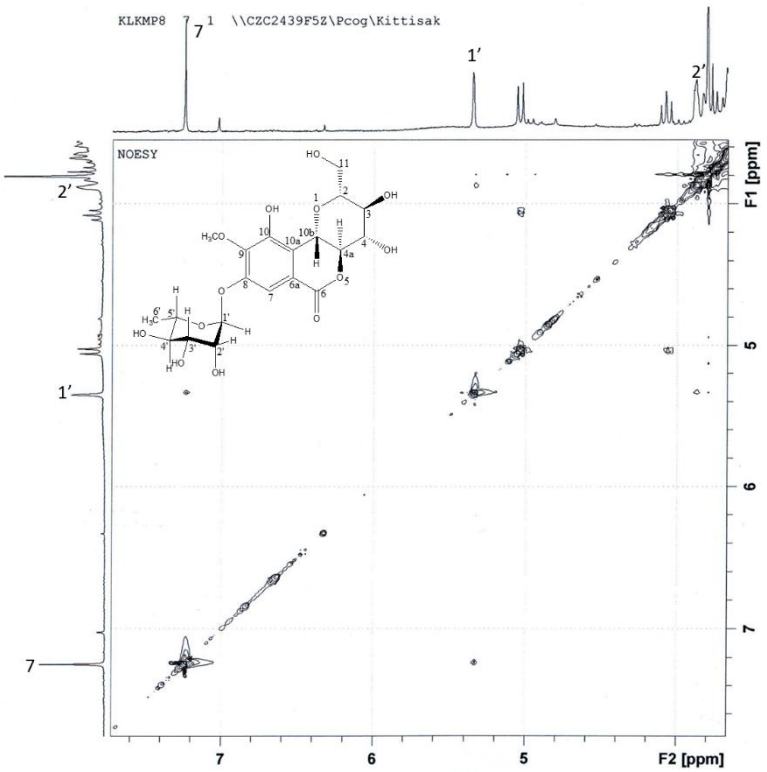

Figure 76 NOESY Spectrum (300 MHz) of compound MP-8 [**142**] (DMSO-d_6)

(δ_H 4.6-7.6, δ_H 4.6-7.6 ppm)

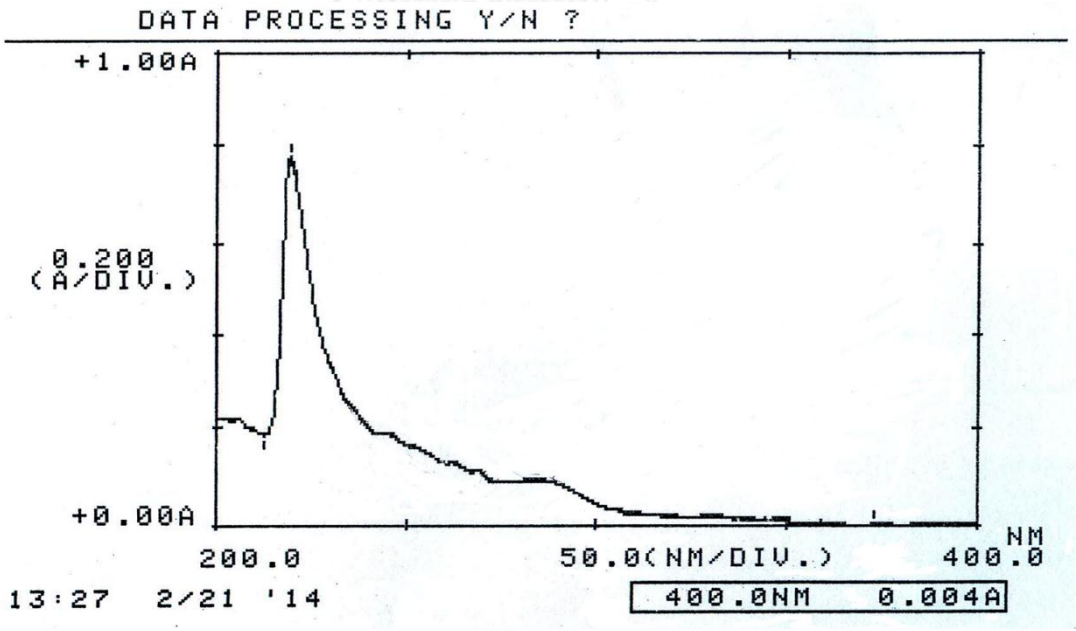

Figure 77 UV Spectrum of compound MP-9 [**143**]

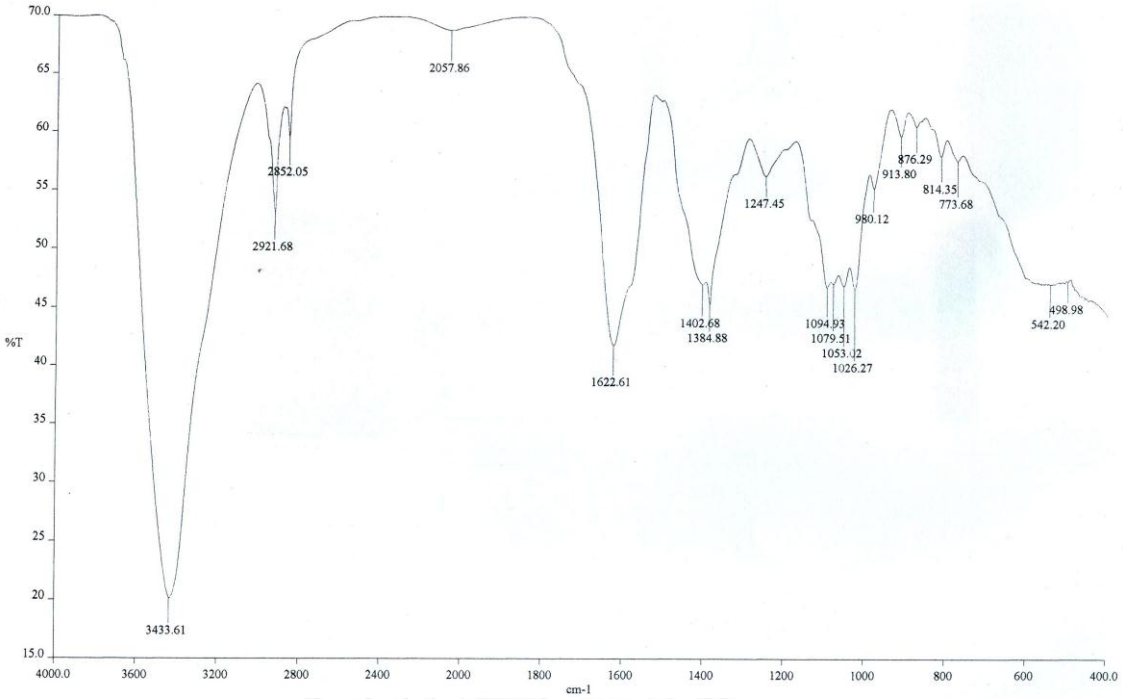

Figure 78 FT-IR Spectrum of compound MP-9 [**143**]

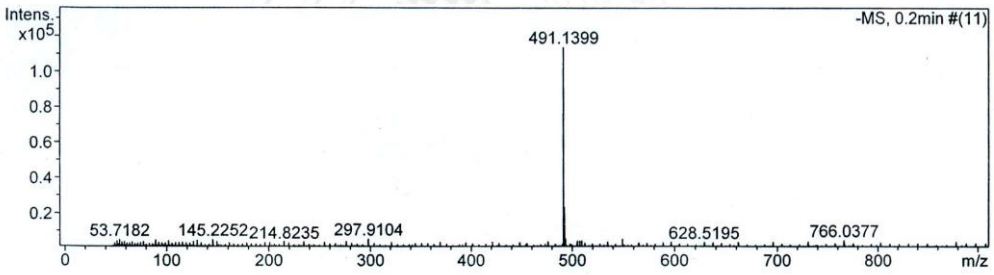

#	m/z	I	I %	S/N	FWHM	Res.
1	51.3861	4150	3.6	3.8	0.0103	4995
2	53.7182	5202	4.6	4.9	0.0082	6524
3	66.3290	3935	3.5	3.6	0.0112	5904
4	77.2931	3855	3.4	3.5	0.0071	10815
5	89.1774	4271	3.8	3.9	0.0084	10587
6	89.2598	4128	3.6	3.8	0.0280	3186
7	126.2721	4109	3.6	3.7	0.0125	10116
8	145.2252	5266	4.6	4.9	0.0161	9030
9	297.9104	5614	4.9	6.0	0.0340	8760
10	491.1399	113839	100.0	134.0	0.0627	7838
11	492.1437	23416	20.6	27.2	0.0642	7668
12	493.1454	5668	5.0	6.2	0.0630	7826
13	504.8712	4450	3.9	4.8	0.0290	17405
14	507.1351	4494	3.9	4.8	0.0613	8267
15	509.1092	4565	4.0	4.9	0.0530	9602
16	549.1025	5412	4.8	5.9	0.0632	8691
17	766.0377	4385	3.9	4.7	0.0451	16990
18	997.1948	4014	3.5	4.2	0.0217	45977
19	1038.9547	3957	3.5	4.2	0.0299	34709
20	1081.5928	4875	4.3	5.2	0.0347	31137
21	1451.3542	5086	4.5	5.4	0.0585	24826
22	1875.3221	3966	3.5	4.2	0.0681	27557
23	1875.3867	4459	3.9	4.7	0.0750	25007
24	2290.6209	3882	3.4	4.0	0.0442	51770
25	2291.0094	3856	3.4	4.0	0.1050	21824
26	2353.3881	6160	5.4	6.6	0.0359	65529
27	2353.5907	5521	4.8	5.8	0.0663	35478
28	2353.7456	4059	3.6	4.2	0.0677	34770
29	2885.5322	4069	3.6	4.3	0.0404	71350
30	2886.2761	5171	4.5	5.6	0.0672	42965

Figure 79 HR-ESI Mass spectrum of compound MP-9 [**143**]

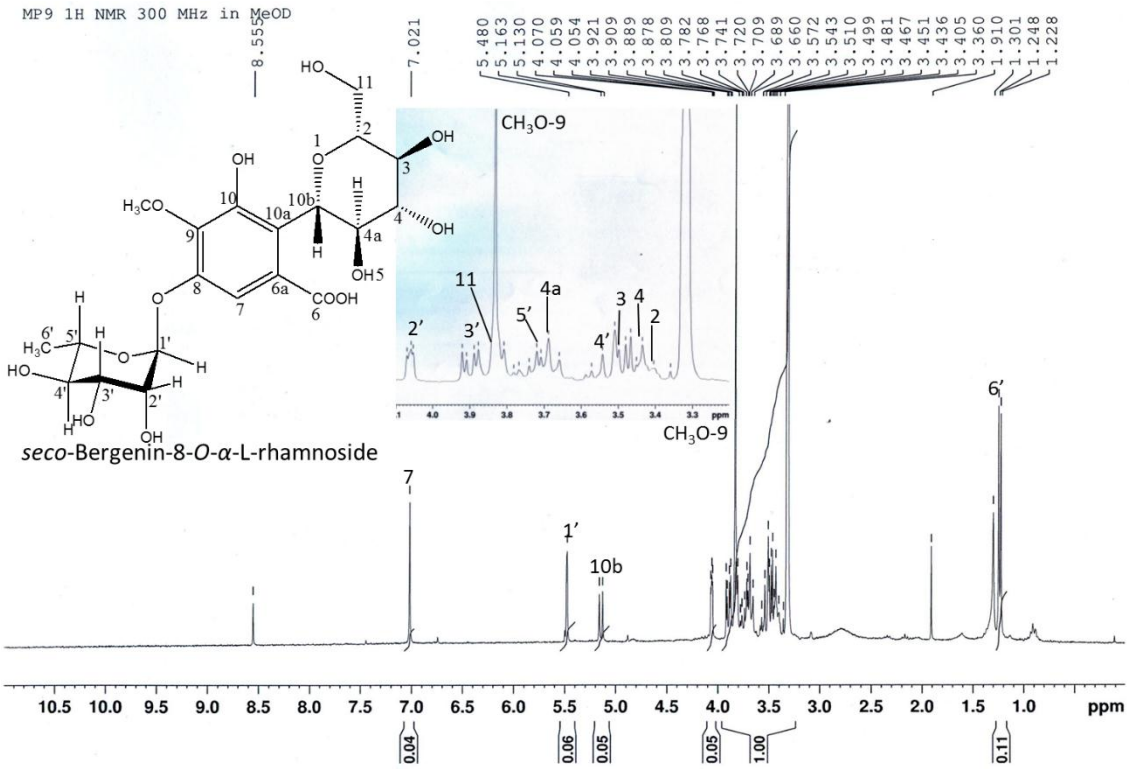

Figure 80 ^{1}H-NMR (300 MHz) Spectrum of compound MP-9 [**143**] (CD_3OD)

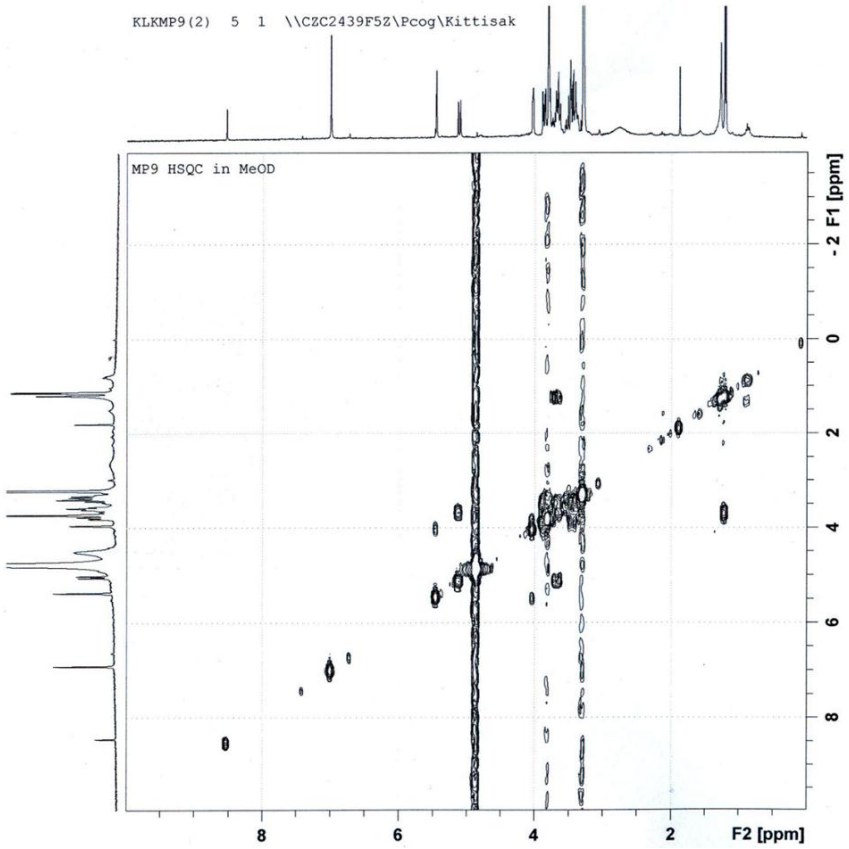

Figure 81 ^{1}H-^{1}H COSY Spectrum (300 MHz) of compound MP-9 [**143**] (CD_3OD)

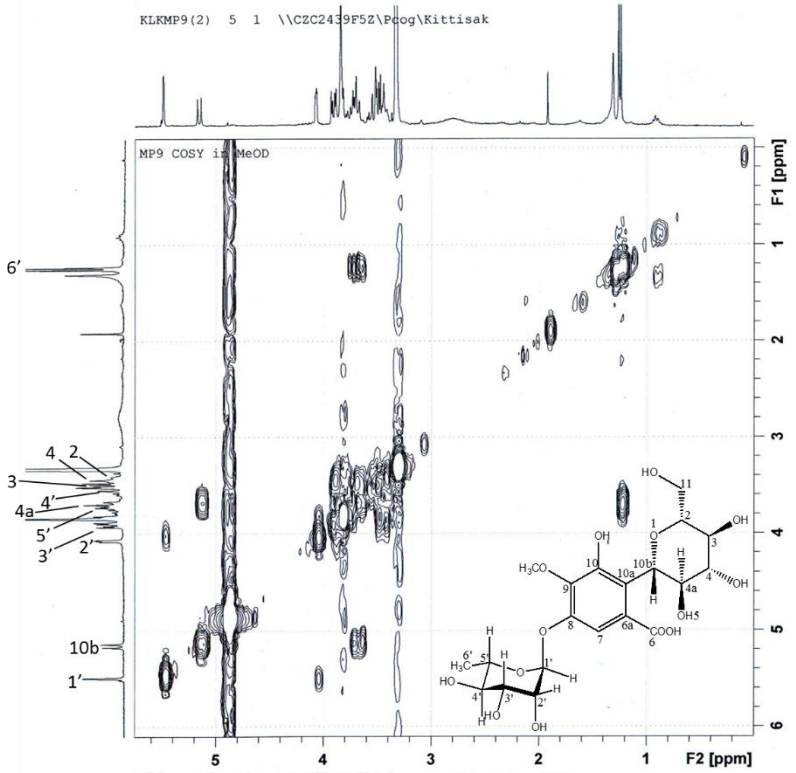

Figure 82 ^{1}H-^{1}H COSY Spectrum (300 MHz) of compound MP-9 [**143**] (CD_3OD) (δ_H 0.0-5.6, δ_H 0.0-5.6 ppm)

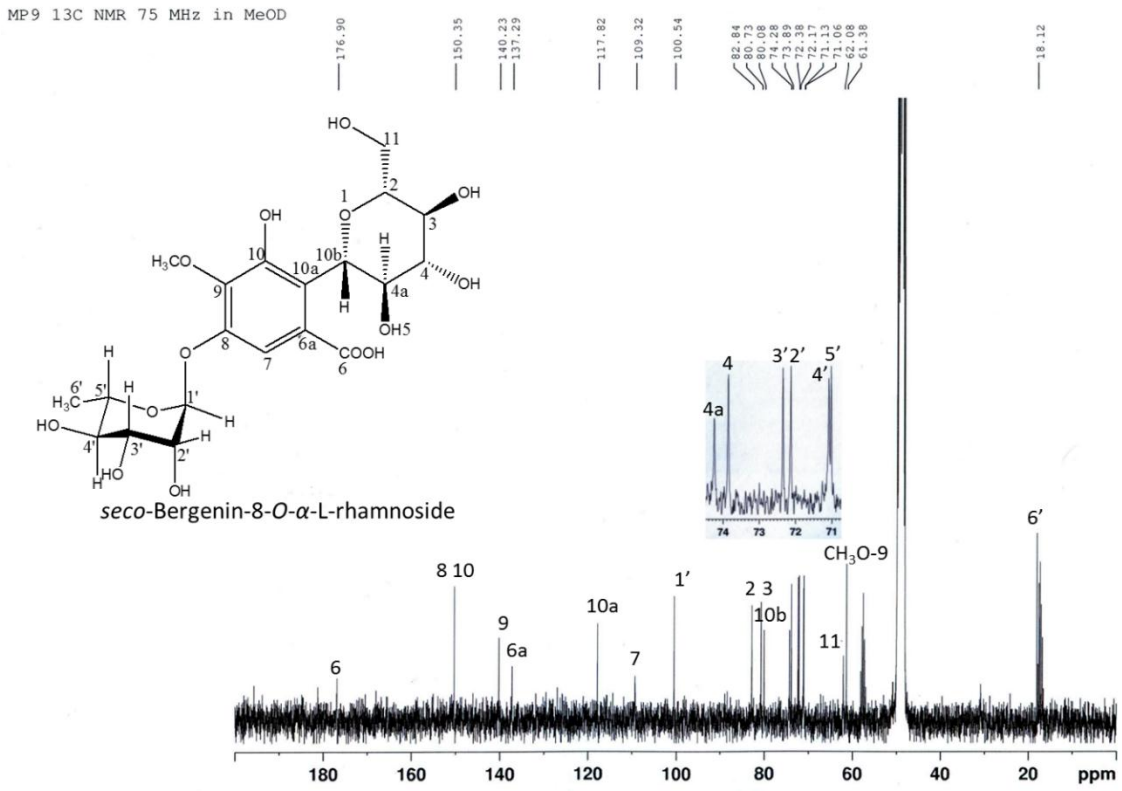

Figure 83 ^{13}C-NMR (75 MHz) Spectrum of compound MP-9 [**143**] (CD_3OD)

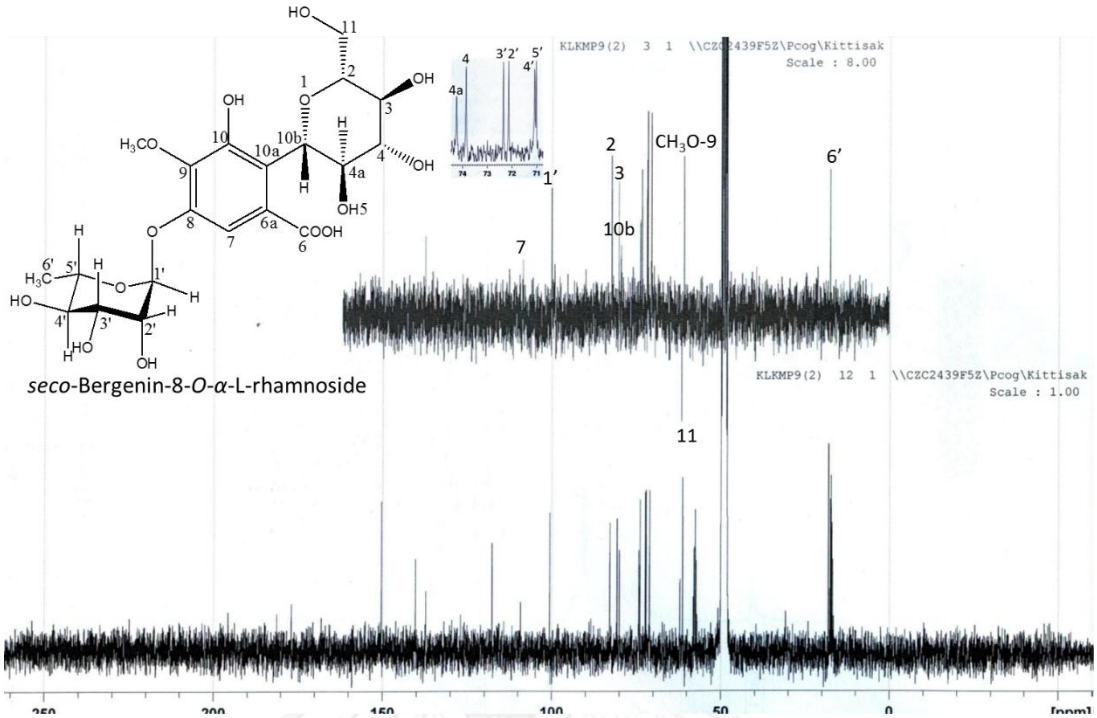

Figure 84 ^{13}C-NMR and DEPT-135 (75 MHz) Spectra of compound MP-9 [**143**] (CD_3OD)

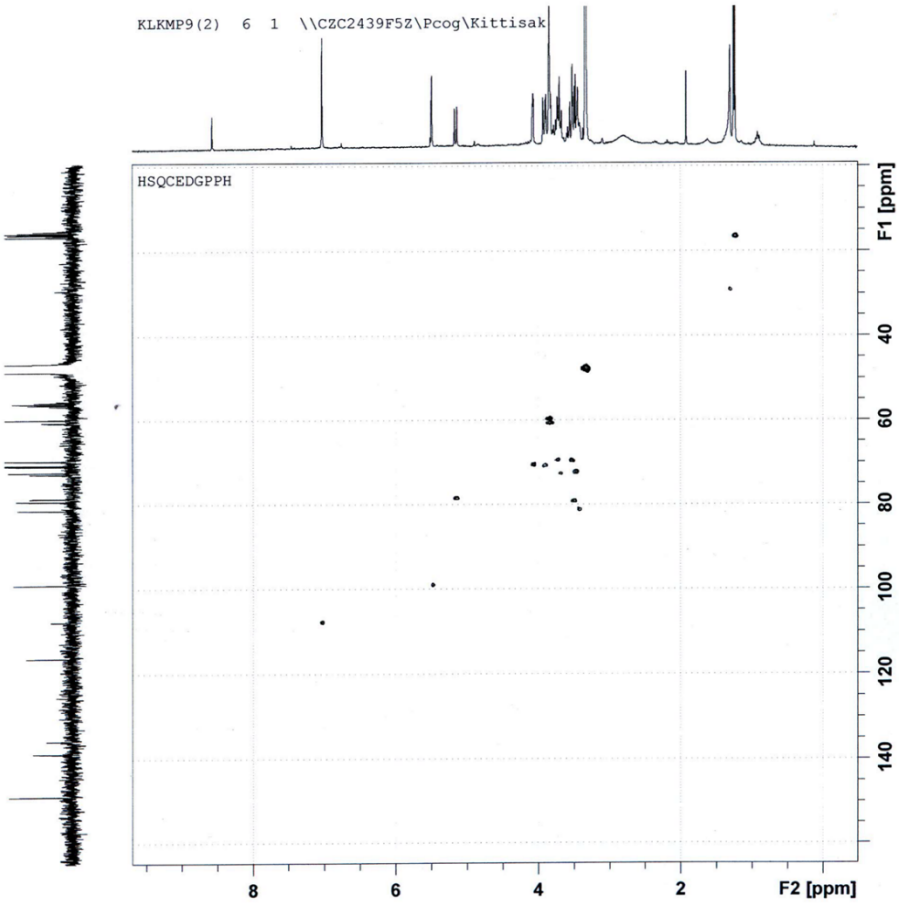

Figure 85 HSQC Spectrum of compound MP-9 [**143**] (CD_3OD)

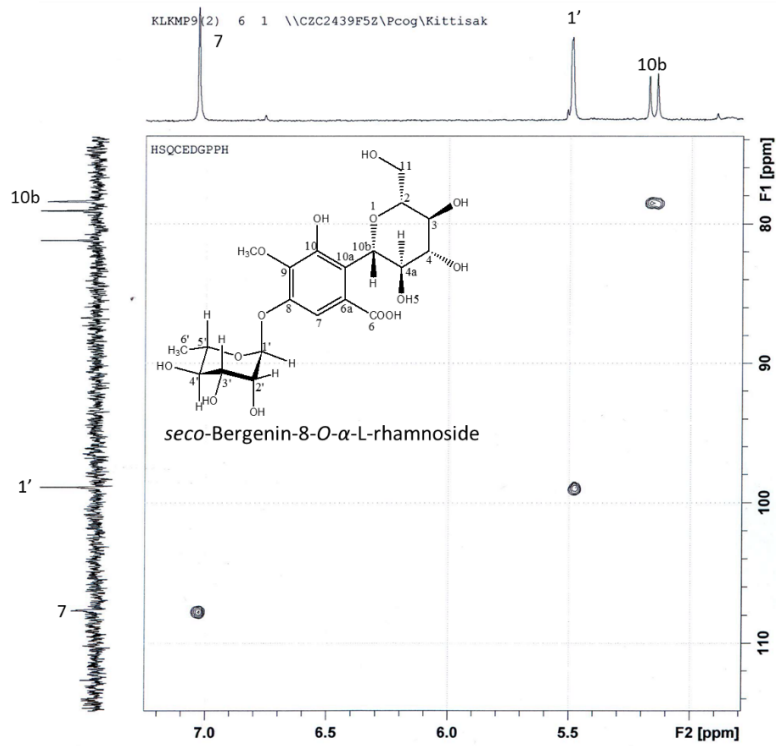

Figure 86 HSQC Spectrum of compound MP-9 [**143**] (CD_3OD)

(δ_H 4.8-7.2, δ_C 74-114 ppm)

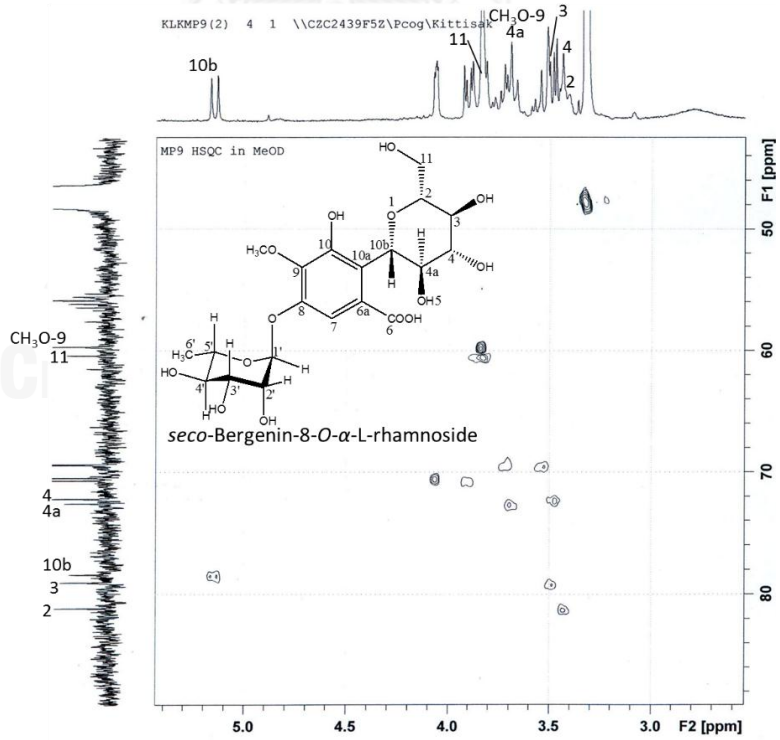

Figure 87 HSQC Spectrum of compound MP-9 [**143**] (CD_3OD)

(δ_H 2.6-5.4, δ_C 52-88 ppm)

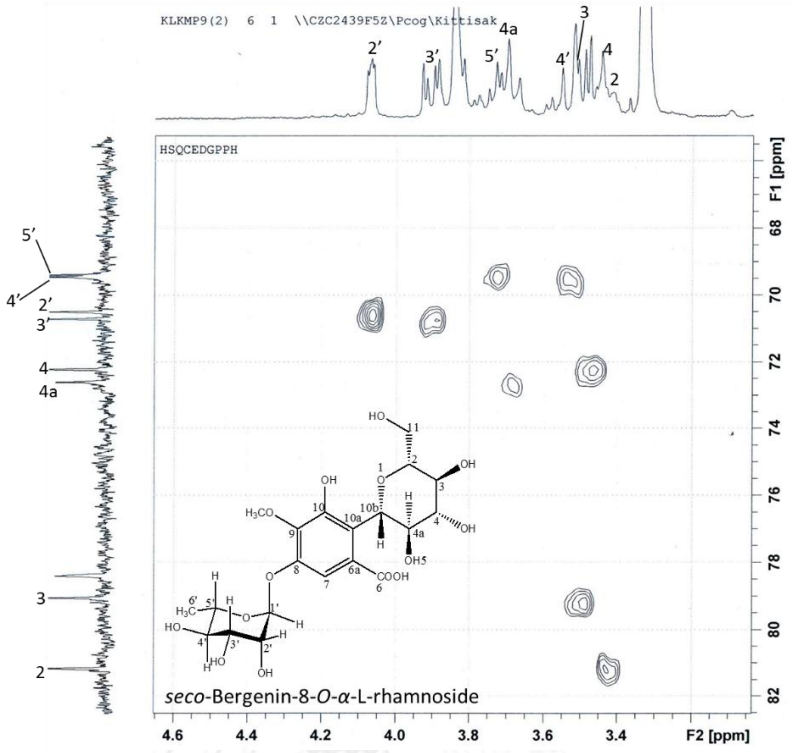

Figure 88 HSQC Spectrum of compound MP-9 [**143**] (CD_3OD)

(δ_H 3.05-4.65, δ_C 65.5-82.5 ppm)

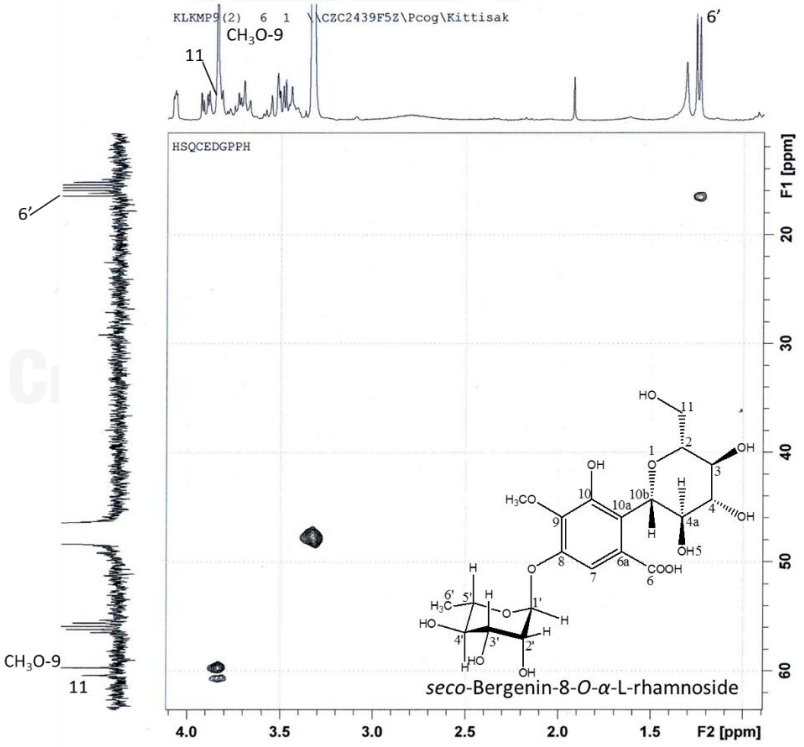

Figure 89 HSQC Spectrum of compound MP-9 [**143**] (CD_3OD)

(δ_H 0.9-4.1, δ_C 12-62 ppm)

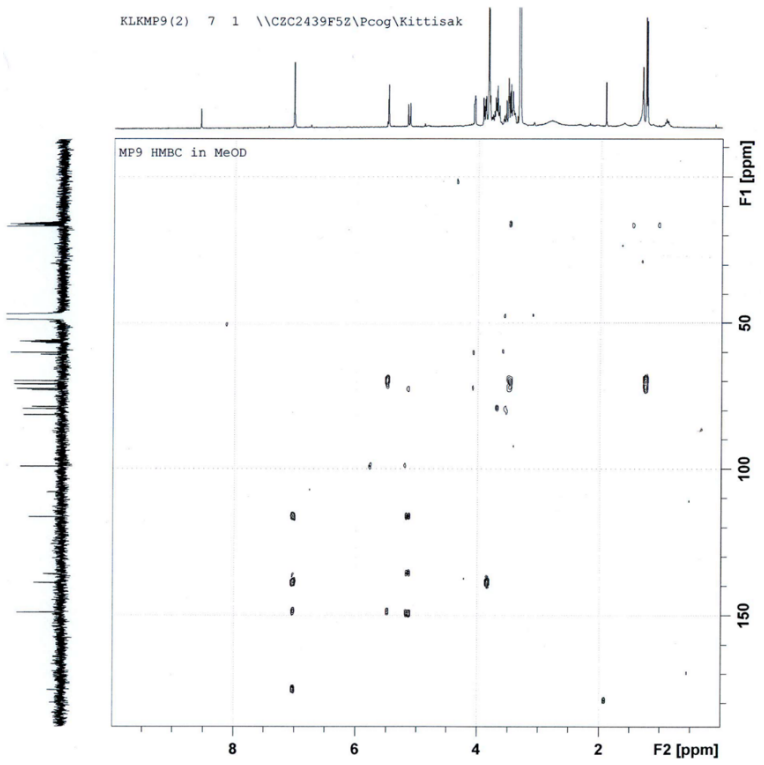

Figure 90 HMBC Spectrum of compound MP-9 [**143**] (CD_3OD)

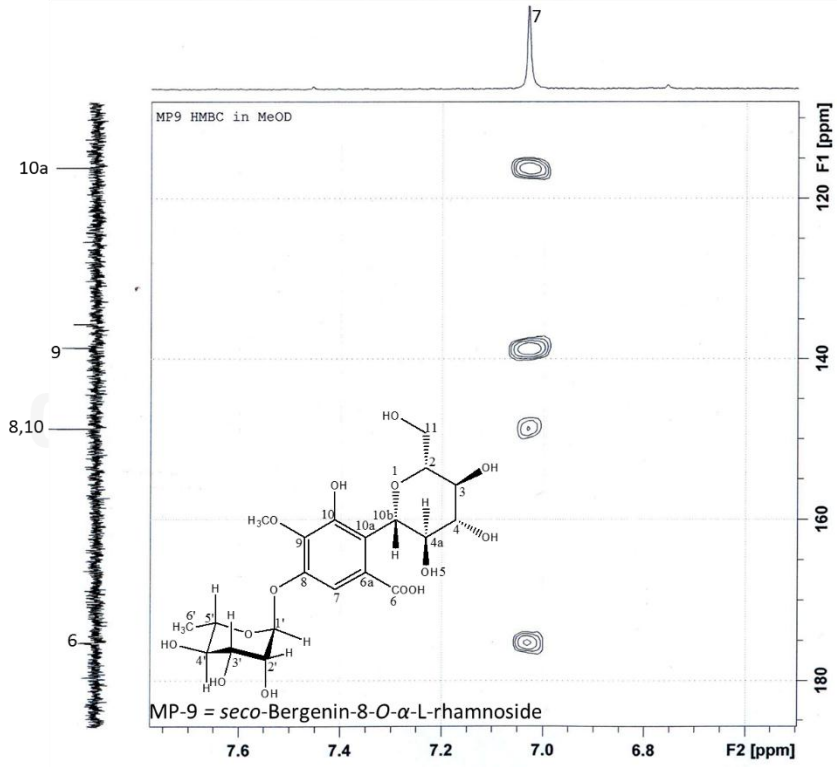

Figure 91 HMBC Spectrum of compound MP-9 [**143**] (CD_3OD)

(δ_H 6.50-7.65, δ_C 110-185 ppm)

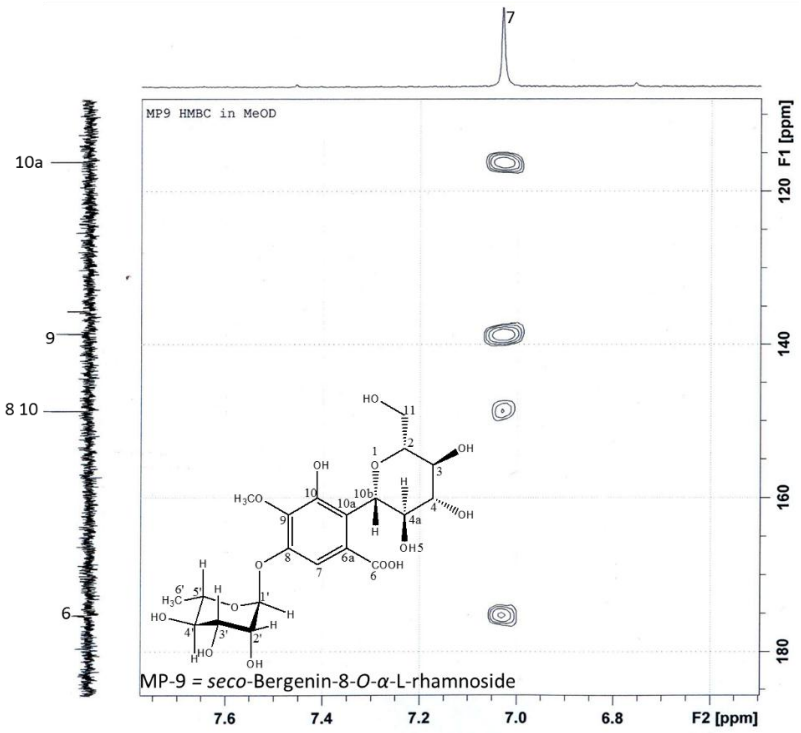

Figure 92 HMBC Spectrum of compound MP-9 [**143**] (CD_3OD)

(δ_H 6.6-7.0, δ_C 65-155 ppm)

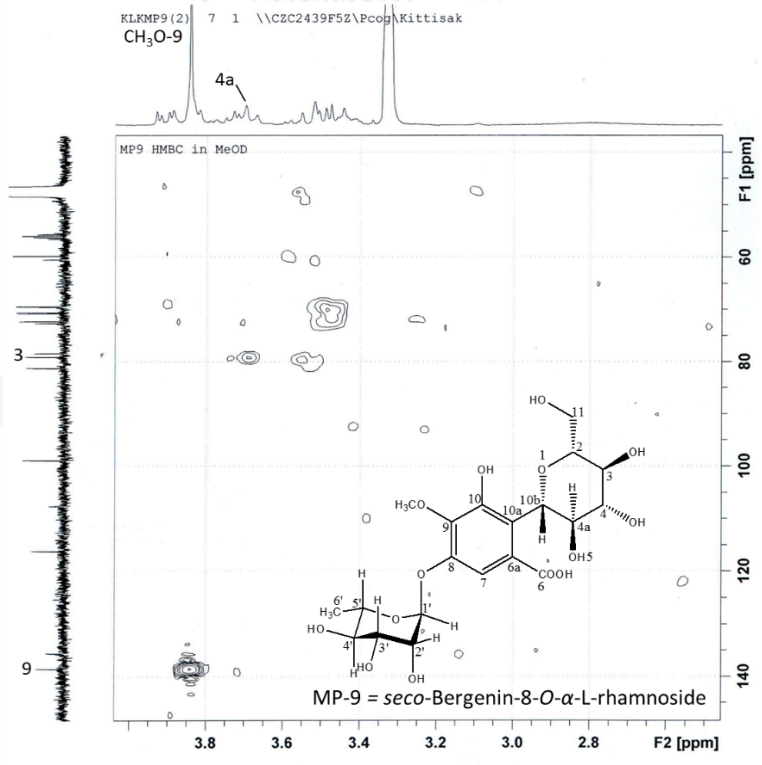

Figure 93 HMBC Spectrum of compound MP-9 [**143**] (CD_3OD)

(δ_H 2.5-4.0, δ_C 40-145 ppm)

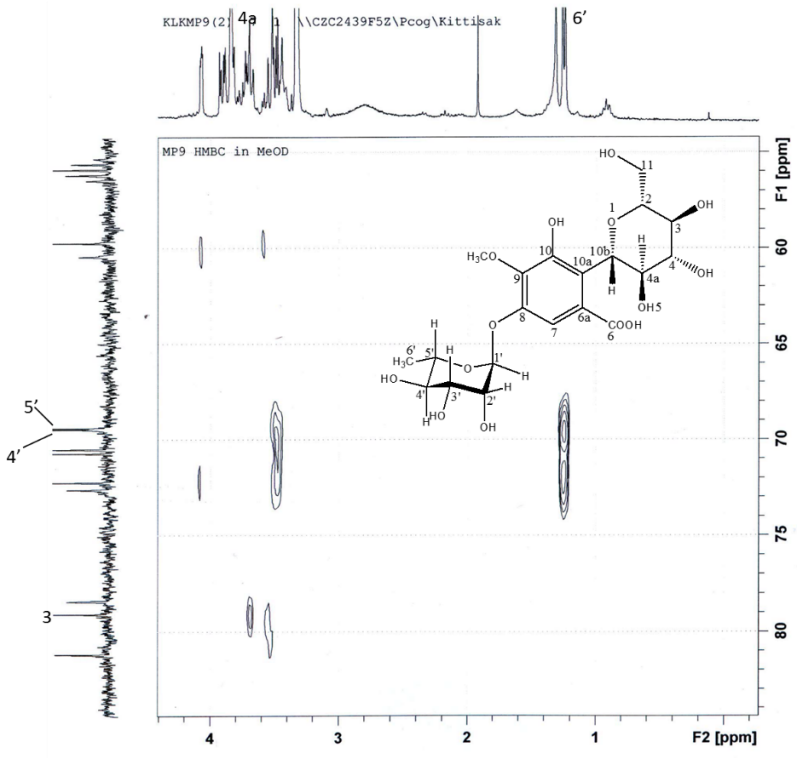

Figure 94 HMBC Spectrum of compound MP-9 [**143**] (CD_3OD)

(δ_H 0.0-4.4, δ_C 55-84 ppm)

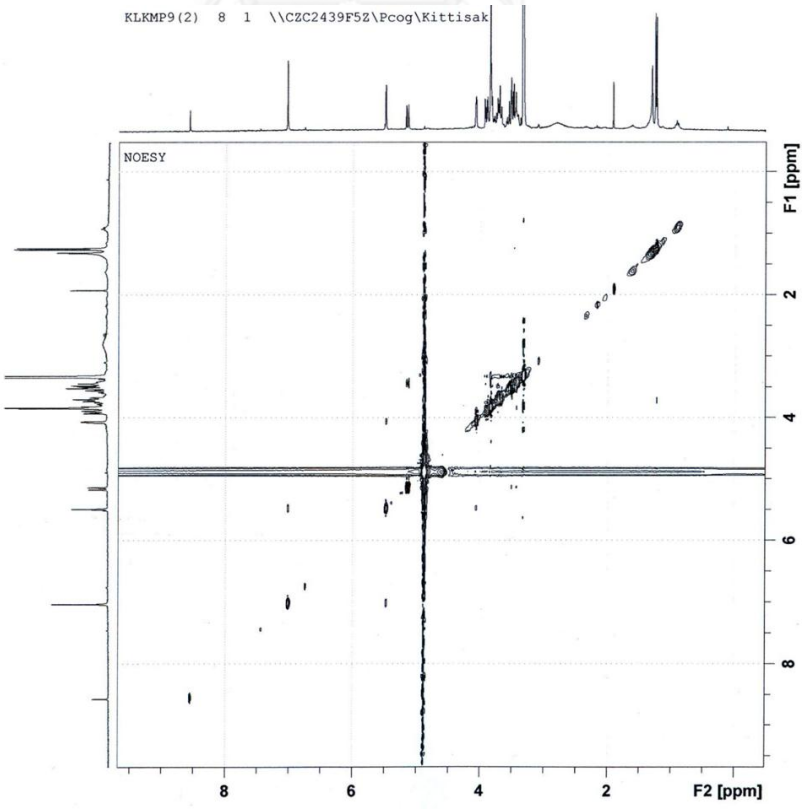

Figure 95 NOESY Spectrum (300 MHz) of compound MP-9 [**143**] (CD_3OD)

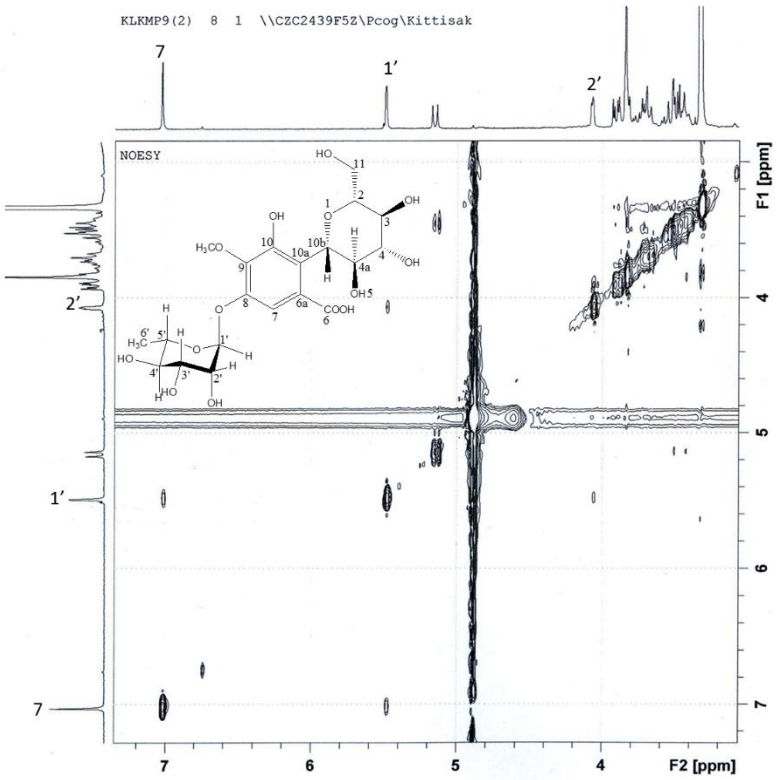

Figure 96 NOESY Spectrum (300 MHz) of compound MP-9 [**143**] (CD_3OD) (δ_H 3.2-7.2, δ_H 3.2-7.2 ppm)

VITA

Mr. Kongsin Luangruangrong was born on March 11, 1988 in Bangkok, Thailand. He received his Bachelor's Degree in Pharmacy in 2010 from the Faculty of Pharmacy, Mahidol University. Thailand.

Poster presentation

Kongsin Luangruangrong, Boonchoo Sritularak, and Kittisak Likhitwitayawuid. Chemical constituents of Mallotus plicatus stem bark. Proceedings of 15th Graduate Research Conferences, March 28, 2014. The Graduate School, Khon Kaen University, Bangkok, Thailand. p. 164.

Publication

Kongsin Luangruangrong, Boonchoo Sritularak, Vimolmas Lipipun, and Kittisak Likhitwitayawuid. New gallic acid glycosides from Mallotus plicatus. Heterocycles, Vol 89, No. 5, 2014, p. 1237-1444.